Interstellar and Intergalactic Medium

1. **Overview**
2. **Gas and dust**
3. **Star Formation**

Wen-Ping CHEN
National Central University
Taiwan

VSOA9 2025 July 07~12 @ Quy Nhon, Vietnam

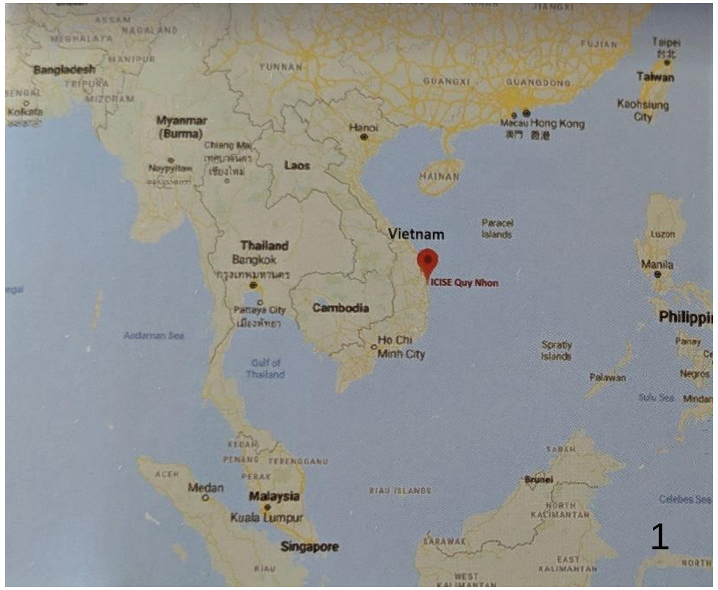

Interstellar Medium

and Radiation

http://www.astro.ncu.edu.tw/~wchen/Courses/ISM/index.htm

Space is not completely empty, but filled with **interstellar medium** (ISM) of various format (*atomic*, *molecular*, *ionized*) under drastically different conditions (*temperature*, *pressure*, *density*, *etc*.) cf. IGM, ICM

Stars are formed out of, and continue to interact with, the ISM.

When stars end their lives, they return enriched "complex" stellar matter back to the ISM, with which the next negation of stars (and planets) are formed.

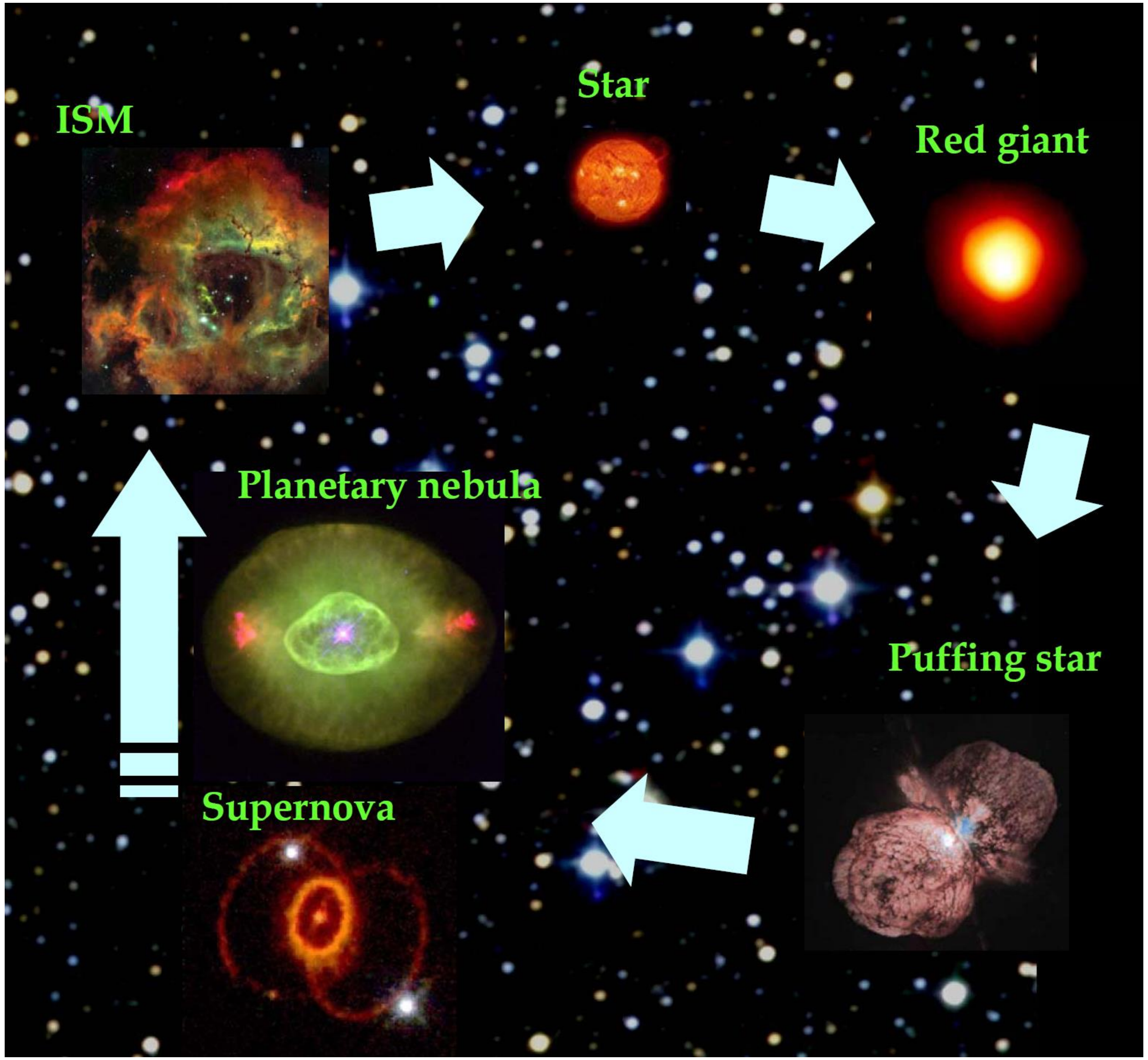

Discovery of the Interstellar Medium

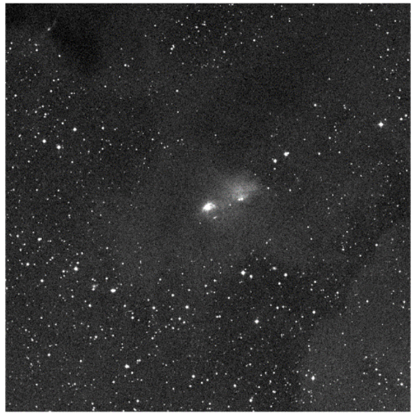

- 1811 William Herschel: "*holes in the starry sky*"
- 1904 J. F. Hartmann "*stationary*" calcium lines in the spectroscopic binary δ Orionis → of interstellar origin
- 1919 E. E. Barnard catalog of dark nebulae
- Photography → emission and reflection nebulae; dark clouds
- 1926 Sir Arthur Eddington lectured "*Diffuse Matter in Space*"
- 1927 Otto Struve "Interstellar Calcium"
- 1930 Robert J. Trumpler: absorption ↗ as distance ↗
→ beginning of ISM as a new branch of astronomy

1904

INVESTIGATIONS ON THE SPECTRUM AND ORBIT OF δ *ORIONIS*.[1]

By J. Hartmann.

One of the first results obtained by M. Deslandres with the new spectrograph attached to the 62 cm refractor of the observatory at Meudon was the discovery of the "oscillation" of δ *Orionis*. I use the term "oscillation" in place of the ponderous expression "variability of velocity in the line of sight;" but the idea of oscillation is still somewhat broader, as it includes every sort of periodic variation in the spectrum, without saying anything as to its explanation.

After the publication[2] of the discovery mentioned, which was communicated to the Paris Academy on February 12, 1900, Director Vogel instructed the observers in the field of stellar spectroscopy at Potsdam to undertake to confirm the interesting phenomenon, and the observations made with the four different spectrographs then in use here proved beyond a doubt that δ *Orionis* belongs to the number of oscillating stars. A confirmation of the discovery was also given by three observations by Wright with the Mills spectrograph of the Lick Observatory.

Deslandres derived from his eleven observations a period of 1.92 days, and concluded that the orbit was very eccentric. The observations which I made at that time with the large Spectrograph III (with three prisms) attached to the 80 cm refractor could not, however, be brought into accord with that length of period; and since the measures showed that the star could be more advantageously observed with low dispersion, on account of the extreme diffuseness of its lines, I included it in the program of Spectrograph I (with only one prism). With this

THE
ASTROPHYSICAL JOURNAL
AN INTERNATIONAL REVIEW OF SPECTROSCOPY AND ASTRONOMICAL PHYSICS

VOLUME XLIX | JANUARY 1919 | NUMBER 1

ON THE DARK MARKINGS OF THE SKY
WITH A CATALOGUE OF 182 SUCH OBJECTS

By E. E. BARNARD

It would be unwise to assume that all the dark places shown on photographs of the sky are due to intervening opaque masses between us and the stars. In a considerable number of cases no other explanation seems possible, but some of them are doubtless only vacancies.

1919

PLATE I

North

Region North of Theta Ophiuchi
$\alpha = 17^h\ 13^m,\ \delta = -21°\ 0'$
Scale: $1^{mm} = 234''$

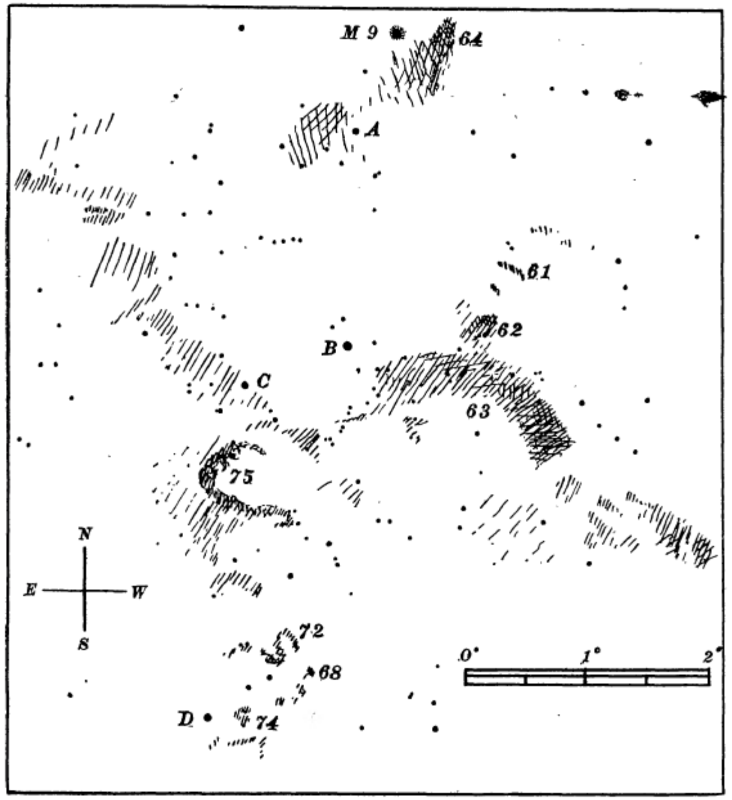

Fig. 2.—Sketch map of Plate I

- The air we breathe: 10^{19} molecules per cc.
- A typical diffuse ISM cloud: 1 particle per cc.
- This includes gas and dust. No liquid (why not?)
- Mutual gravitational force brings them closer together → denser

Gas remains transparent, but dust (grains) blocks background luminous sources.

- These "dark clouds" are dense ($10^4/cm^3$) and cold (a few K or –260°C) ; seen silhouetted

Barnard 72 in Ophiuchus

http://www.robgendlerastropics.com/B72JMM.jpg

Star Shadows Remote Observatory

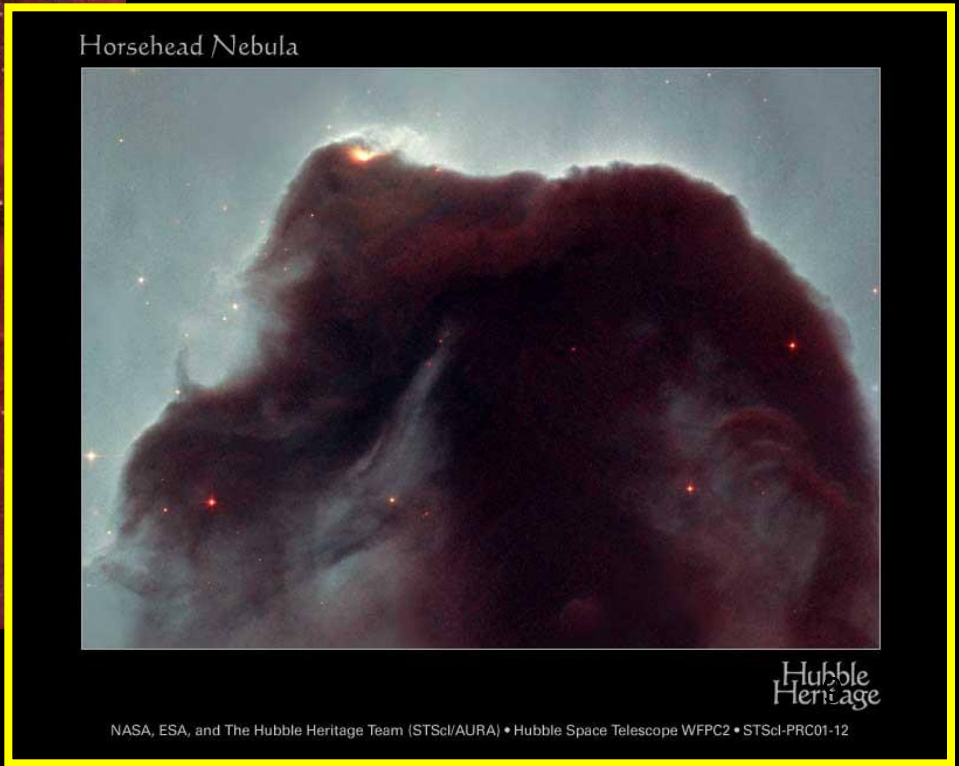

(Bok) Globules silhouetted against emission nebulosity

A dark cloud core seen against a star field

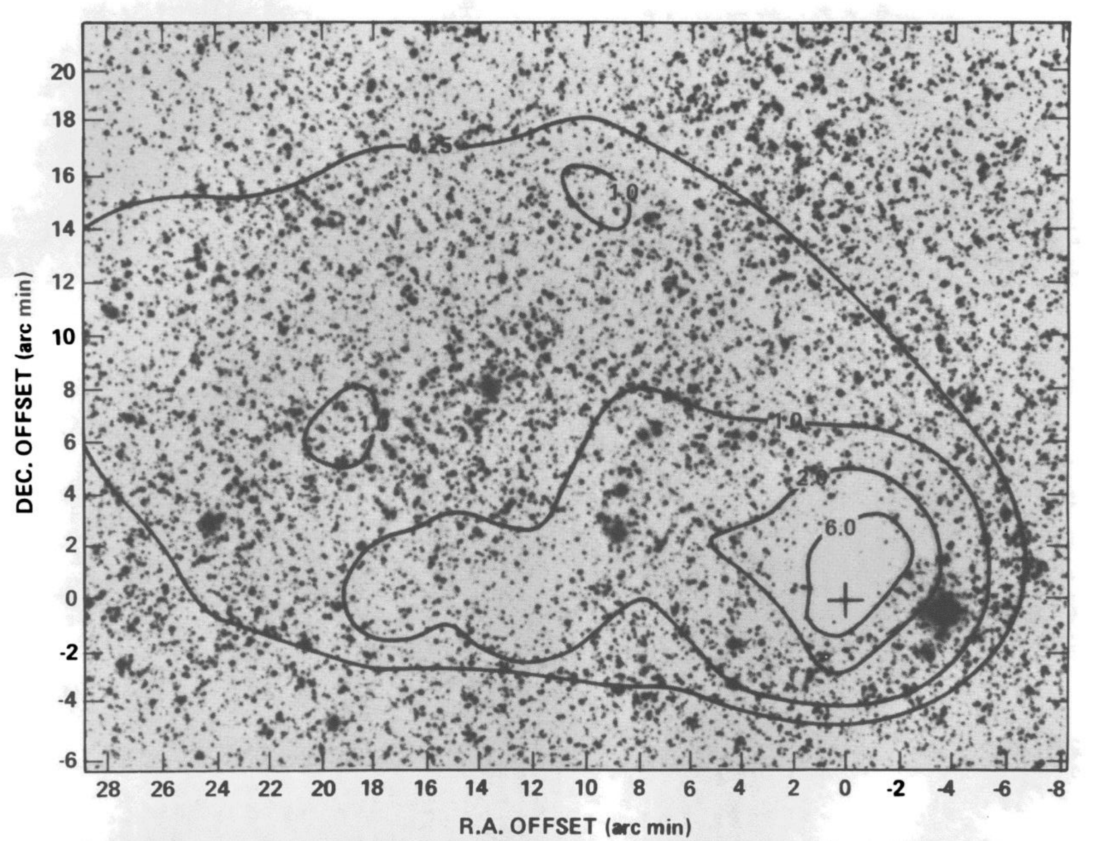

FIG. 1.—The optical image of B335 on the blue POSS print. Superposed on it are the $N(H_2)$ contours in units of 10^{21} cm^{-2}; the derivation of $N(H_2)$ is discussed in § III*a*(i). In the SW corner there is a highly obscured core region ~2′ × 3′ surrounded by an extended envelope covering ~34′ × 20′.

Frerking et al. (1987)

Optical Composite | Optical/IR composite

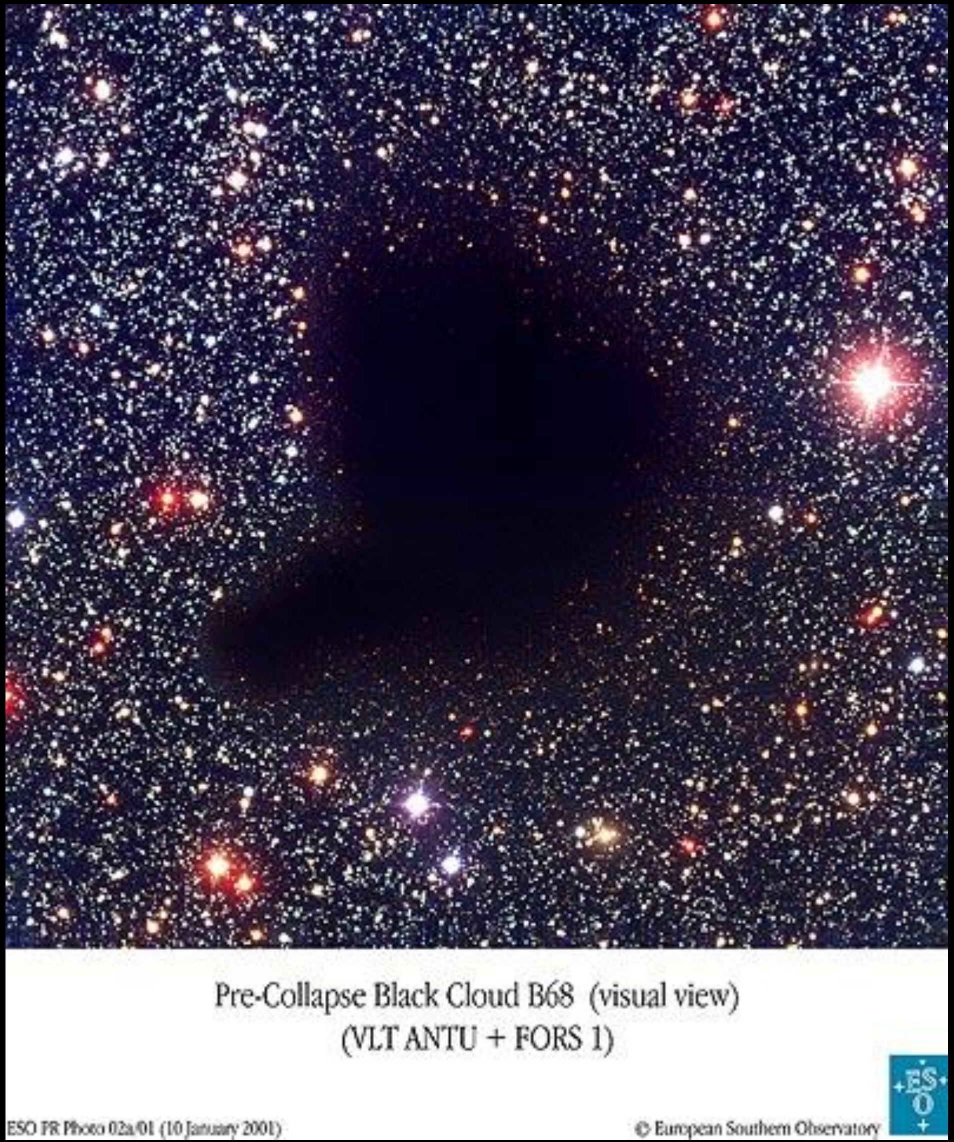

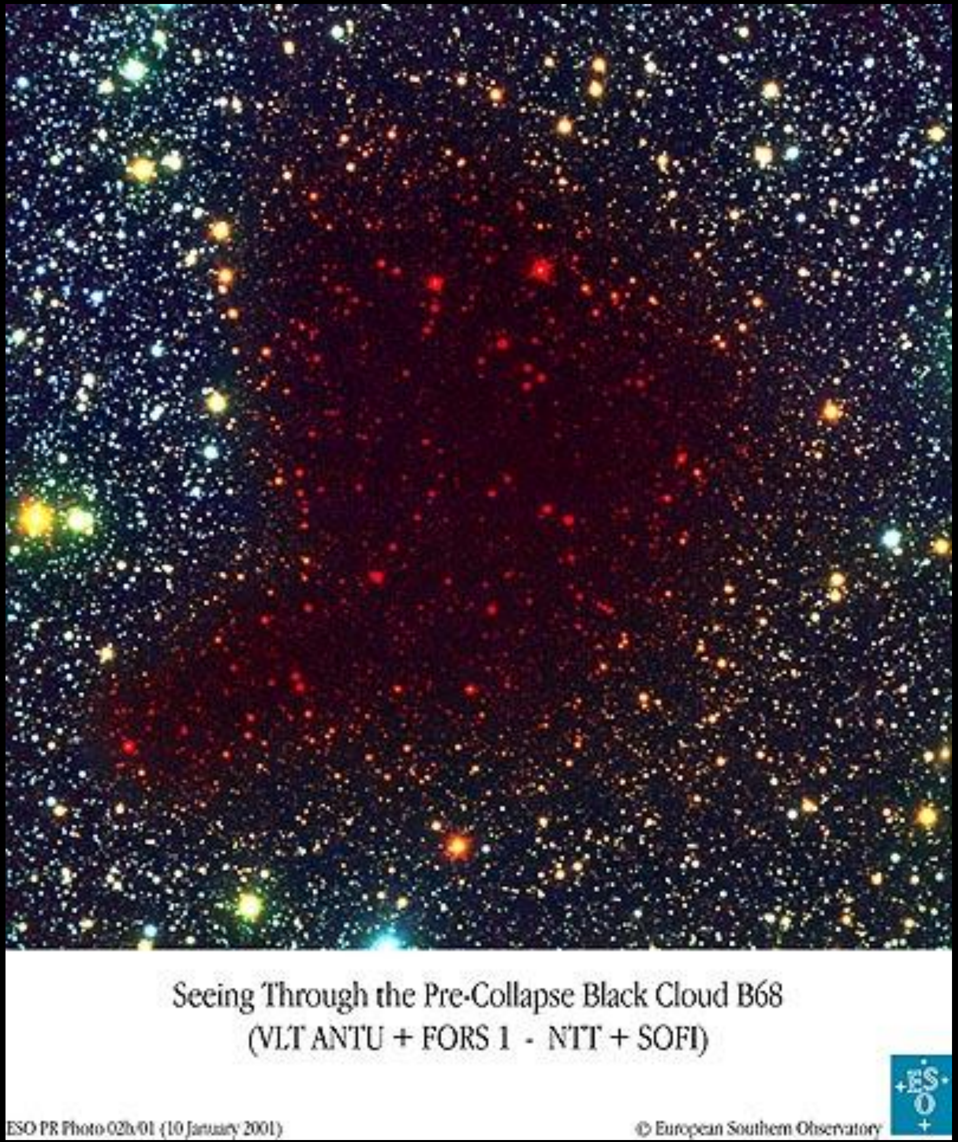

ρ Ophiuchi cloud complex

Visible

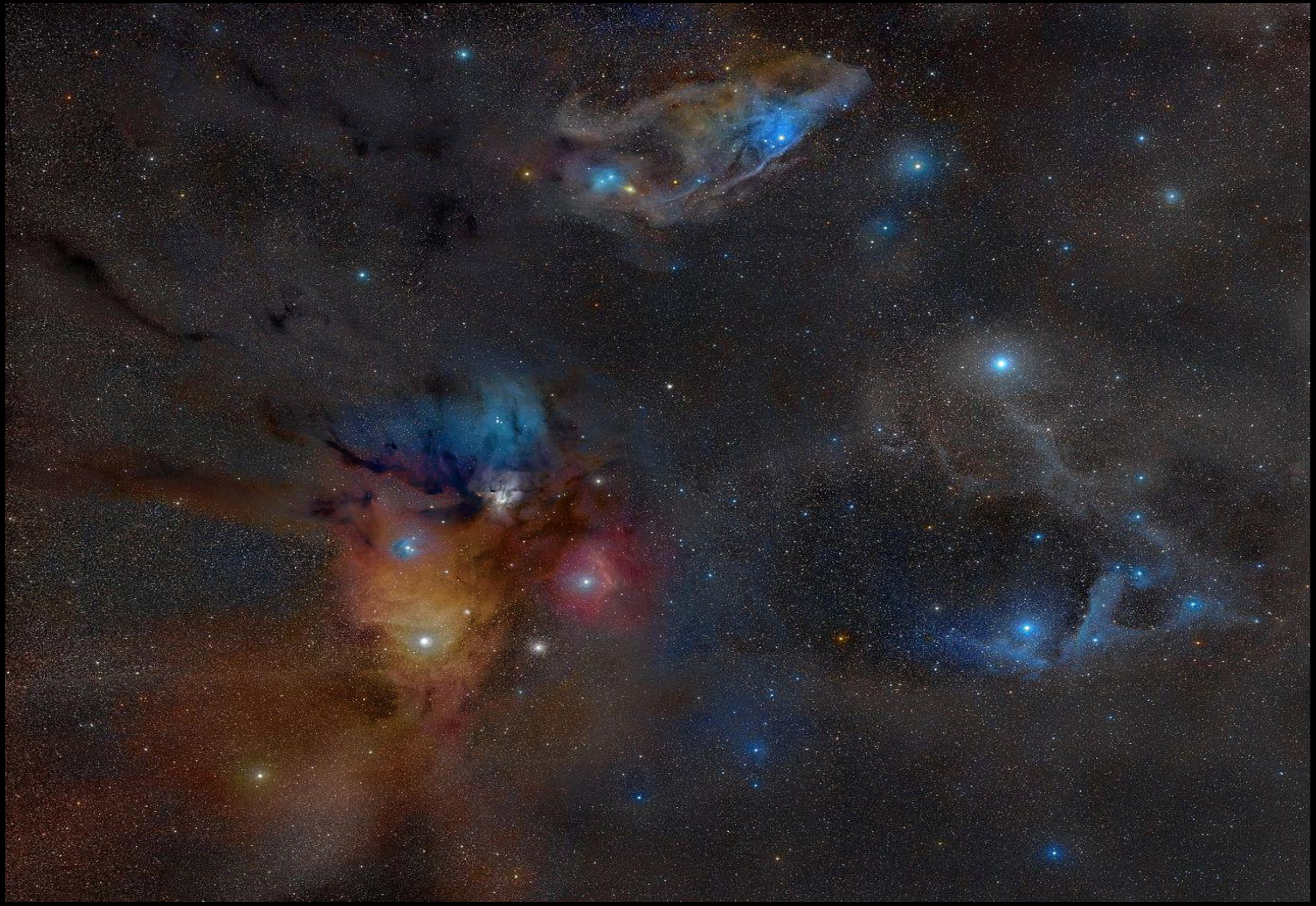

Infrared

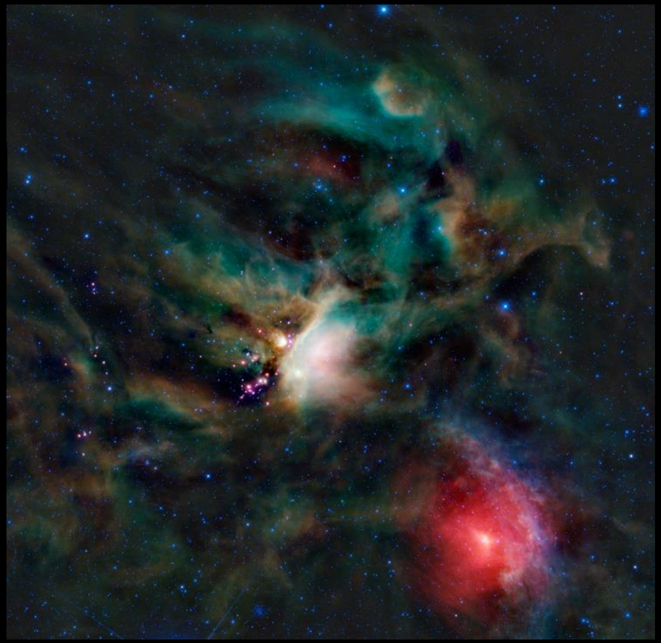

WISE

https://en.wikipedia.org/wiki/Rho_Ophiuchi#/media/File:Rho_Ophiucus_Widefield.jpg

Interstellar Medium (ISM)

- ISM very sparse --- gas and dust (solid)

  [star-star distance] / [stellar diameter]
  $\sim 1\ \mathrm{pc}/10^{11}\ \mathrm{cm} \sim 3 \times 10^{7}: 1$; in terms of volume (space) $\sim 10^{22}$

  Parsec (pc): a unit of distance, about 3.26 ly or 3×10^{16} m

  (What about galaxies?)

  ➔ Stars truly tiny compared to space in between

- Mass: [gas + dust] / total ~ 10%, but density very low

  (What is the number density of air in this room?
  Of the solar atmosphere?)

- **Milky Way galaxy**: stars/planets, gas, dust, radiation, magnetic fields, cosmic rays (i.e., charged particles)
- ISM mass = 10% of the total visible matter of the MW galaxy
- Of the ISM: 99% mass in gas, 1% in dust

"gas-to-dust ratio" ≈ 100 *nominally, but …*

- Of the gas: 90% H; 10% He
- Hydrogen: mainly H I (atomic), H II (ionized), and H_2 (molecular)

H I: H^0, neutral; H II: H^+, singly ionized; e.g., He III, Fe XXVI

- Studies of ISM ---
  - Beginning of evolution of baryonic matter "recombination"
  - Stars form out of ISM
  - Important ingredient of a galaxy

Table 1.2 Mass of H II, H I, and H_2 in the Milky Way ($R < 20$ kpc)

Phase	$M(10^9\, M_\odot)$	fraction	Note
Total H II (not including He)	1.12	23%	see Chapter 11
Total H I (not including He)	2.9	60%	see Chapter 29
Total H_2 (not including He)	0.84	17%	see Chapter 32
Total H II, H I and H_2 (not including He)	4.9		
Total gas (including He)	6.7		

Material Constituents of the ISM

Name	T (K)	n (cm^{-3})	Properties
Hot, intercloud and "coronal" gas	10^6	10^{-4}	
Warm intercloud gas	10^4	10^{-1}	
Diffuse cloud (H I)	10^2	$10^{-1} - 1$	Mostly H I; $n_e/n_0 \approx 10^{-4}$
H II regions	10^4	>10	
Dark Molecular Clouds	10	$> 10^3$	Mostly H_2 and dust
Supernova Remnants	$10^4 \sim 10^7$	>1	
Planetary Nebulae			

Energy Density in the Local ISM

Component	u (eV/cm^{-3})	Properties
Cosmic microwave background	0.265	$T_{\rm CMB} = 2.725$ K
FIR radiation from dust	0.31	
Starlight	0.54	$h\nu < 13.6$ eV
Thermal kinetic energy	0.49	
Turbulent kinetic energy	0.22	$\langle n_H \rangle = 1$ cm^{-3}
Magnetic field	0.89	$B^2/8\pi; \langle B \rangle = \mu$G
Cosmic rays	1.39	

There seems to be equipartition between these energies. Why?

Draine

McKee & Ostriker (1977)

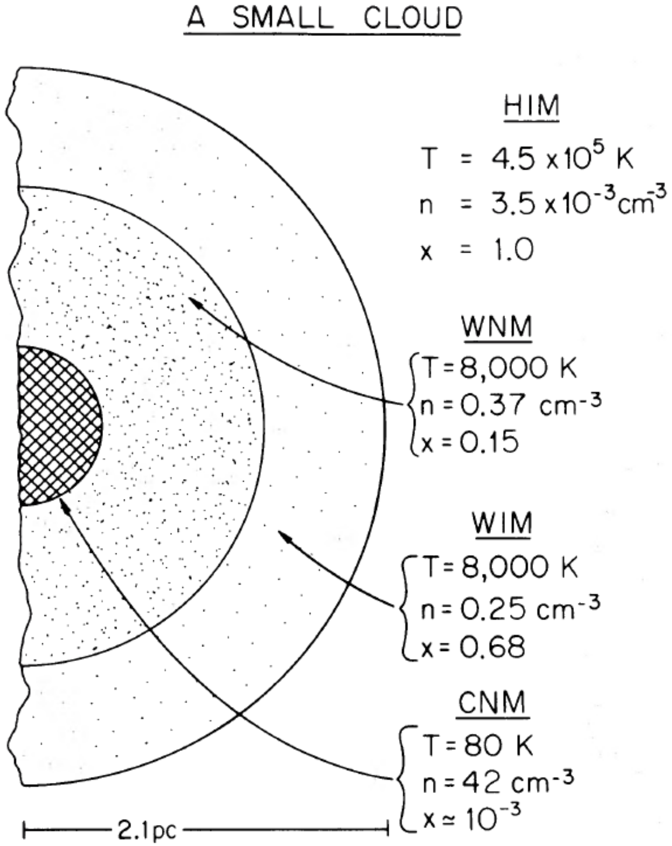

FIG. 1

Zooming out from Fig. 1

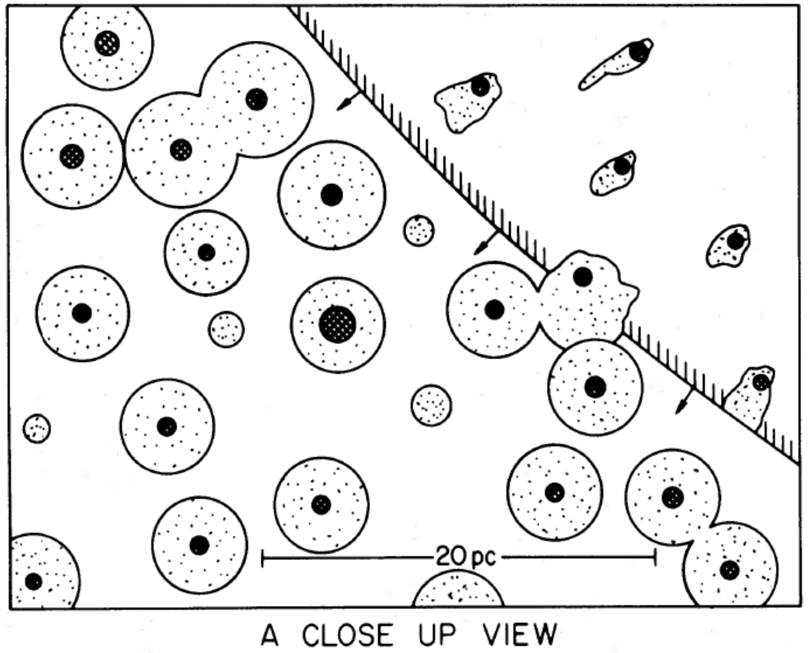

FIG. 2

Zooming out further from Fig. 2

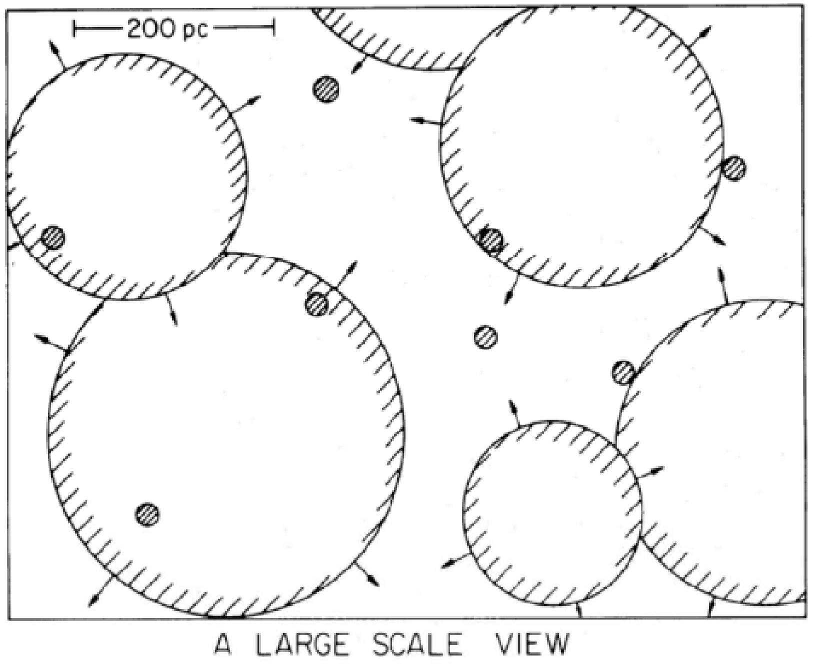

600×800 pc

FIG. 1.—Cross section of a characteristic small cloud. The crosshatched region shows the cold core, which gives the usual optical absorption lines. Next is the warm neutral medium (WNM) with ionization produced by soft X-ray background. The outer layer (WIM) is gas largely ionized by stellar UV background. Typical values of hydrogen density *n*, temperature *T*, and ionization $x = n_e/n$ are shown for each component, except that a higher than average value of the soft X-ray flux has been assumed in order to produce a significant amount of WNM at this pressure.

FIG. 2.—Small-scale structure of the interstellar medium. A cross section of a representative region 30 pc × 40 pc in extent is shown, with the area of the features being approximately proportional to their filling factors. A supernova blast wave is expanding into the region from the upper right. The radius of the neutral cores of the clouds (represented by crosshatching) ranges from about 0.4 to 1 pc in this small region; all the clouds with cores have warm envelopes (*dotted regions*) of radius $a_w \sim 2.1$ pc. A few clouds are too small to have cores. The envelopes of clouds inside the SNR are compressed and distorted.

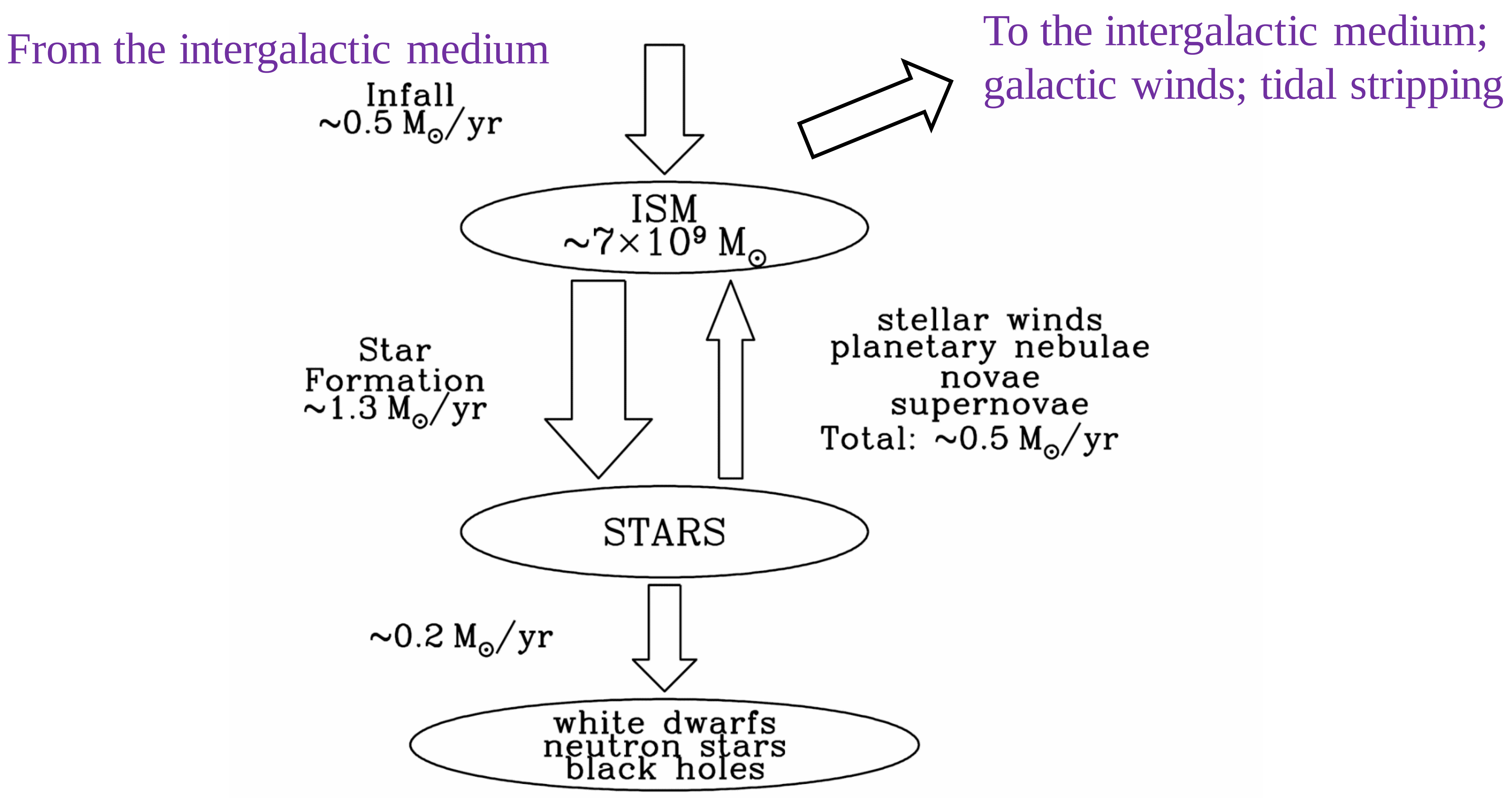

Draine

Flow of baryons in the Milky Way galaxy

The ISM is far from thermodynamic equilibrium.

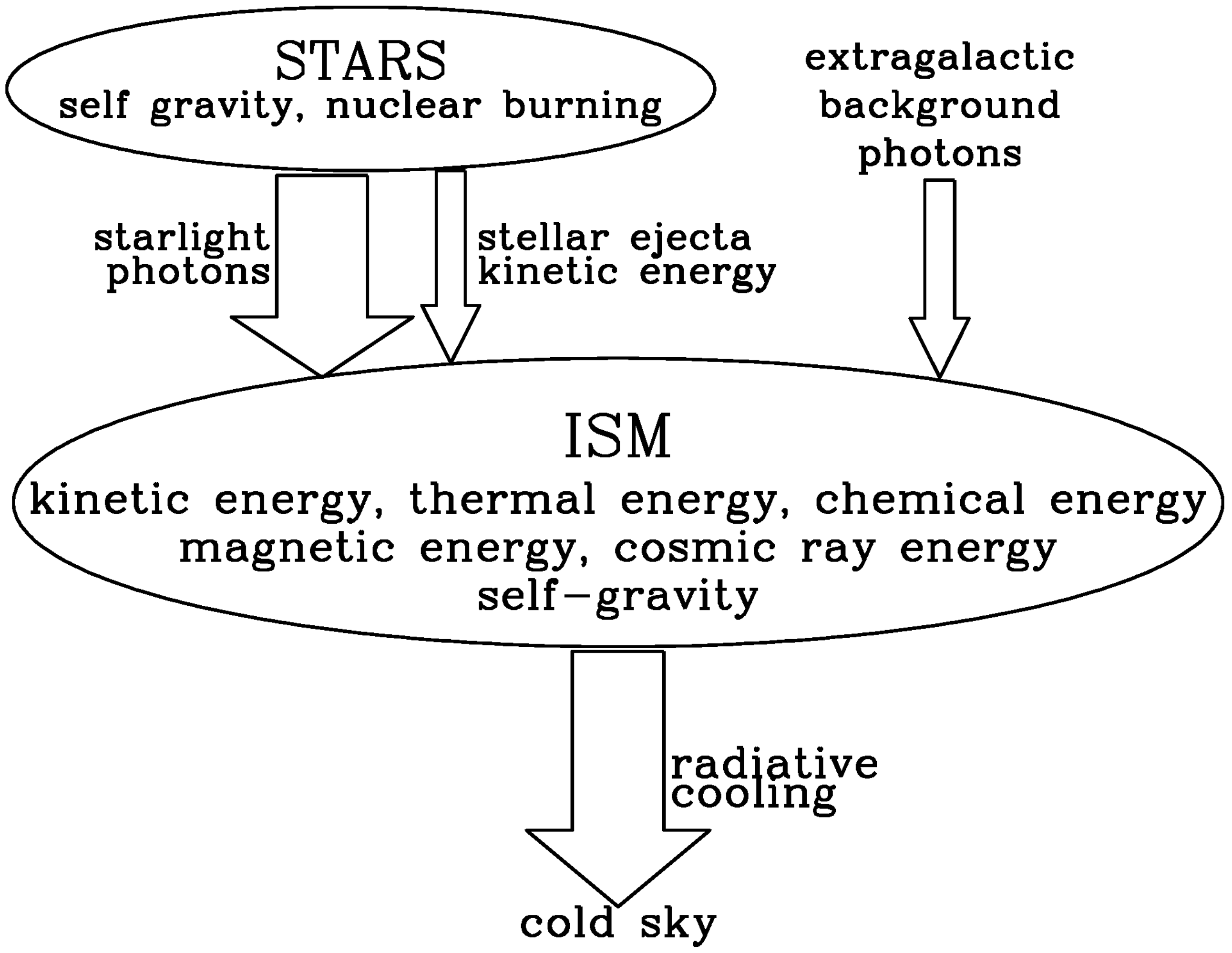

Draine

Flow of energy in the Milky Way

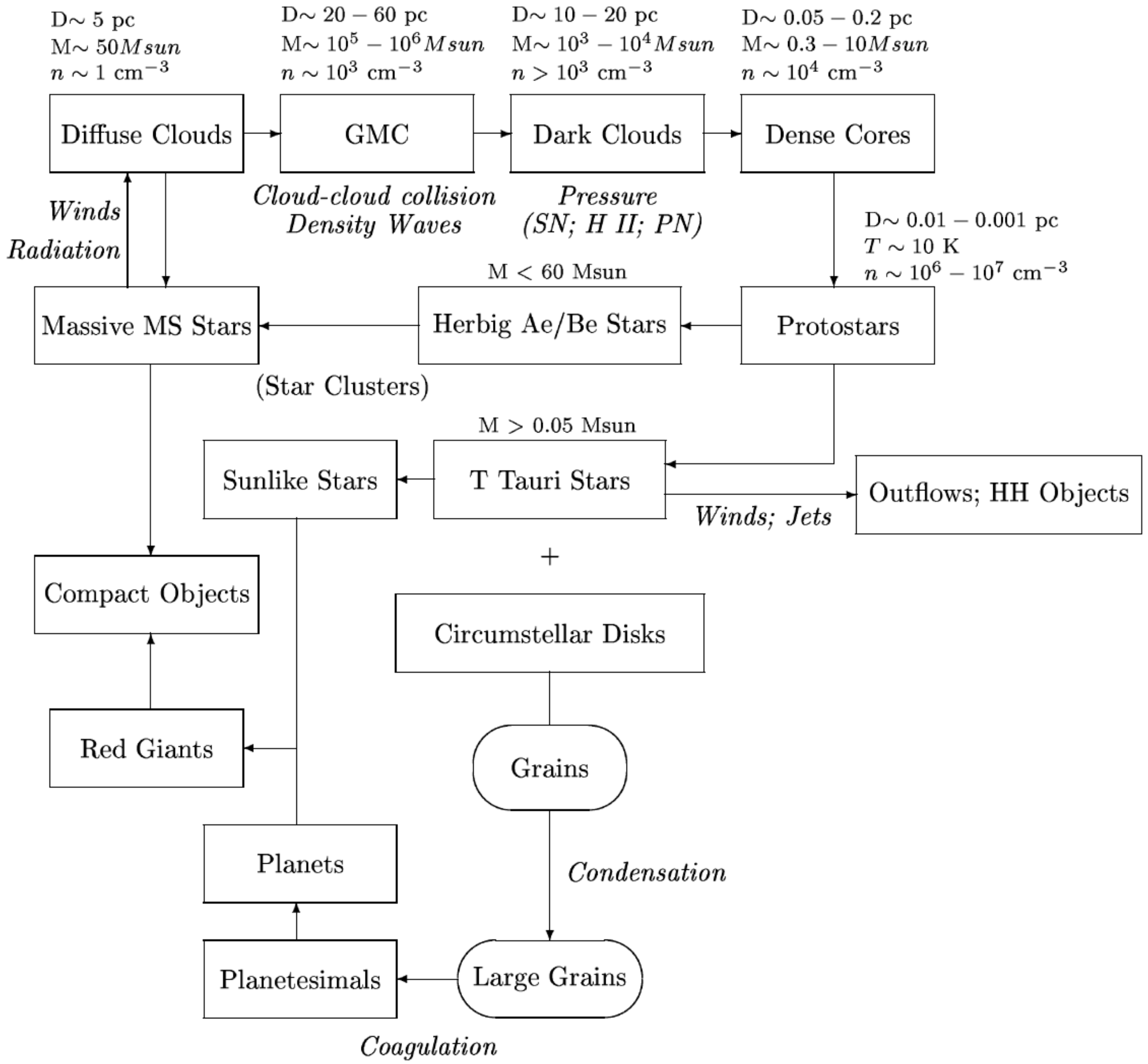

Galactic Ecology

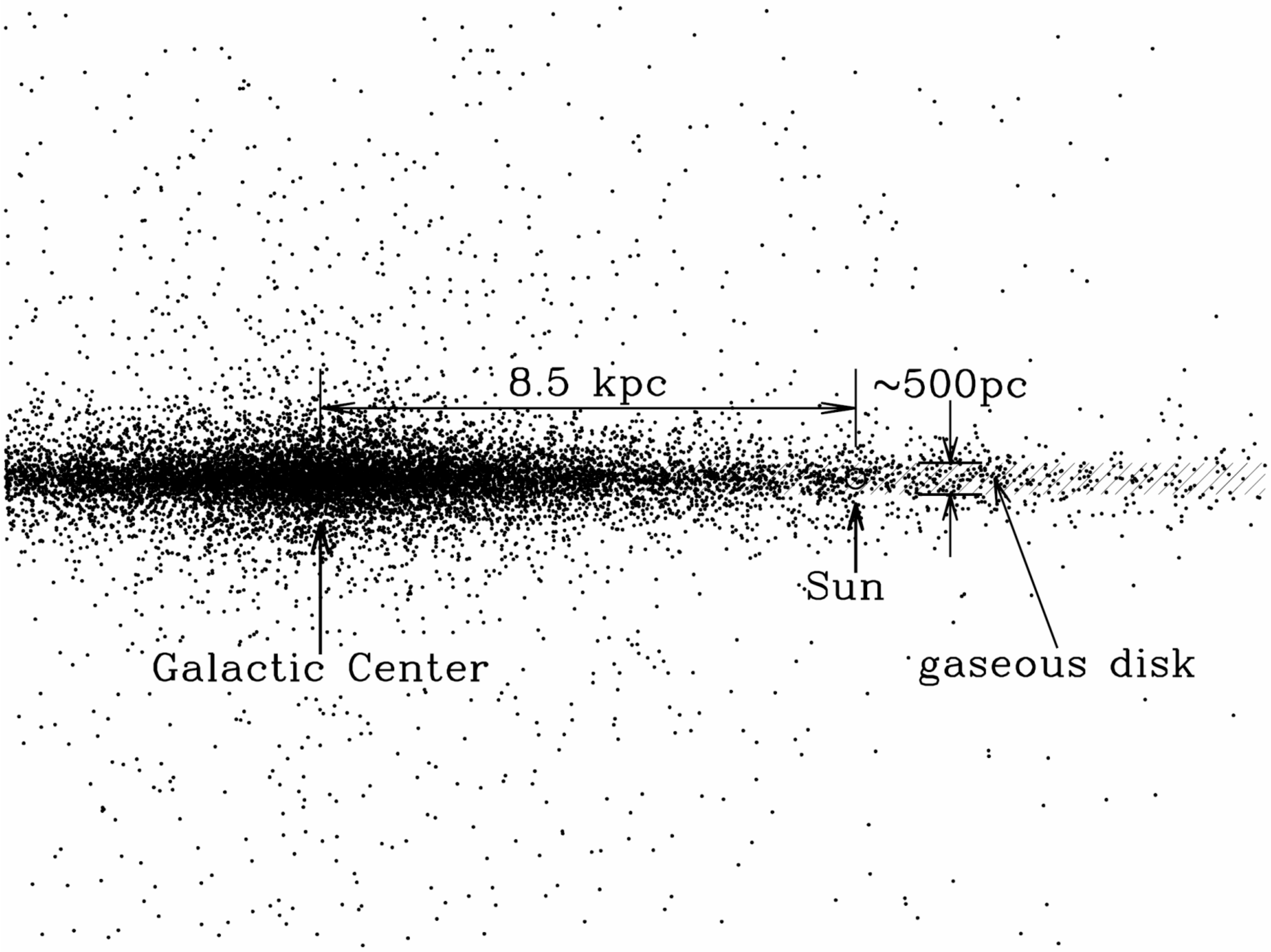

Draine

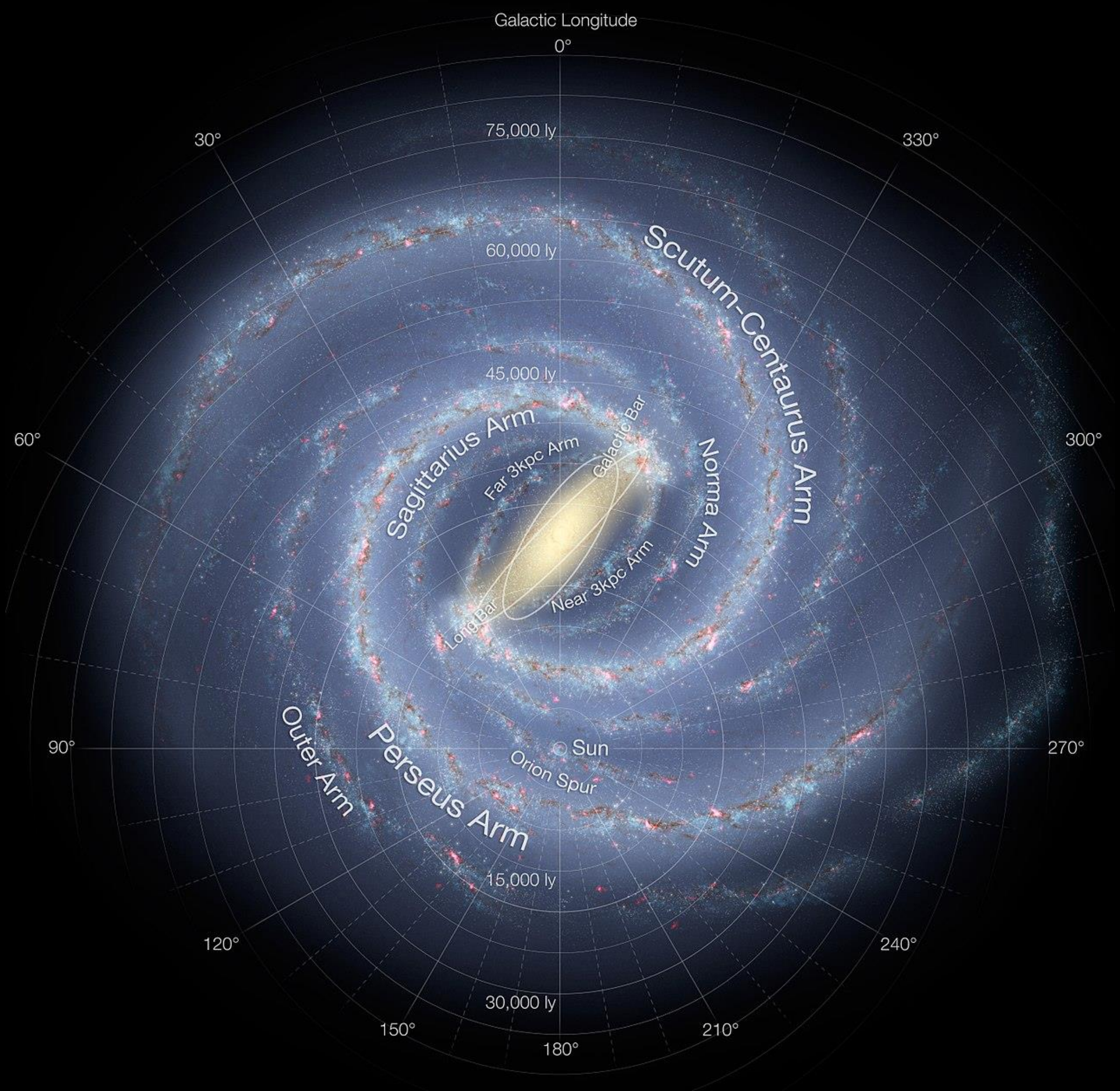
Galactic Longitude
0°
30°
330°
60°
300°
90°
270°
120°
240°
150°
210°
180°
75,000 ly
60,000 ly
45,000 ly
30,000 ly
15,000 ly
Scutum-Centaurus Arm
Sagittarius Arm
Far 3kpc Arm
Galactic Bar
Norma Arm
Near 3kpc Arm
Long Bar
Outer Arm
Perseus Arm
Sun
Orion Spur

The Local Bubble A cavity of sparse, hot gas in the Orion Arm; ~100 pc across; $n \sim 0.05\ \mathrm{cm}^{-3} \sim 0.1$ of ISM; likely by SN explosions 10--30 Myr ago?

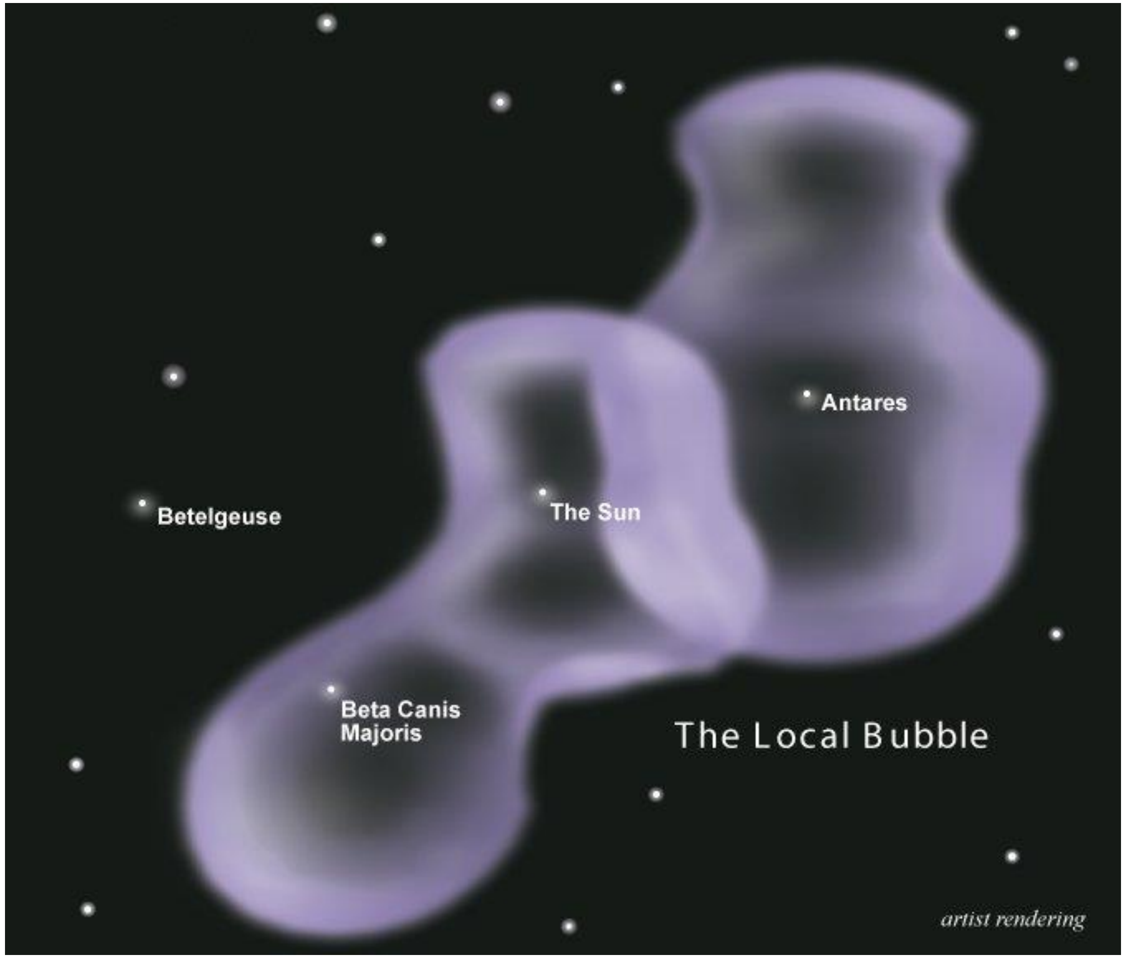

Where is the supernova (remnant)?
Check out the Orion-Eridanus Superbubble

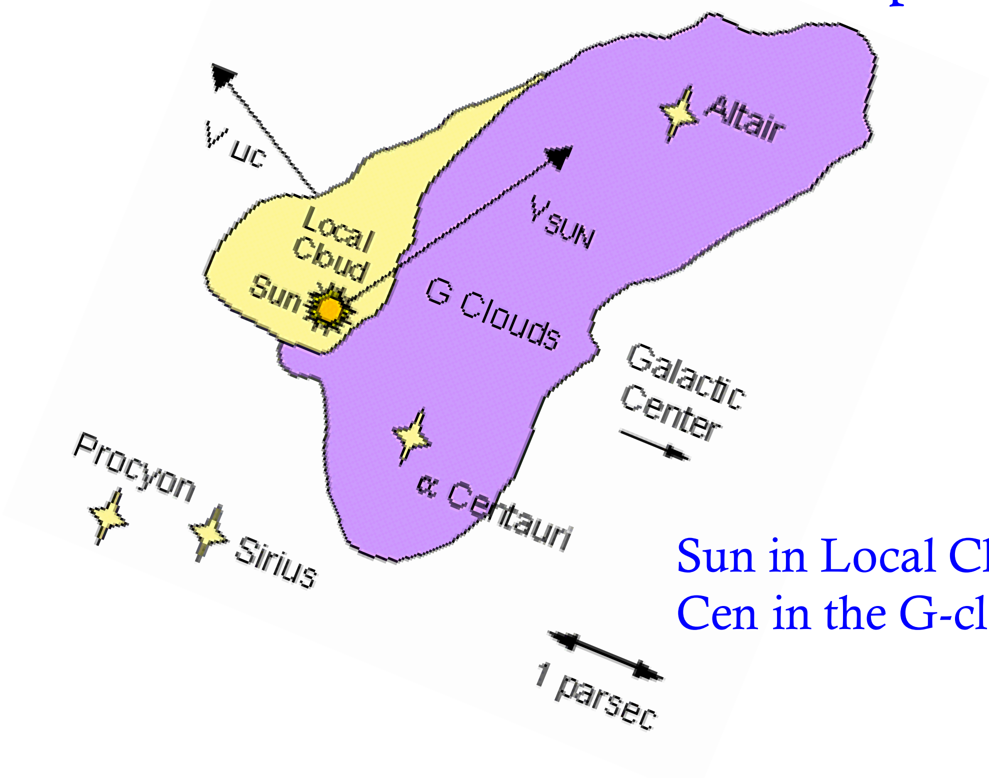

Sun in Local Cloud; Alpha Cen in the G-cloud complex

https://en.wikipedia.org/wiki/Local_Bubble

The **Gould Belt**, a (partial) ring in the sky, ~1 kpc across, centered on a point 100 pc from the Sun and tilted about 20 deg to the Galactic plane, containing star-forming molecular clouds and OB stars = local spiral arm

Origin unknown (dark matter induced star formation?)

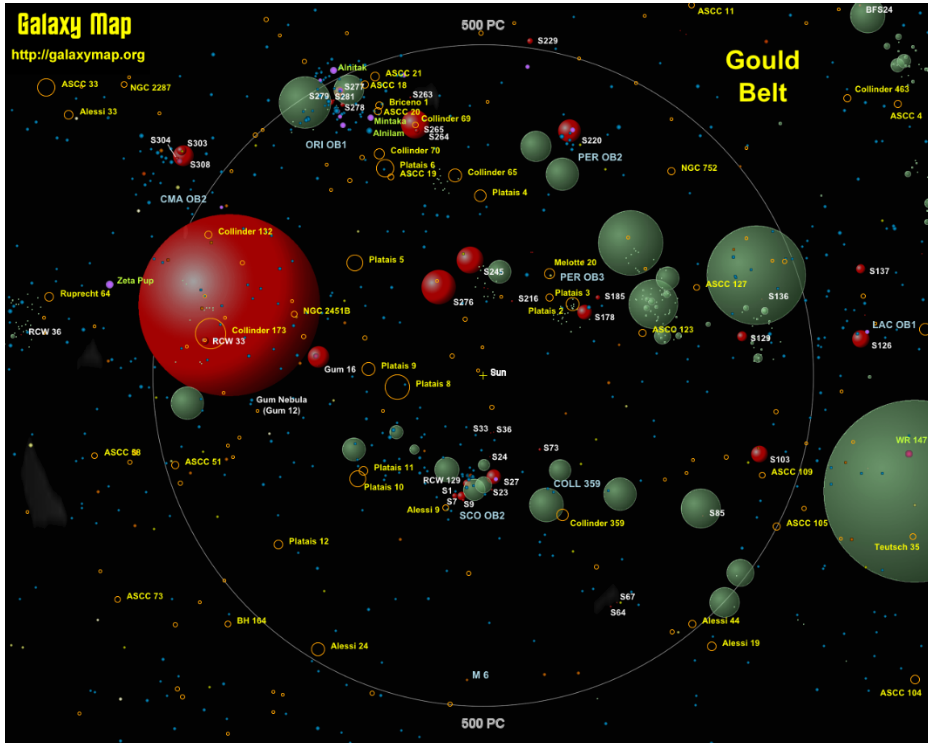

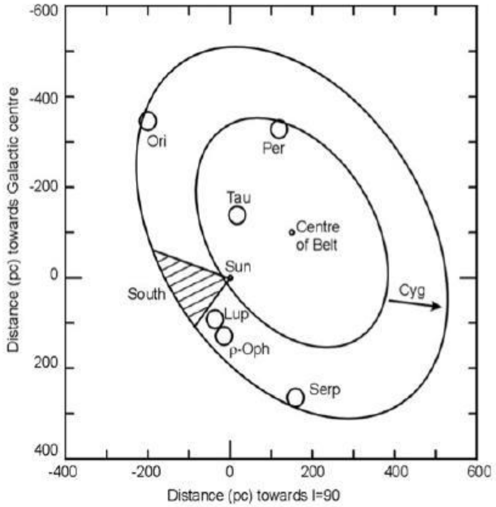

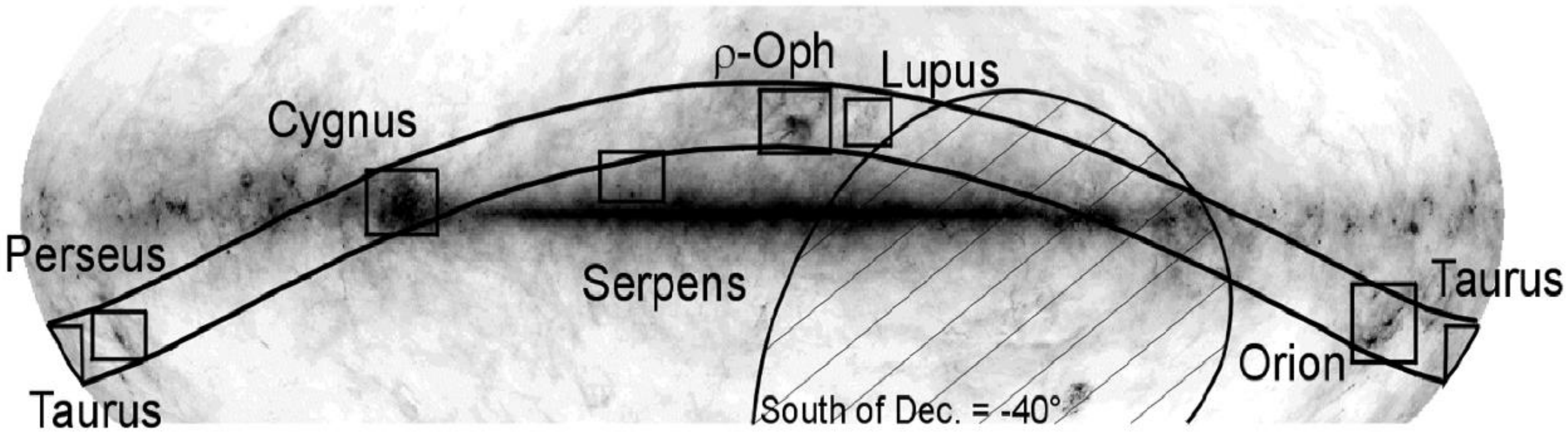

http://www.jach.hawaii.edu/JCMT/surveys/gb/

Gould's Belt superimposed on to an IRAS 100 micron emission map

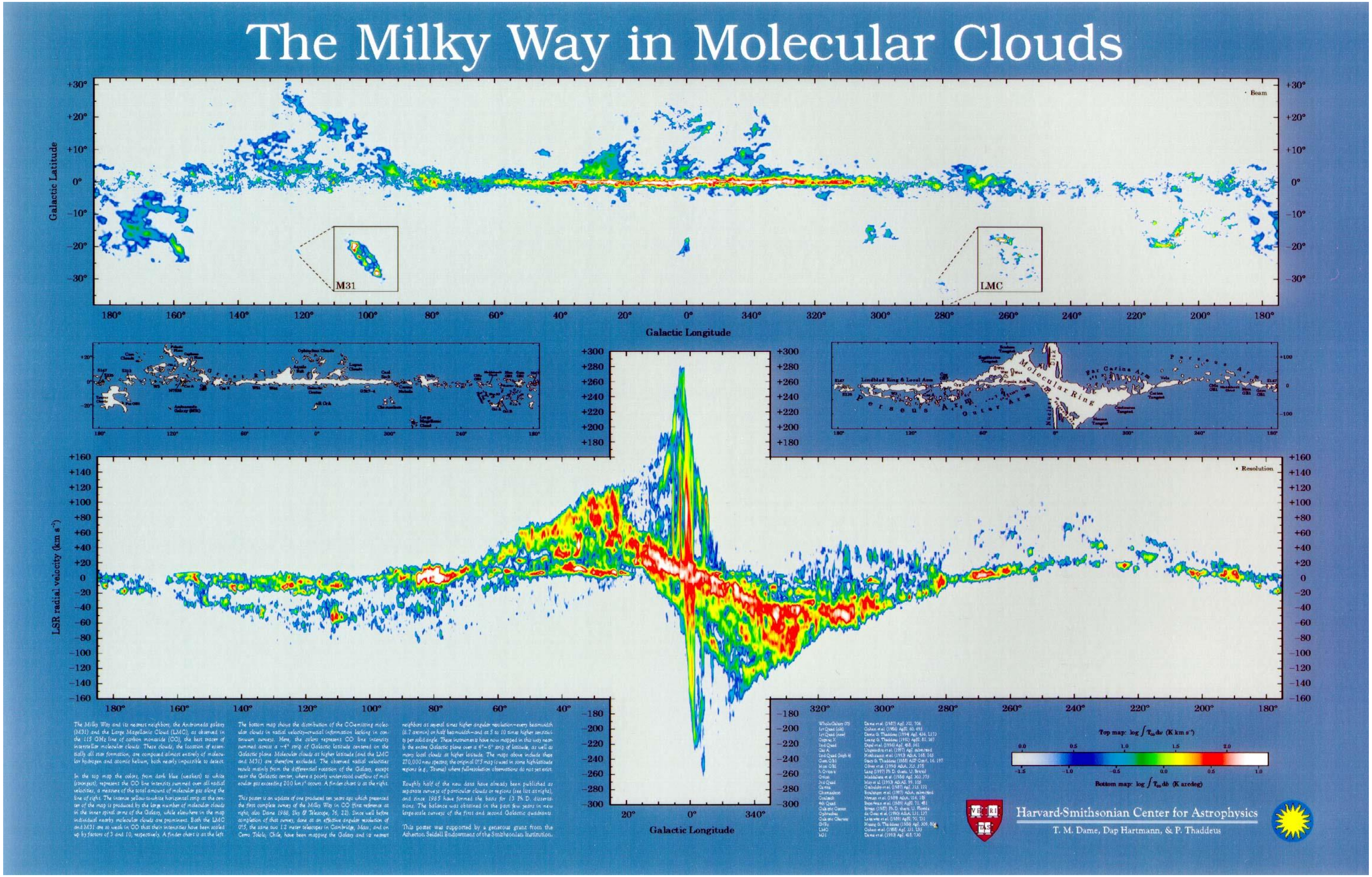
The Milky Way in Molecular Clouds
Beam
Galactic Latitude
+30° +20° +10° 0° −10° −20° −30°
M31
LMC
180° 160° 140° 120° 100° 80° 60° 40° 20° 0° 340° 320° 300° 280° 260° 240° 220° 200° 180°
Galactic Longitude
Resolution
LSR radial velocity (km s⁻¹)
+300 +280 +260 +240 +220 +200 +180 +160 +140 +120 +100 +80 +60 +40 +20 0 −20 −40 −60 −80 −100 −120 −140 −160 −180 −200 −220 −240 −260 −280 −300
Molecular Ring
Perseus Arm
Outer Arm
Far Carina Arm
Local Arm
The Milky Way and its nearest neighbors, the Andromeda galaxy (M31) and the Large Magellanic Cloud (LMC), as observed in the 115 GHz line of carbon monoxide (CO), the best tracer of interstellar molecular clouds. These clouds, the location of essentially all star formation, are composed almost entirely of molecular hydrogen and atomic helium, both nearly impossible to detect.
In the top map the colors, from dark blue (weakest) to white (strongest), represent the CO line intensity summed over all radial velocities, a measure of the total amount of molecular gas along the line of sight. The intense yellow-to-white horizontal strip at the center of the map is produced by the large number of molecular clouds in the inner spiral arms of the Galaxy, while elsewhere in the map individual nearby molecular clouds are prominent. Both the LMC and M31 are so weak in CO that their intensities have been scaled up by factors of 3 and 10, respectively. A finder chart is at the left.
The bottom map shows the distribution of the CO-emitting molecular clouds in radial velocity—crucial information lacking in continuum surveys. Here, the colors represent CO line intensity summed across a ~4° strip of Galactic latitude centered on the Galactic plane. Molecular clouds at higher latitude (and the LMC and M31) are therefore excluded. The observed radial velocities result mainly from the differential rotation of the Galaxy, except near the Galactic center, where a poorly understood outflow of molecular gas exceeding 200 km s⁻¹ occurs. A finder chart is at the right.
This poster is an update of one produced ten years ago which presented the first complete survey of the Milky Way in CO (first reference at right; also Dame 1988, Sky & Telescope, 76, 22). Since well before completion of that survey, done at an effective angular resolution of 0°.5, the same two 1.2 meter telescopes in Cambridge, Mass., and on Cerro Tololo, Chile, have been mapping the Galaxy and its nearest neighbors at several times higher angular resolution—every beamwidth (8.7 arcmin) or half beamwidth—and at 5 to 10 times higher sensitivity per solid angle. These instruments have now mapped in this way nearly the entire Galactic plane over a 4°–6° strip of latitude, as well as many local clouds at higher latitude. The maps above include these 270,000 new spectra; the original 0°.5 map is used in some high-latitude regions (e.g., Taurus) where full-resolution observations do not yet exist.
Roughly half of the new data have already been published as separate surveys of particular clouds or regions (see list at right), and since 1985 have formed the basis for 13 Ph.D. dissertations. The balance was obtained in the past few years in new large-scale surveys of the first and second Galactic quadrants.
This poster was supported by a generous grant from the Atherton Seidell Endowment of the Smithsonian Institution.
Top map: log ∫ T_mb dv (K km s⁻¹)
Bottom map: log ∫ T_mb db (K arcdeg)
Harvard-Smithsonian Center for Astrophysics
T. M. Dame, Dap Hartmann, & P. Thaddeus

Intergalactic medium

Warm to hot (10^5 to 10^7 K)
sparse ($1/m^3$)

Intracluster medium

Hot (10^7 to 10^8 K)
sparse ($1000/m^3$)

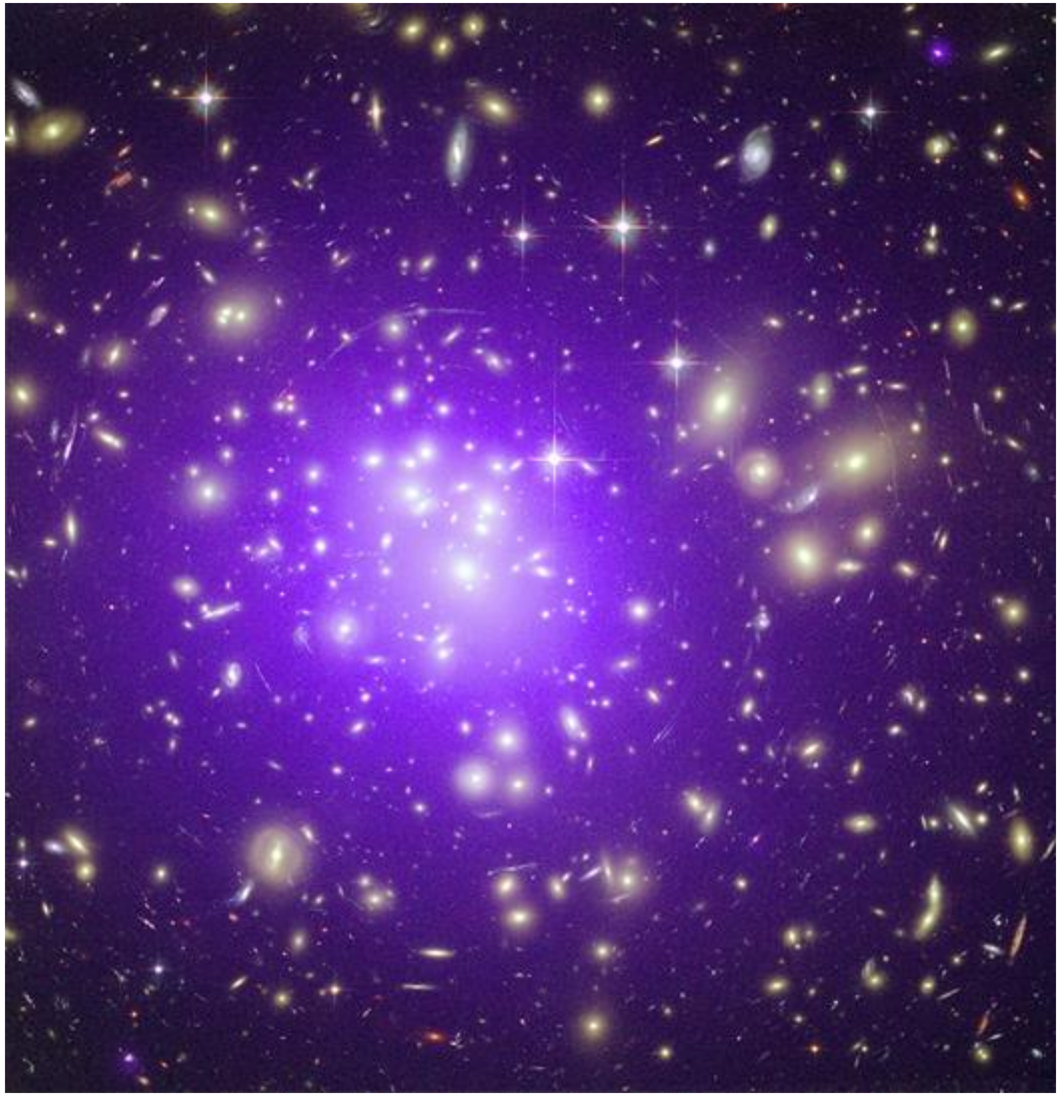

Chandra image (100 MK) of Abell1689

Radiation and Matter

Electronic transitions Matter ↔ matter; matter ↔ photons

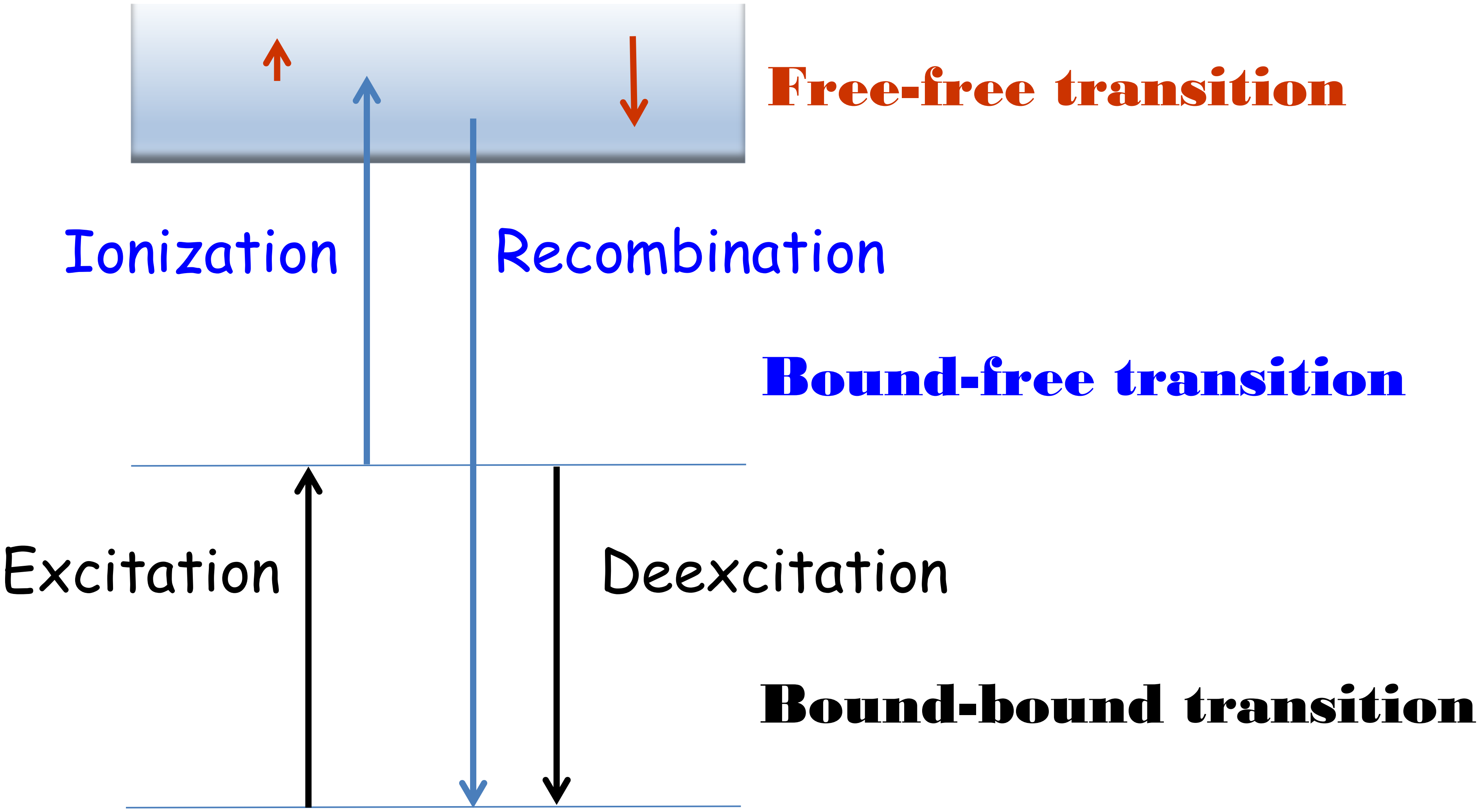

Rotational transition, vibrational transition, ...

Line Formation: Kirchhoff's Laws of Spectroscopy

cf. circuit/current law

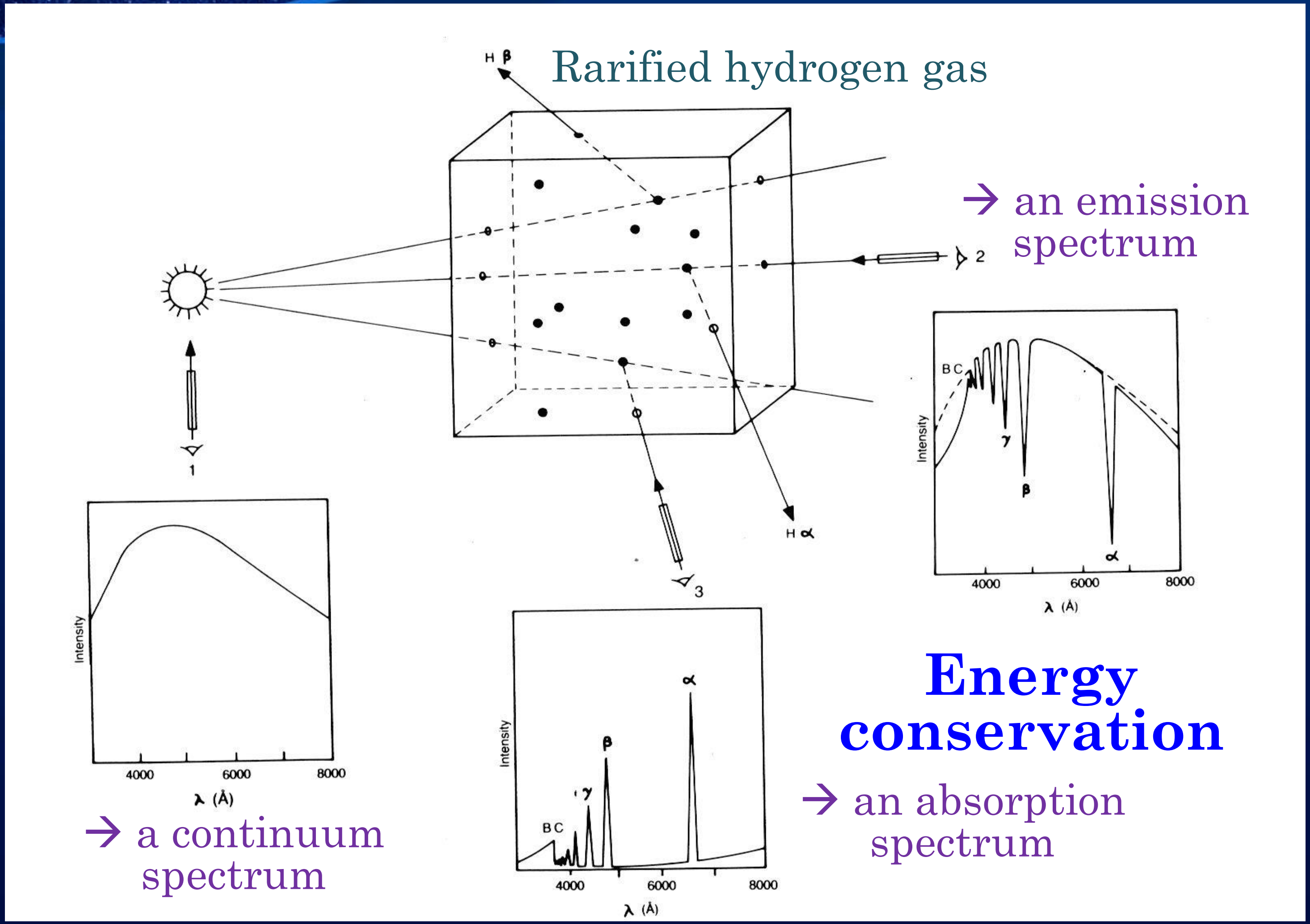

Kaler

Interstellar Clouds

- **Emission nebula**
  Gas itself emits light
  (excited by starlight, collision, etc.)
  e.g., Balmer alpha → reddish

- **Reflection nebula**
  Gas reflects/scatters light
  → bluish

- **Dark nebula**
  Dust blocks background light
  (stars, emission/reflection nebulae)
  → dark/black

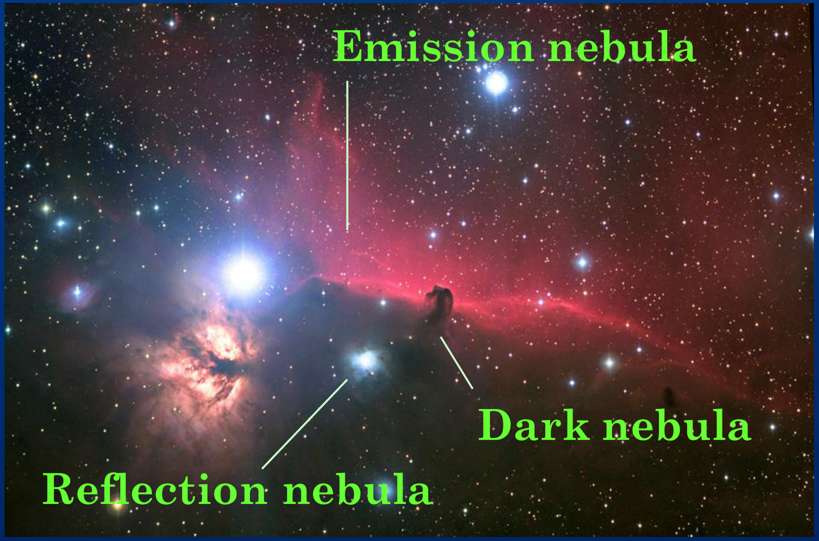

A photograph may be a false-color composite. How to display a radio or X-ray image?


Star Shadows Remote Observatory

- Electromagnetic (EM) radiation (from gamma rays to radio waves) + cosmic rays + neutrinos + gravitational waves …

Interactions between matter, between matter and energies/photons. We detect photons.

- Diagnosed by photometry, spectroscopy, polarization, etc.
  - **line** (absorption, emission) in a narrow range of frequency
    e.g., $h\nu +$ H(^{1}S) $\rightarrow$ H(^{2}P) ($h\nu$ =10.2 eV or λ=121.6 nm)
  - **continuum** (absorption, emission) over a continuous range of ν
    e.g., $h\nu$+ H(^{1}S) → $H^+ + e^-$ ($h\nu \geq$ 13.6 eV or $\lambda \leq$91.2 nm)

Spectrum of a star

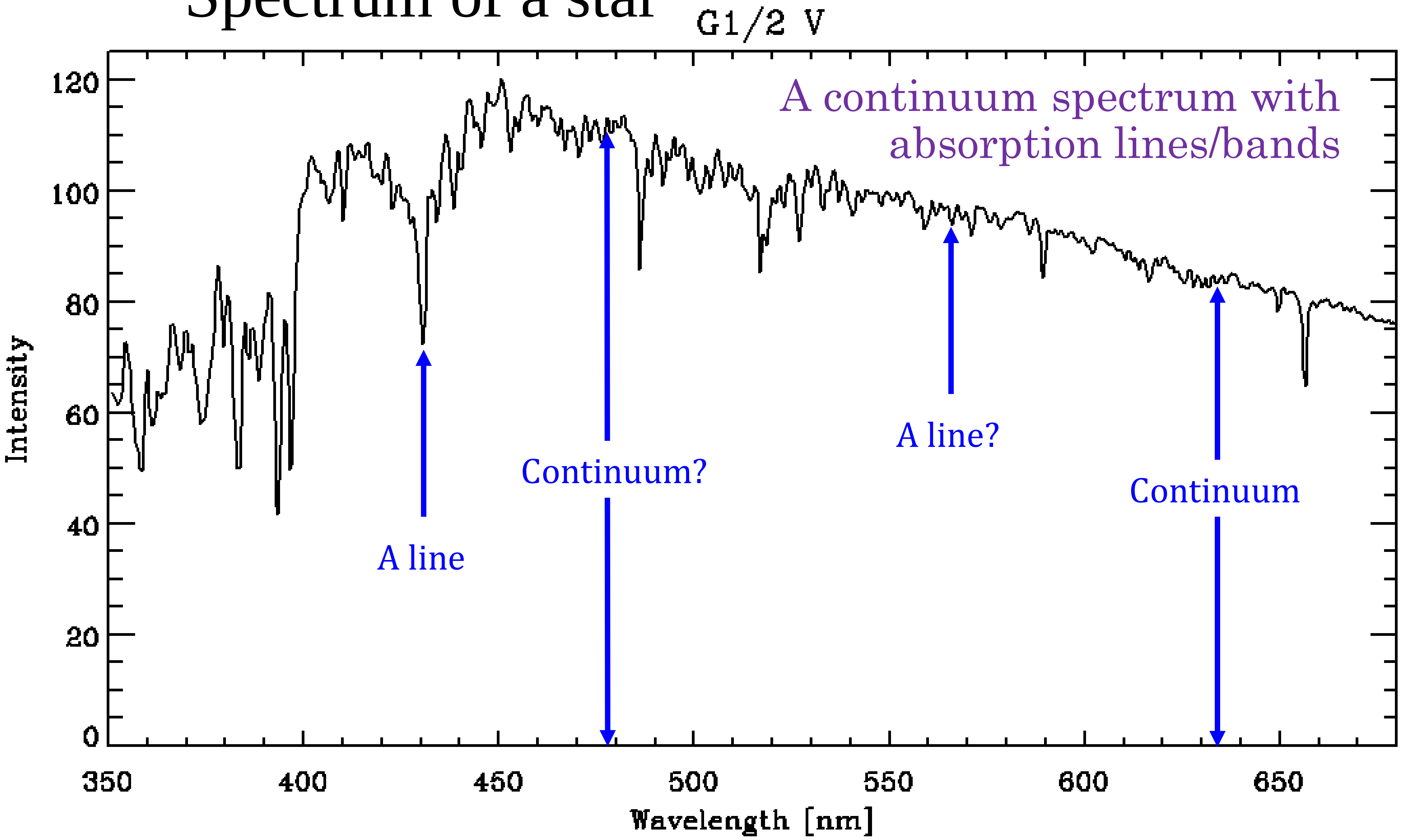

A weak continuum with prominent emission lines

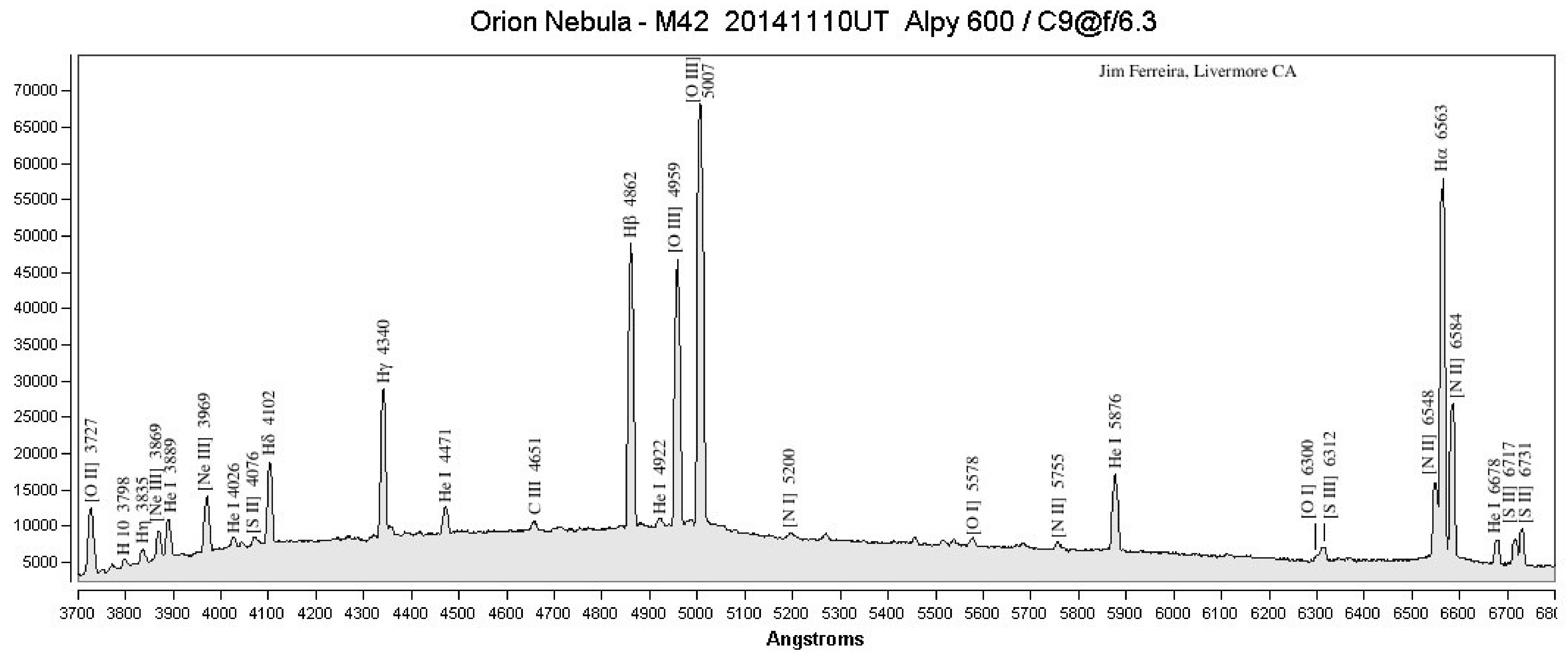

- **Photometry**

  measurement of brightness of radiation (of a source, or a position in sky)

  Astronomers use "magnitude" ↔ flux density

  At the V band (λ_{eff} =550 nm; $\Delta\lambda$ =86 nm), $F_{\nu}^{\text{v}=0} = 3.64 \times 10^{-23}$ [W m^{-2} Hz^{-1}]

  $F_{\lambda}^{\text{v}=0} = 3.61 \times 10^{-11}$ [W m^{-2} nm^{-1}]; $N_{\lambda} = 1000$ [photons s^{-1} cm^{-2} Å^{-1}]

- **Spectroscopy**

  measurements of brightness distribution with wavelength or frequency

Spectrophotometry; Integral Field Unit (IFU); IF Spectrograph

- **Polarimetry**

  measurements of the polarization level (polarized intensity/total intensity) and polarization angle

Observations of the ISM

- Difficult: typical temps either too **low** or too **high**, so observable usually only outside visible wavelengths.

  Planck function (1901) to describe a blackbody radiation

$$B_\nu \, d\nu = \frac{2h\nu^3}{c^2} \frac{n_\nu^2}{e^{h\nu/k_B T} - 1} \, d\nu \; [\mathrm{erg\ s^{-1}\ cm^{-2}\ sr^{-1}\ Hz^{-1}}]$$

$$B_\lambda \, d\lambda = \frac{2hc^2}{\lambda^5} \frac{n_\nu^2}{e^{hc/\lambda k_B T} - 1} \, d\lambda \; [\mathrm{erg\ s^{-1}\ cm^{-2}\ sr^{-1}\ \text{Å}^{-1}}]$$

$\lambda_{\mathrm{max}} T \approx 2900\ [\mu\mathrm{m} \cdot \mathrm{K}]$ ... Wien's displacement law

Not possible until the second half of the 20th century (detector technology, from space, etc.)

Low ν High ν

Blackbody radiation (prescribed by the Planck function) is a continuum radiation.

$$B_\nu \, d\nu = \frac{2h\nu^3}{c^2} \frac{n_\nu^2}{e^{h\nu/k_B T} - 1} \, d\nu$$

$$\nu^3 \Longleftrightarrow e^{-\nu}$$

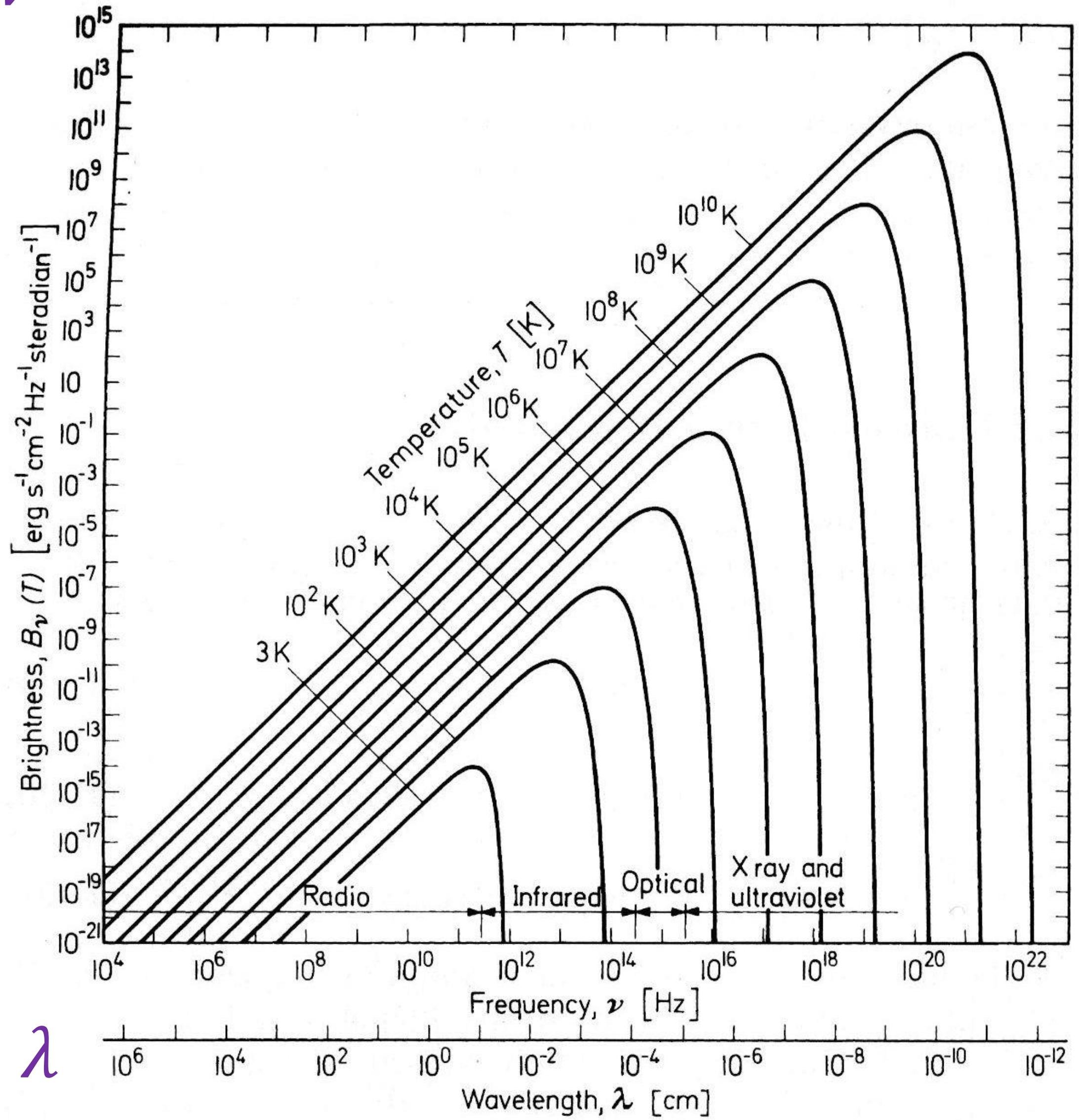

Short λ Long λ

Fig. 1.1. The brightness, $B_\nu(T)$, of a black-body radiator at frequency, ν, and temperature, T. The Planck function $B_\nu(T)$, is given by Eq. (1.119)

Lang

Spectra of hot stars

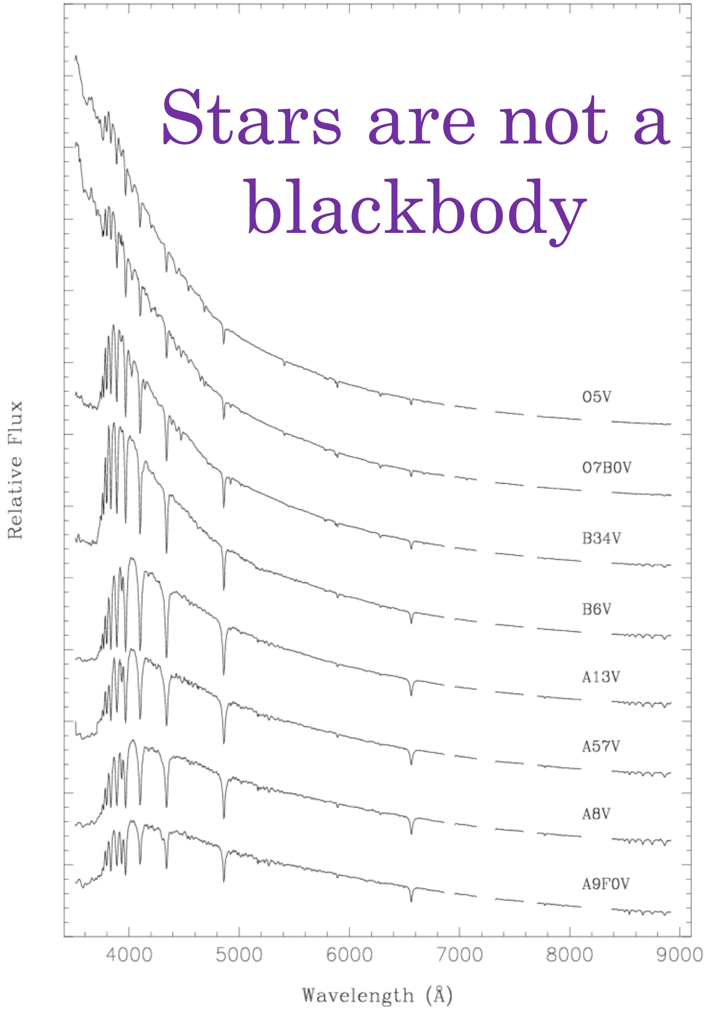

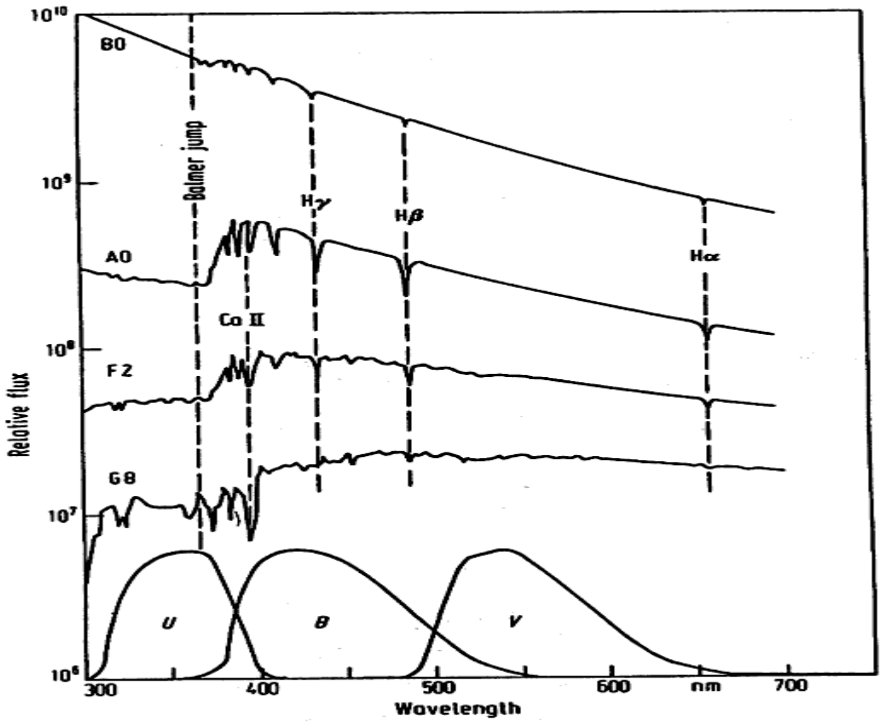

Imaging photometry

Photometry and polarization of background stars of a globule

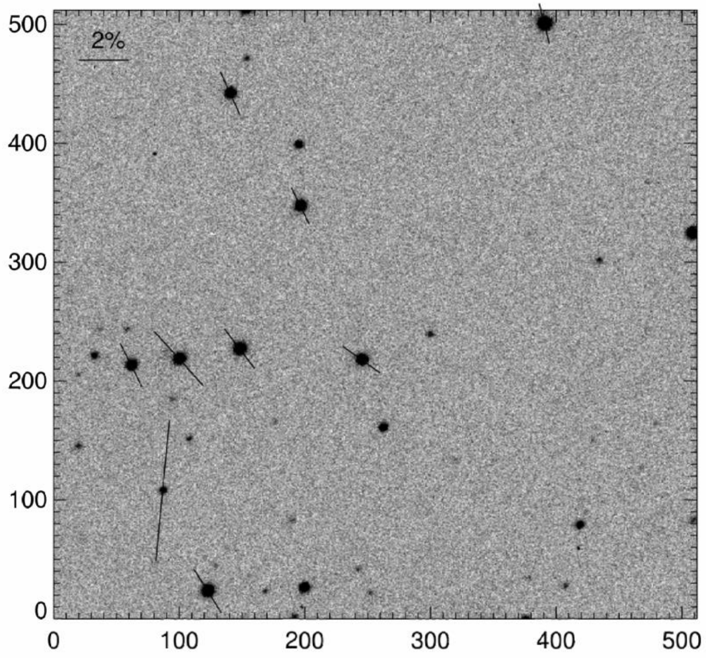

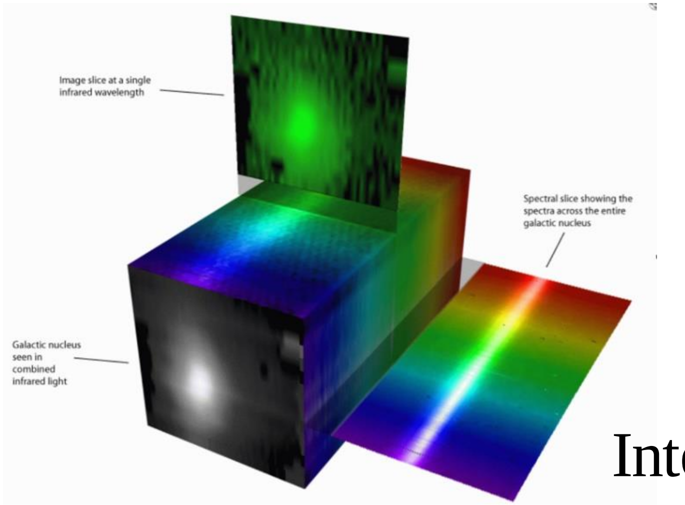

Integral field spectroscopy

Stellar spectrum = a blackbody modified by absorption

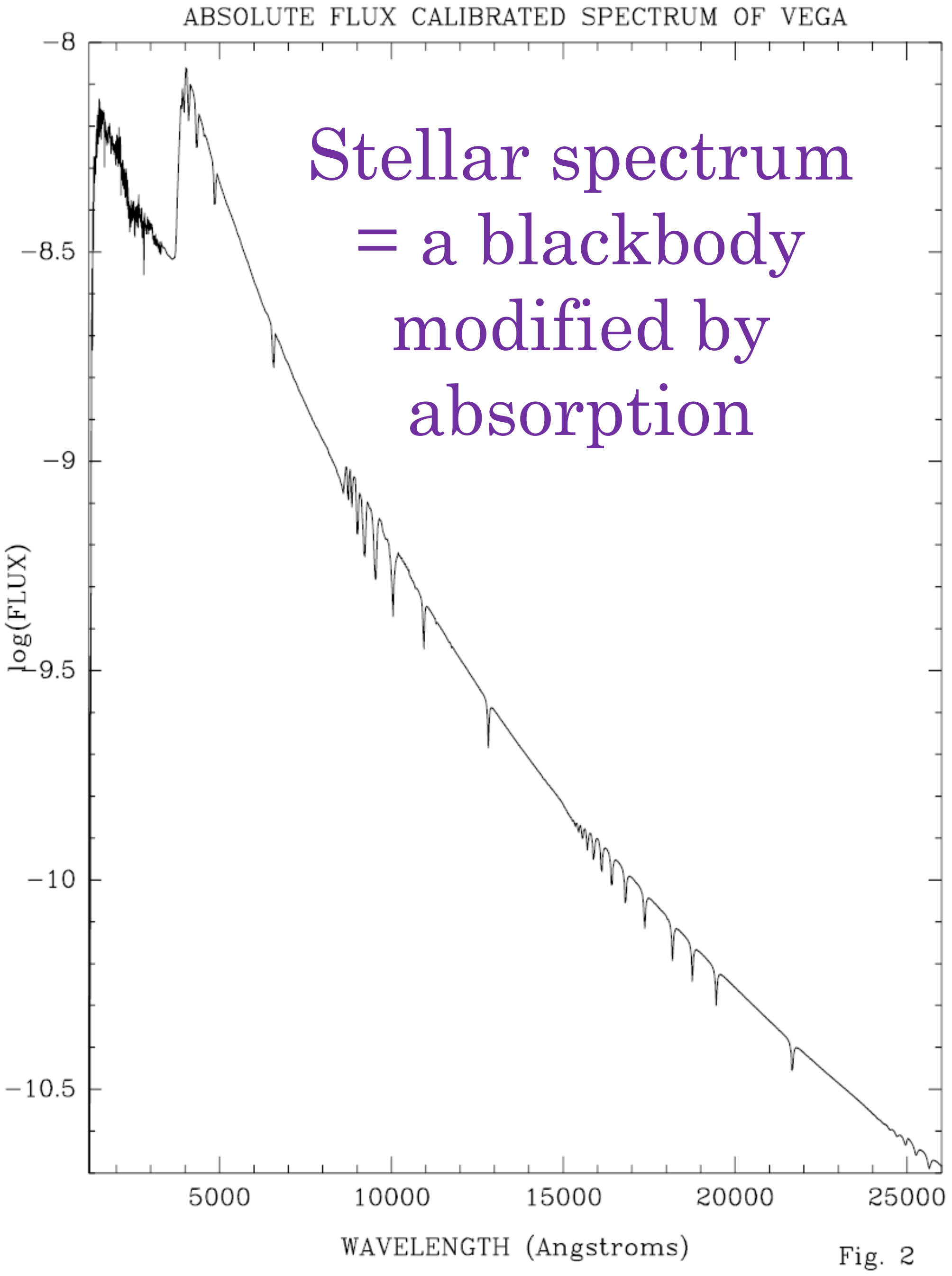

Spectrum diagnosed by photometry,

e.g., $(B-V)$ for T_{eff}, $(U-B)$ for metallicity

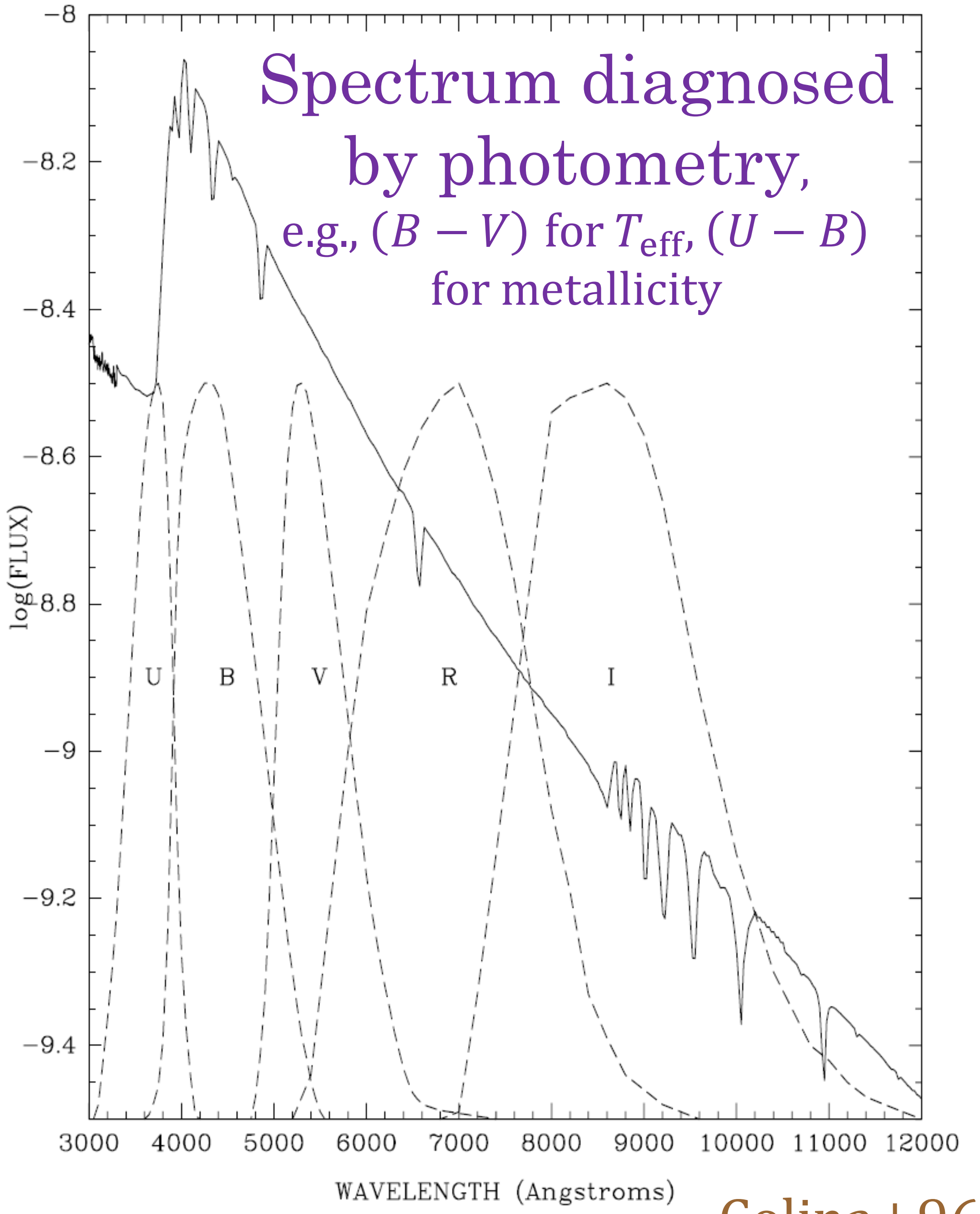

Colina+96

The Spectral Energy Distribution: photometry as a proxy of (a very low-dispersion) spectroscopy

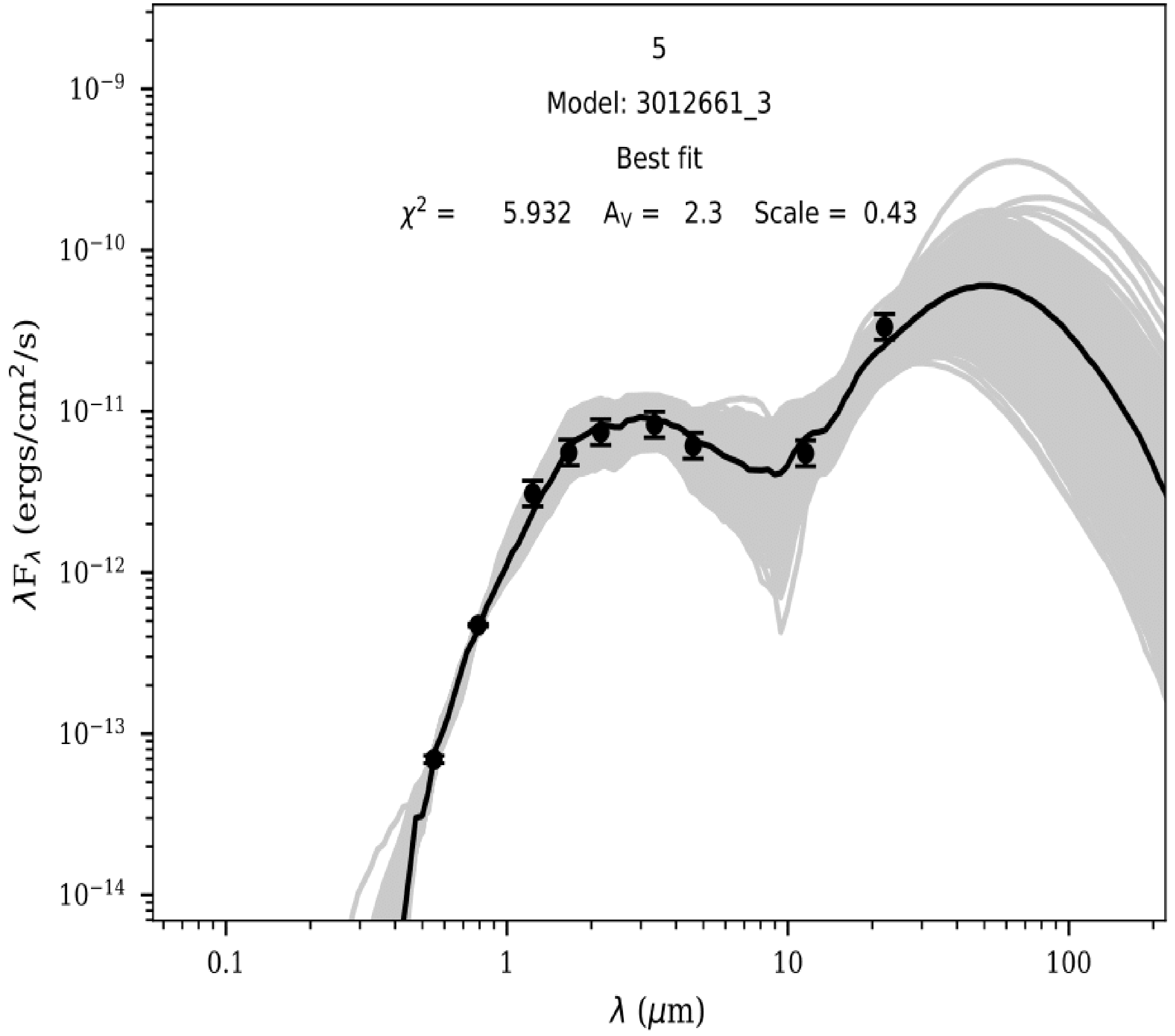

Continuum

Absorption --- bound-free (ionization); free-free
Emission --- (thermal) blackbody; bremsstrahlung
(non-thermal) synchrotron; Čerenkov Cherenkov

Matter $\Leftrightarrow$ energy $\longrightarrow$ what we observe

Thermodynamics (ISM cooling, heating, physical interactions; chemical reactions …)

Line

- Emission --- atom/ion/molecule already excited (by collisions or absorption of a photon from, e.g., a star)

- Absorption --- atom initially in a lower state and absorbs an incoming photon

Transition between 2 quantum levels
(electronic, rotational, vibrational, stretching…)

- Collision ($u \rightarrow l$) or ($l \rightarrow u$) (upwards or downwards)
  spontaneous emission ($u \rightarrow l$) (only downwards)
  absorption ($l \rightarrow u$) (only upwards)

- Diagnosis: line strength, central wavelength, shape, …

ISM in Gaseous and Solid States

Cosmic Matter

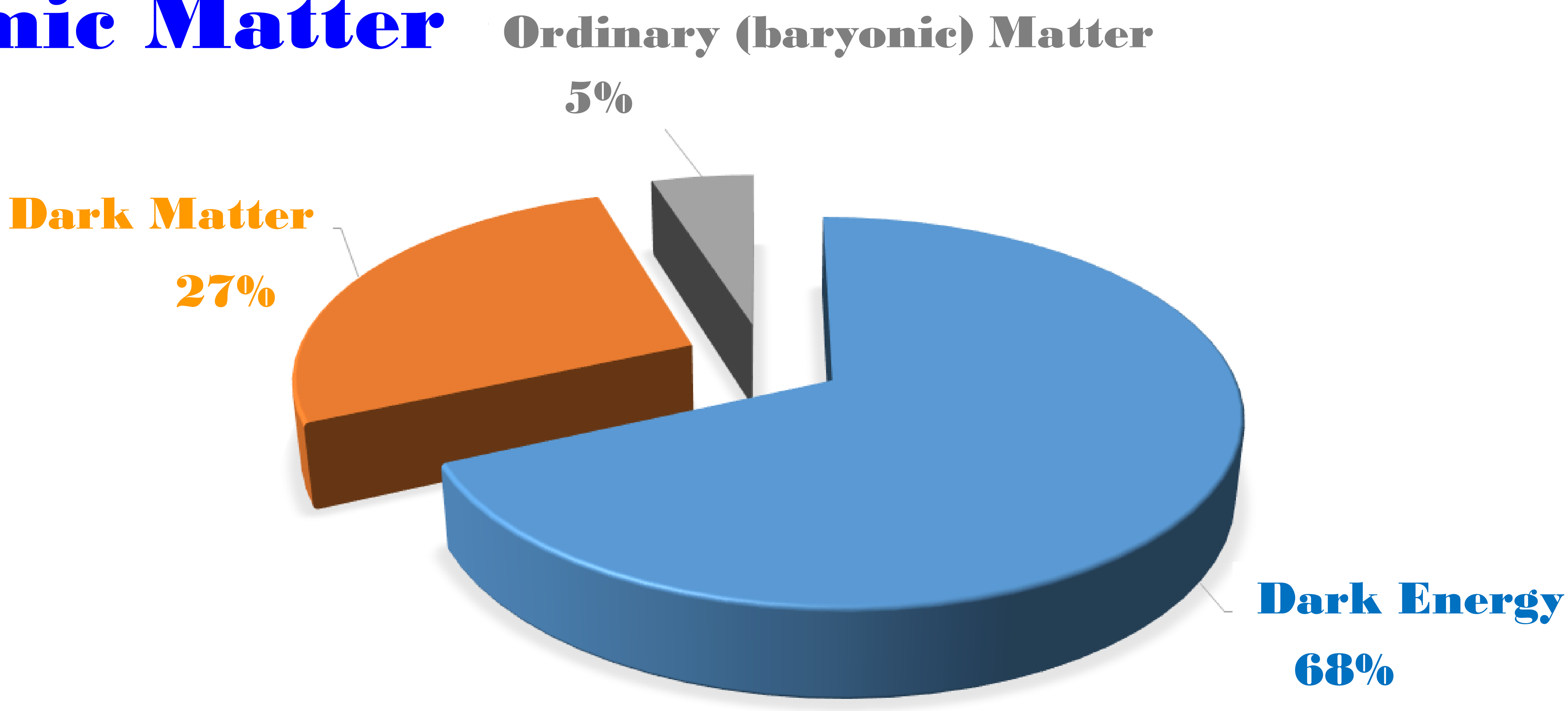

Early Universe: Energy ⟶ Matter condensed + Energy
⟶ ISM being gaseous ⟶ Stars (light + complex elements)
⟶ ISM of gas and dust (planets → life) → summer school

Excitation

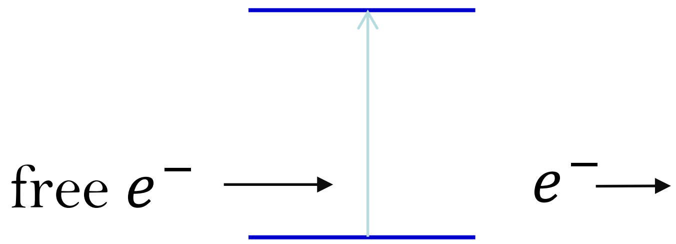

Collision

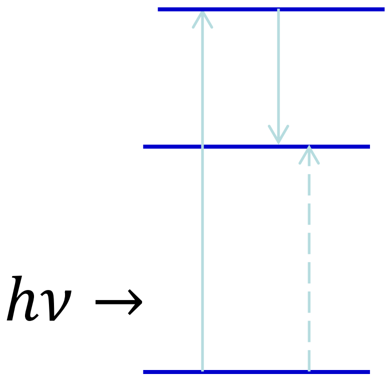

Photon Pumping

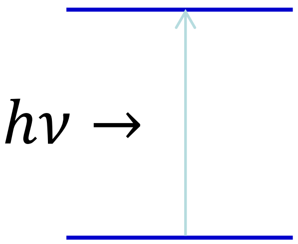

Radiation

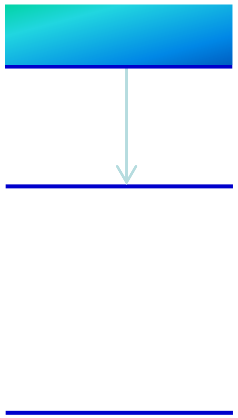

Recombination

Emission and Absorption

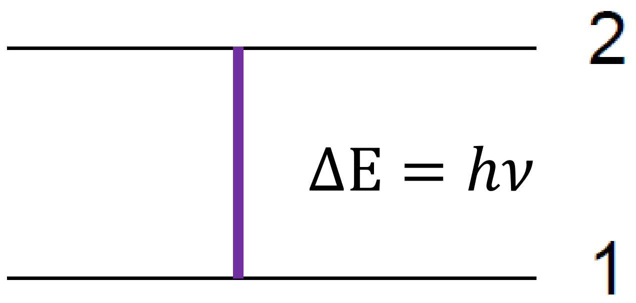

<u>Two ways</u> to jump down from an excited state

Colliding up
✓colliding down, or
✓jumping down

- **Spontaneous emission**

$$X_2 \rightarrow X_1 + h\nu$$

occurrence rate ↔ atomic properties

- **Stimulated emission**

$$X_2 + h\nu \rightarrow X_1 + 2\,h\nu$$

occurrence rate ↔ density of incoming photons of the same ν, polarization, and direction of propagation

- **Collisional deexcitation** → **no emission of photons**

Boltzmann Excitation Equation

$e^{-E_{21}/kT}$: Boltzmann factor

Population ratio between two excited states (of the same r-times ionized species)

$$\frac{n_2}{n_1} = \frac{g_2}{g_1} \; e^{-E_{21}/kT}$$

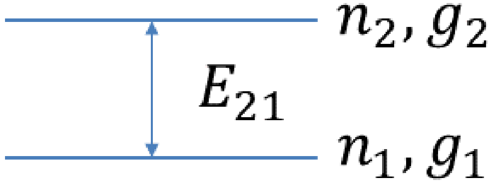

n_i: number density of the particles in the i-th energy state

g_i: statistical weight of the i-th energy state
= degeneracy of the level
= number of states with different quantum numbers but with the same energy

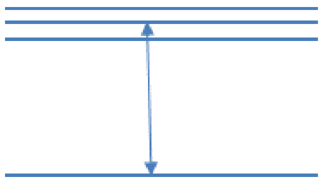

E_{21}: difference in excitation energies (wrt to ground state) $= h\nu$

It really should have been n_i^r or g_i^r for the same r-times ionization.

Saha Ionization Equation

Population ratio between two ionization stages

$$\frac{n_{r+1}\, n_e}{n_r} = \frac{G_{r+1}\, g_e}{G_r} \frac{(2\pi m_e\, kT)^{3/2}}{h^3} e^{-\chi_r/kT}$$

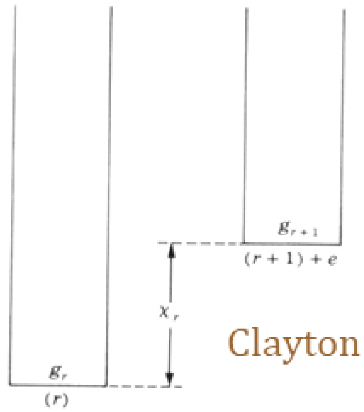

Clayton

n_r: number density of the particles in the r-th ionized state
n_e: number density of free electrons

G_r, g_e: partition functions of the ionized species, and of the electron = sum of the statistical weights of all bound states, each weighted by the Boltzmann factor

$G_r = \sum_i g_{r,i}\, e^{-\frac{E_i}{kT}}$, very often G_1 dominates; $g_e = 2$

χ_r: ionization potential from the ionization stage r to $r+1$

Einstein Coefficients

Einstein (1917)

Spontaneous emission

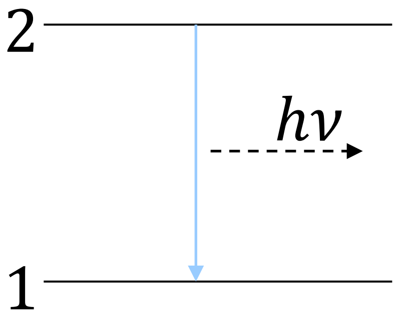

$$X_2 \longrightarrow X_1 + h\nu$$
$$\nu = (E_2 - E_1)/h$$

$\boldsymbol{A_{21}}$ --- probability $[\mathrm{s}^{-1}]$

$n_2\, A_{21} dt$: # of spontaneous radiative transitions during dt

Stimulated (induced) emission

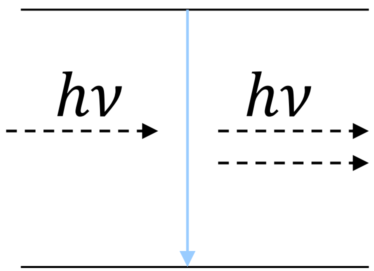

$$X_2 + h\nu \longrightarrow X_1 + 2\, h\nu$$

$\boldsymbol{B_{21}}$

(Stimulated) absorption

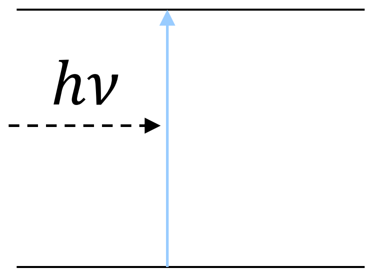

$$X_1 + h\nu \longrightarrow X_2$$

$\boldsymbol{B_{12}}$

$\boldsymbol{B\, I_\nu}$ --- probability or $\boldsymbol{B\, u_\nu}$ then unit different

$n_2\, B_{21} I_\nu\, dt$ or $n_1\, B_{12}\, I_\nu\, dt$: # of (stimulated) or radiative transitions during dt when irradiated with $\boldsymbol{I_\nu}$

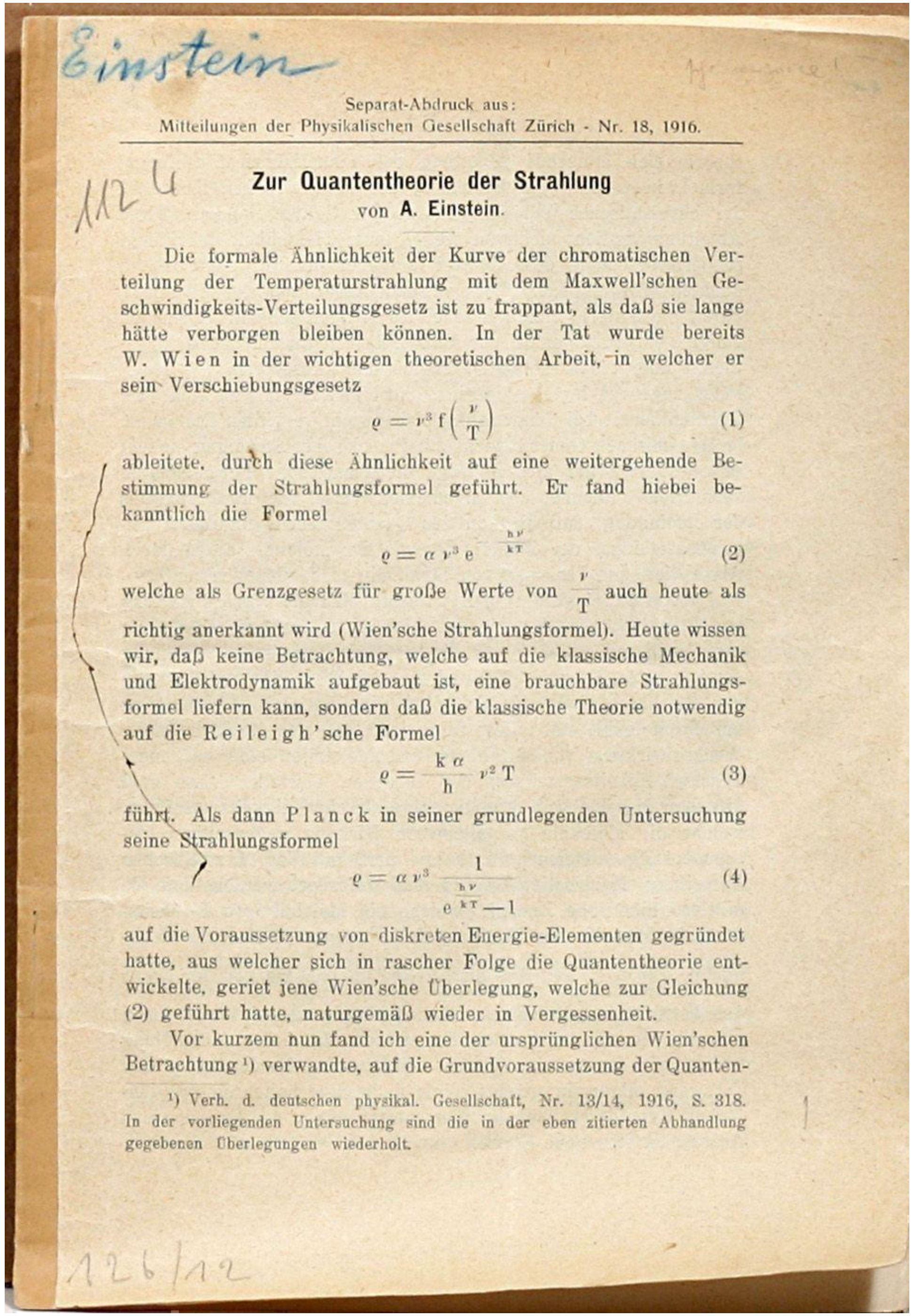

Separat-Abdruck aus:
Mitteilungen der Physikalischen Gesellschaft Zürich - Nr. 18, 1916.

Zur Quantentheorie der Strahlung

von **A. Einstein.**

Die formale Ähnlichkeit der Kurve der chromatischen Verteilung der Temperaturstrahlung mit dem Maxwell'schen Geschwindigkeits-Verteilungsgesetz ist zu frappant, als daß sie lange hätte verborgen bleiben können. In der Tat wurde bereits W. Wien in der wichtigen theoretischen Arbeit, in welcher er sein Verschiebungsgesetz

$$\varrho = \nu^3 f\left(\frac{\nu}{T}\right) \qquad (1)$$

ableitete, durch diese Ähnlichkeit auf eine weitergehende Bestimmung der Strahlungsformel geführt. Er fand hiebei bekanntlich die Formel

$$\varrho = \alpha \nu^3 e^{-\frac{h\nu}{kT}} \qquad (2)$$

welche als Grenzgesetz für große Werte von $\frac{\nu}{T}$ auch heute als richtig anerkannt wird (Wien'sche Strahlungsformel). Heute wissen wir, daß keine Betrachtung, welche auf die klassische Mechanik und Elektrodynamik aufgebaut ist, eine brauchbare Strahlungsformel liefern kann, sondern daß die klassische Theorie notwendig auf die Reileigh'sche Formel

$$\varrho = \frac{k\alpha}{h} \nu^2 T \qquad (3)$$

führt. Als dann Planck in seiner grundlegenden Untersuchung seine Strahlungsformel

$$\varrho = \alpha \nu^3 \frac{1}{e^{\frac{h\nu}{kT}} - 1} \qquad (4)$$

auf die Voraussetzung von diskreten Energie-Elementen gegründet hatte, aus welcher sich in rascher Folge die Quantentheorie entwickelte, geriet jene Wien'sche Überlegung, welche zur Gleichung (2) geführt hatte, naturgemäß wieder in Vergessenheit.

Vor kurzem nun fand ich eine der ursprünglichen Wien'schen Betrachtung [1]) verwandte, auf die Grundvoraussetzung der Quanten-

[1]) Verh. d. deutschen physikal. Gesellschaft, Nr. 13/14, 1916, S. 318. In der vorliegenden Untersuchung sind die in der eben zitierten Abhandlung gegebenen Überlegungen wiederholt.

"On the Quantum Theory of Radiation" by A. Einstein

Einstein relations

$$g_1 B_{12} = g_2 B_{21}$$

$$A_{21} = \frac{2h\nu^3}{c^2} B_{21}$$

These relate to the intrinsic properties of an atom.

https://einstein.manhattanrarebooks.com/pages/books/17/albert-einstein/zur-quantentheorie-der-strahlung-on-the-quantum-theory-of-radiation

Define the **excitation rate coefficient** γ_{01}, so that

# of excitation $\mathrm{s}^{-1}\ \mathrm{cm}^{-3}$ $(= n_e n_1\ v\sigma) \equiv n_e n_1 \gamma_{12}$,

where both n_e and n_1 have units of [cm^{-3}]

$$\gamma_{12} \equiv \langle \sigma v \rangle = \int_{\chi=\frac{1}{2}mv^2}^{\infty} \sigma_{01}(v) v\, f(\vec{v})\, d^3\vec{v}$$

Here σ_{12} is the excitation cross section, and $f(\vec{v})$ is the Maxwellian distribution function,

$$f(\vec{v})\, dv = 4\pi \left(\frac{m}{2\pi kT}\right)^{3/2} v^2\, e^{-\frac{mv^2}{2kT}}\, dv$$

So

$$\gamma_{12} = \frac{4}{\sqrt{\pi}} \left(\frac{1}{2kT}\right)^{1/2} \int_{\chi=\frac{1}{2}mv^2}^{\infty} v^3\, \sigma_{12}(v)\, e^{-\frac{mv^2}{2kT}}\, dv$$

This is the <u>upward</u> transition $1 \rightarrow 2$.

For the downward transition $2 \rightarrow 1$,
the spontaneous emission rate $= n_2 A_{21}$,
and the deexcitation rate by collisions $= n_2 n_e \gamma_{21}$,
where $\gamma_{21} = \int_0^\infty v\, \sigma_{21}(v)\, f(\vec{v})\, d^3\vec{v} = \gamma_{21}(T)$

In a steady state, [upward rate]=[downward rate],
i.e., in **detailed balancing**,

$$n_1 n_e\, \gamma_{12}(T) = n_2\, [A_{21} + n_e\, \gamma_{21}(T)]$$

The competition for downward transition between the two terms in the bracket → **critical density** (radiative deexcitation = collisional deexcitation)

$$n_{\rm crit} = A_{10}/\gamma_{10}$$

When $n_e > n_{\rm crit}$, collisions dominate the deexcitation process
→ LTE, populations governed by the Boltzmann equation

For example, NH_3 (ammonia) is a good tracer of clumps of cold dense gas, and has a critical density of $n_{H_2} \approx 10^4\ \mathrm{cm}^{-3}$

$A_{21} \Leftrightarrow n_e\, \gamma_{21}$ 1/A_{21} : Lifetime in the excited state

If staying up too long (?) $1/A_{21}$ → colliding down → no emission, unless in a very low-density environment (space)

- ☐ **Allowed (regular) Lines** (no bracket), $A \approx 10^{+8}\ \mathrm{s}^{-1}$, e.g., C IV
- ☐ **Semi-forbidden Lines** (a single bracket), $A \approx 10^{+2}\ \mathrm{s}^{-1}$, e.g., [OII
- ☐ **Forbidden Lines** (a pair of square brackets), $A \approx 10^{0}$ to $10^{-4}\ \mathrm{s}^{-1}$, e.g., [O III], [N II]

- Normally an atom stays in an excited state for 10^{-8} s.
- A forbidden transition occurs for excitation levels $<$ a few eV (for heavy ions, cf. for H 10^{+} eV) ; an electron remains excited for seconds or longer before returning to the ground state.
- On Earth n ↑↑, both excitation and de-excitation take place frequently, so radiative transition (emitting a photon) is unlikely.
- In ISM, the electrons are not energetic enough to excite the atoms to normal levels (10 to 20 eV) , but enough to excite to metastable levels. In hot, low-density environments, e.g., in H II regions, PNe, solar corona, earth aurora …

  Once (collisionally) excited → emission
  → photons escaped → **cooling** *'Metals' are efficient coolants.*

Some examples:

Lyman α $(H, n = 3 \rightarrow 2)$, $A_{21} \approx 6.25 \times 10^8\ \mathrm{s}^{-1}$

[O III] $A_{21} = 0.021\ \mathrm{s}^{-1}, \lambda_{21} = 5007\ \text{Å}$

$A_{21} = 0.0281\ \mathrm{s}^{-1}, \lambda_{21} = 4959\ \text{Å}$

$A_{32} = 1.60\ \mathrm{s}^{-1}, \lambda_{32} = 4364\ \text{Å}$

[S II] $A_{21} = 4.7 \times 10^{-5}\ \mathrm{s}^{-1}, \lambda_{21} = 6716\ \text{Å}$

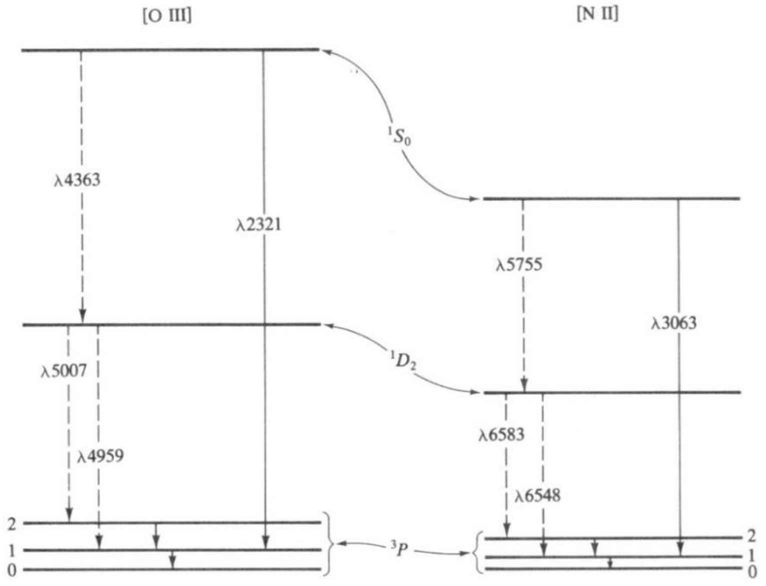

Rosette Nebula and NGC 2244 (H II)

Red: H-alpha
Blue: [S II]
Green: [O III]

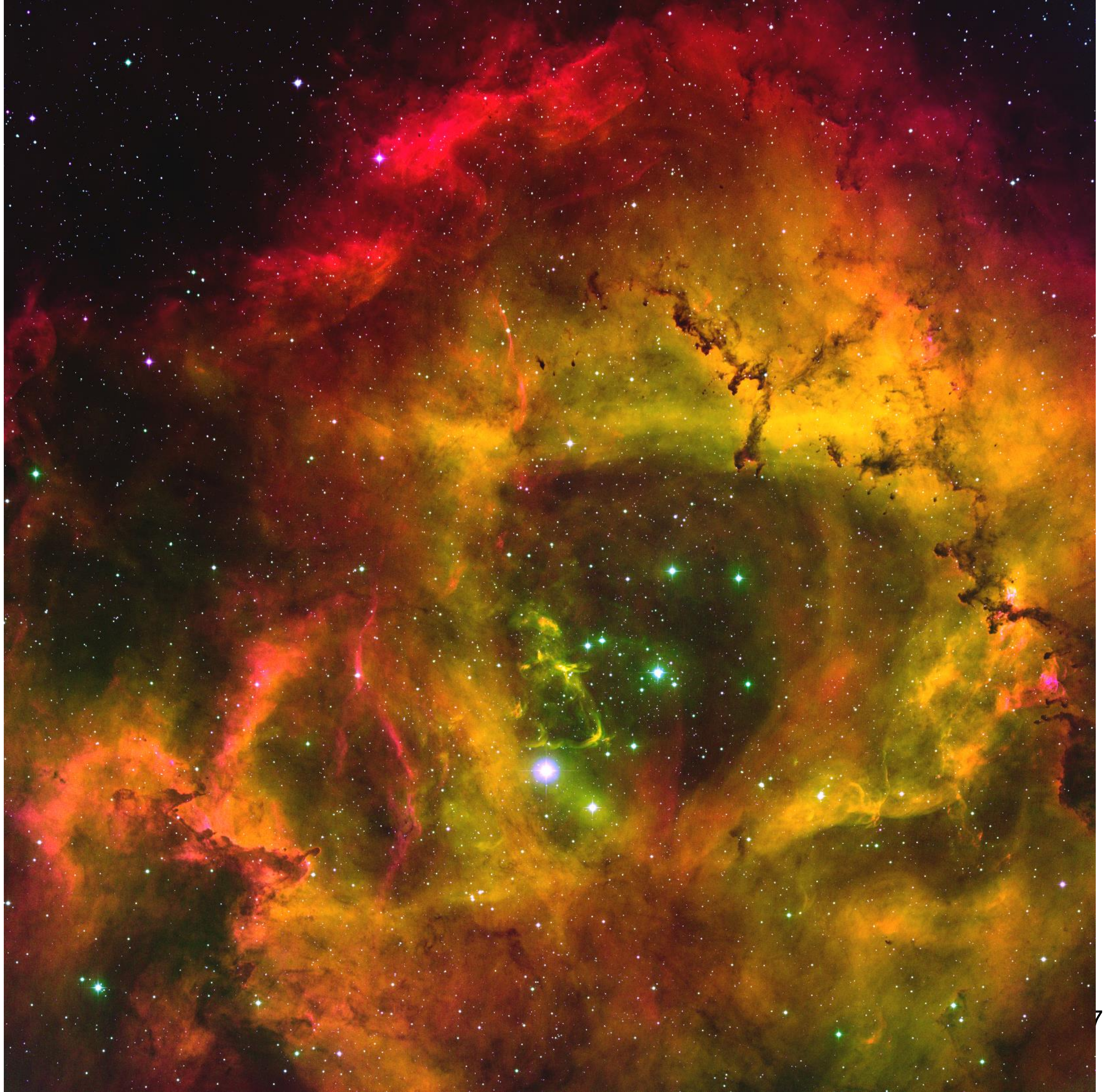

For H, the ground electronic state $1s\ 2S_{1/2}$ has $J = 1/2$, and the proton has $I = 1/2$. The state splits into (total) $F = I + J = 0$ or $F = 1$, $\Delta E = 6.7 \times 10^{-6}$ eV (hyperfine structure) , $\nu \approx 1420.405751$ MHz, $\lambda \approx 21$ cm.

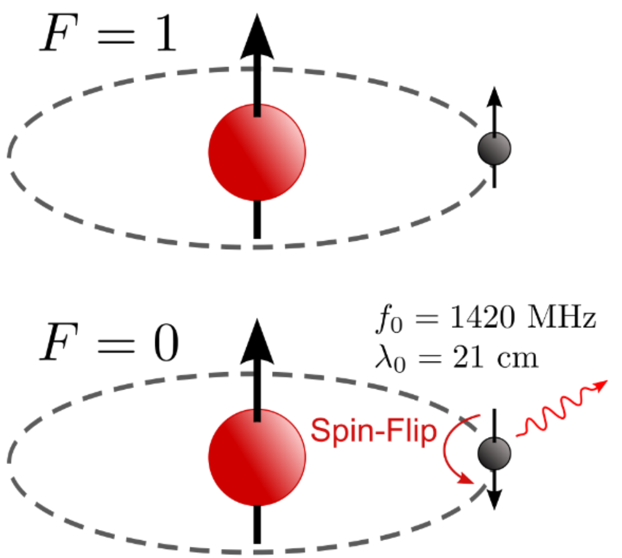

https://en.wikipedia.org/wiki/Hydrogen_line

The H I **21 cm line** $A_{21} \approx 2.8 \times 10^{-15}\ \mathrm{s}^{-1}$; $\tau_{1/2} \approx A_{10}^{-1} \approx\ 3.5 \times 10^{7}$ s $\approx$ 10 million yrs; transition probability extremely low; useful in detecting atomic hydrogen (amount, motion, etc.) in space.

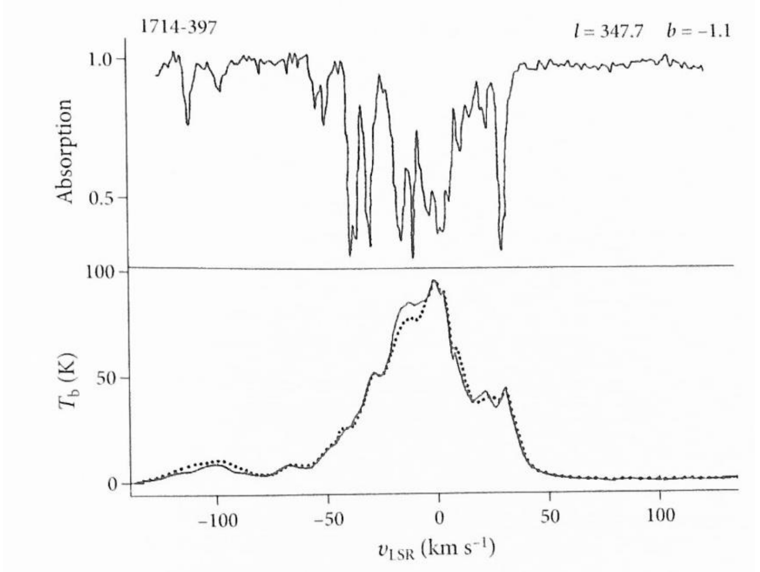

For $n = 2$, ℓ =1, and with spin, a total angular momentum of
$\ell(\ell + 1)\hbar^2 = 2\hbar^2$
3 substates, $\hbar$, 0, $-\hbar$, $m = 1, 0, -1$ (magnetic quantum number)

Fine structure, $\Delta\mathcal{E}$ very small, $\sim 10^{-5}$ eV

But with an external **B** field → **Zeeman splitting**

With a typical ISM field of 10 μG, the 21-cm line shifts 10^{-8}, equivalent to an RV of a few km s^{-1}; very difficult to detect

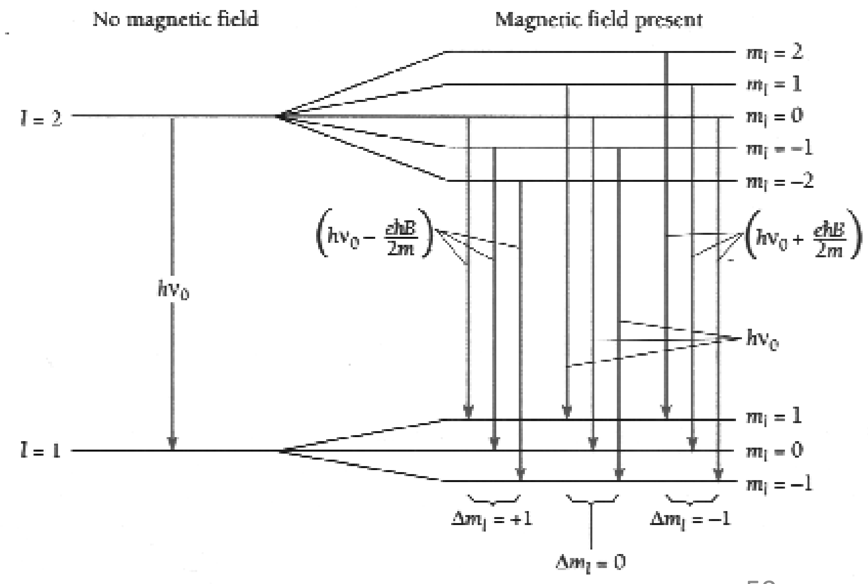

Detectable by the difference of the two circular polarization signals.

Also in OH 18 cm and 6 cm, H_2CO 6 cm lines → to derive B and $n\ (HI)$

Zeeman Effect

… the split of a spectral line into several components in the presence of a **magnetic field**. It is analogous to the **Stark effect**, the splitting of a spectral line into several components in the presence of an **electric field**.

In (kG) and out (1 G) of sunspots

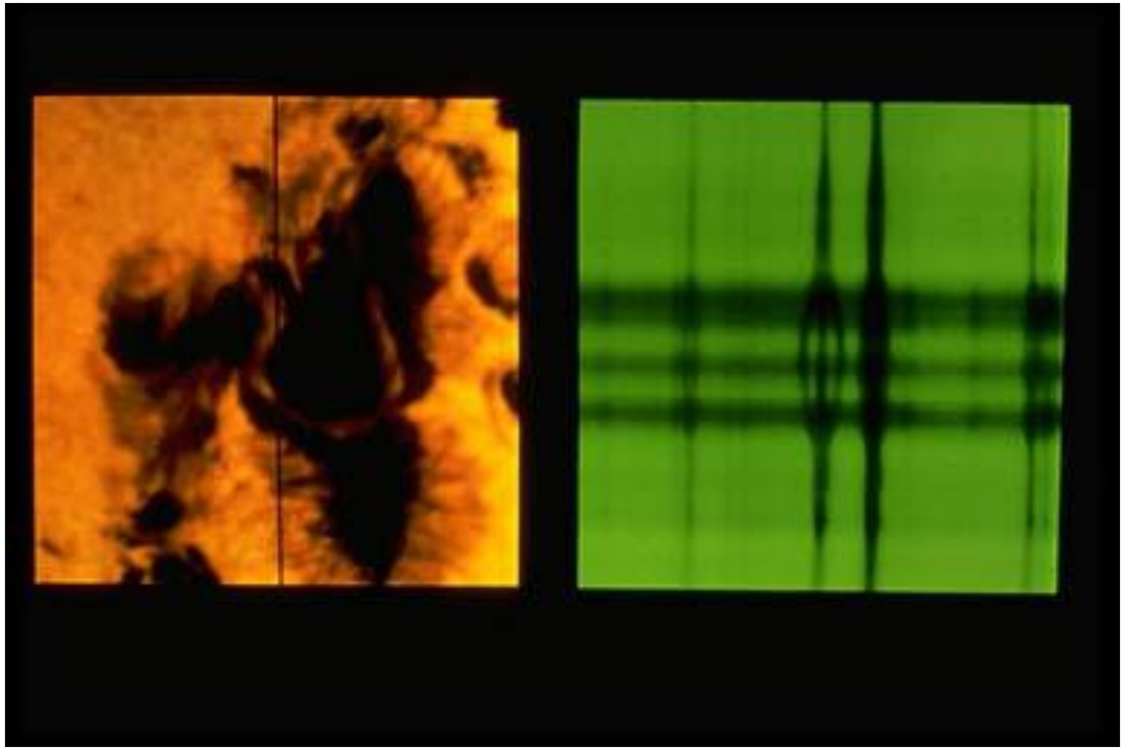

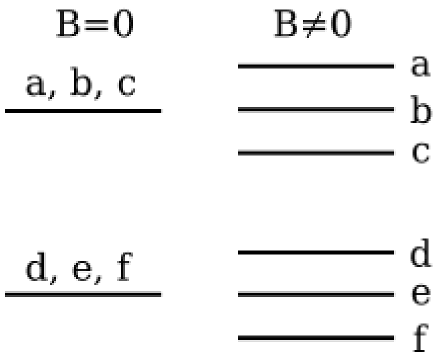

Ionization Processes

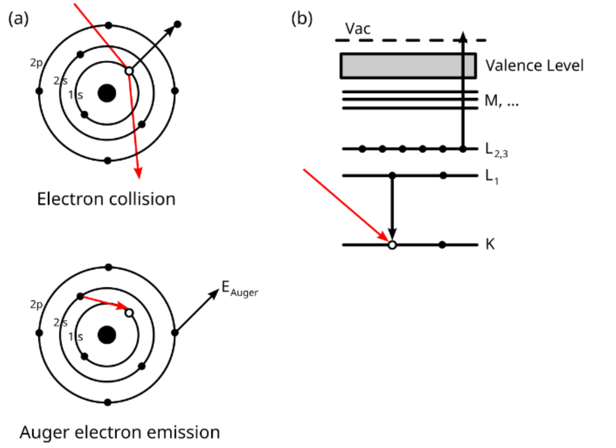

https://en.wikipedia.org/wiki/Auger_effect

- Photoionization
- Auger ionization

  an inner-shell electron is photoionized → a higher-level electron fills in → emitting a photon, or energy transferred to an electron → excited or ionized of an Auger electron

- Collisional ionization
- Cosmic Ray Ionization

  non-thermal electrons and ions

Auger-Meitner effect:
1922 by Lise Meitner:
1923 by Pierre Victor Auger

Recombination → photons

Some of the photons can also ionize or excite other species

H 114 β: $n = 116 \rightarrow 114$

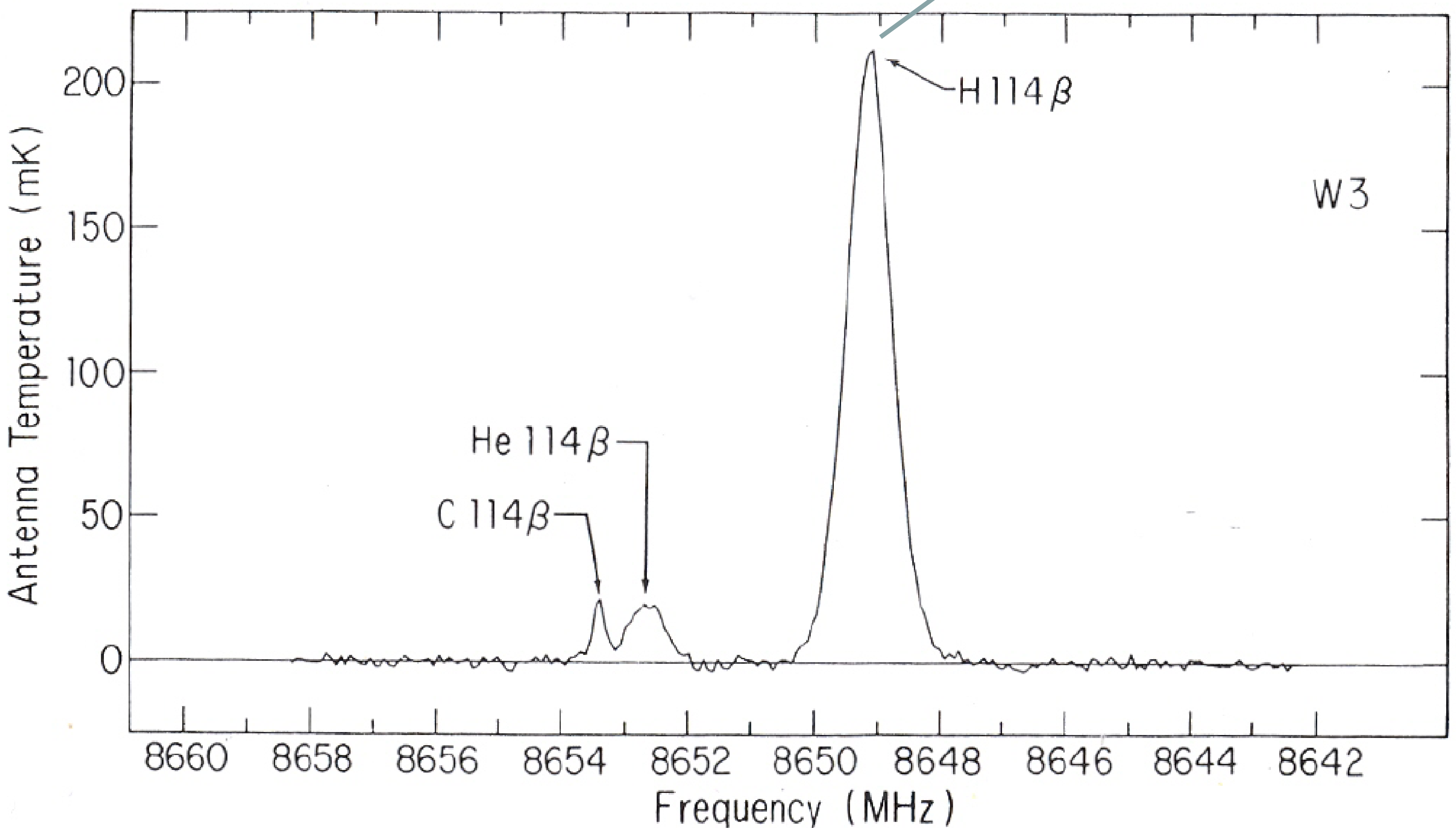

H II Regions of Photoionization

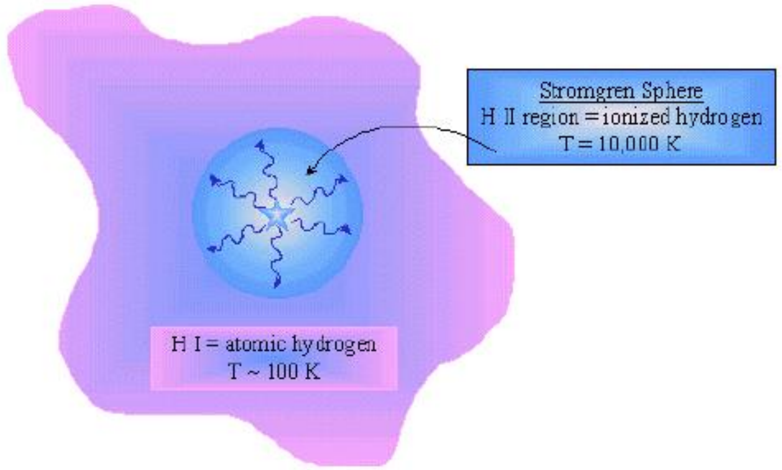

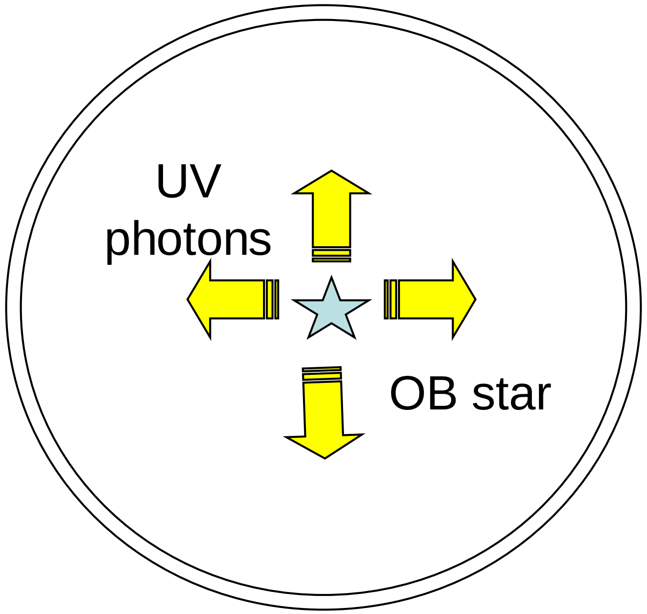

Radiation $\lambda <$ 912 Å
→ ionization of H from gr state

If e^- already in an excited state, a longer λ will do.

Collisional ionization negligible in HII regions

Once ionized, the e^- recombines with a p^+, emitting Balmer, Paschen, Pfund lines or continua → e^- cascading → we see Hα 656.3 nm

lobules in
4 (HST/WFPC2)

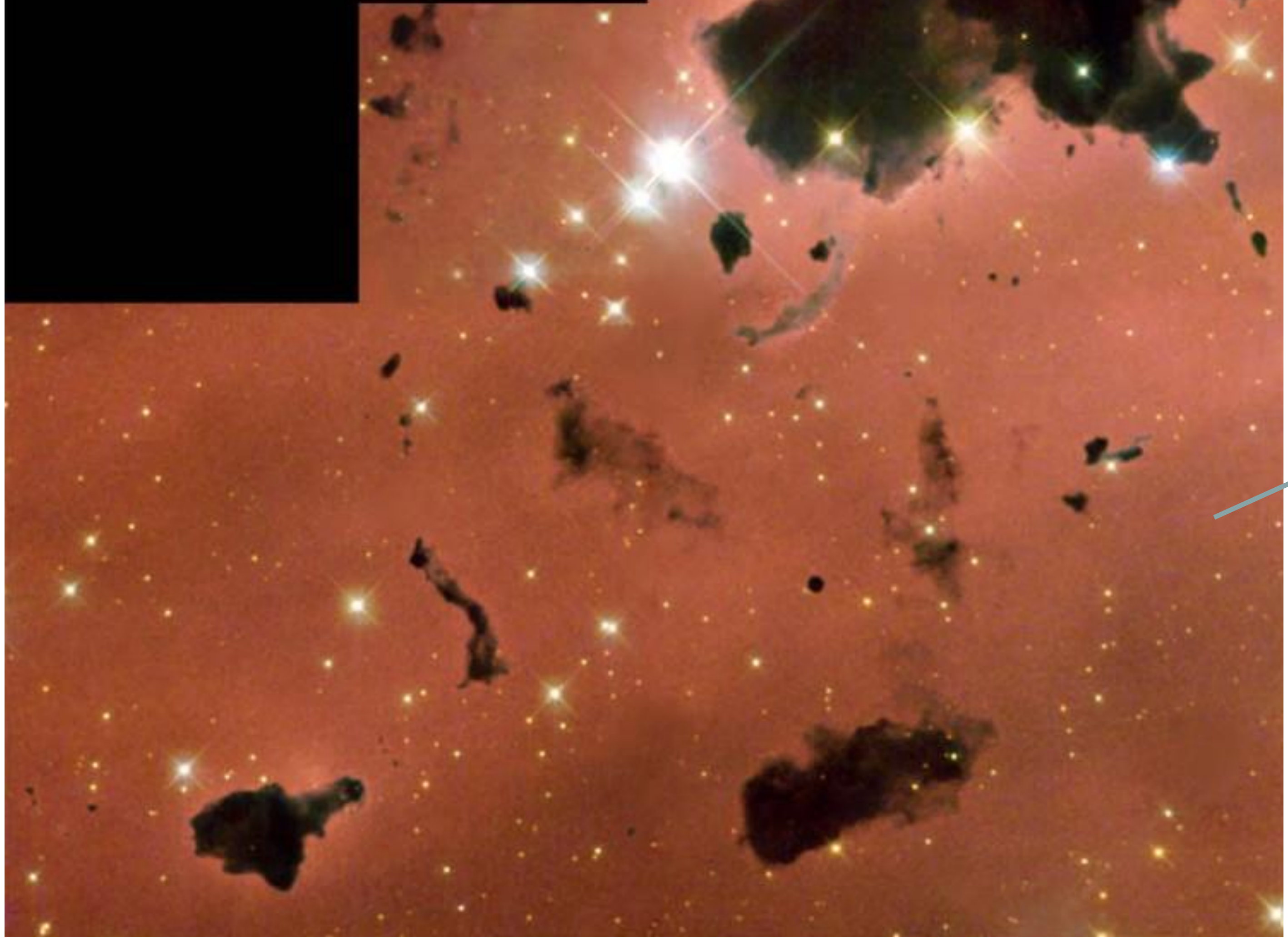

Trifid Nebula
(M20)
(H II)

Ring Nebula (M57) (PN)

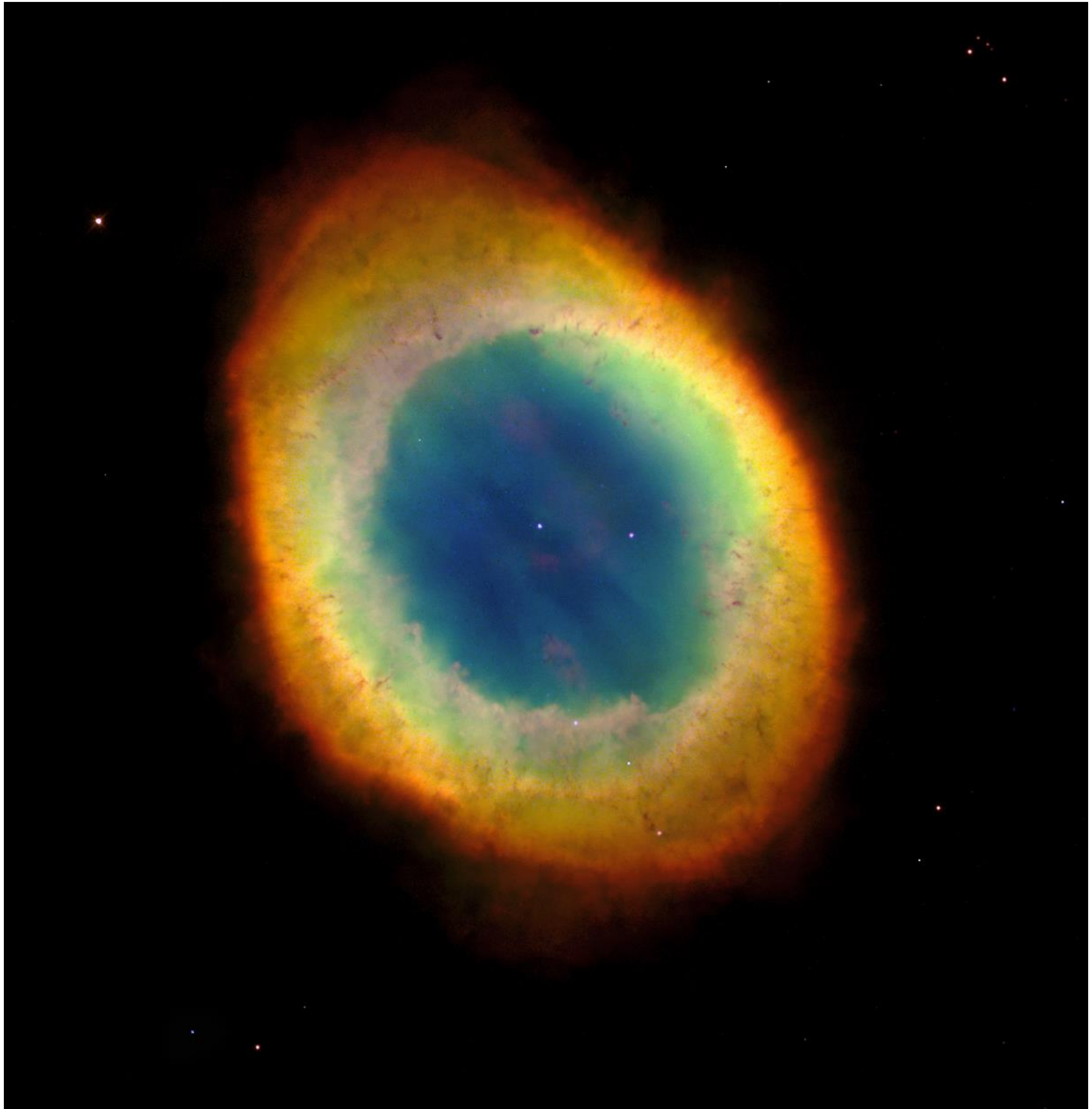

Blue: He
Green: O
Red: N
WD 120,000 K

Helix Nebula (NGC 7293) (PN)

Photoionized cometary knots

Spiral galaxy NGC 300 in H-alpha (ESO)

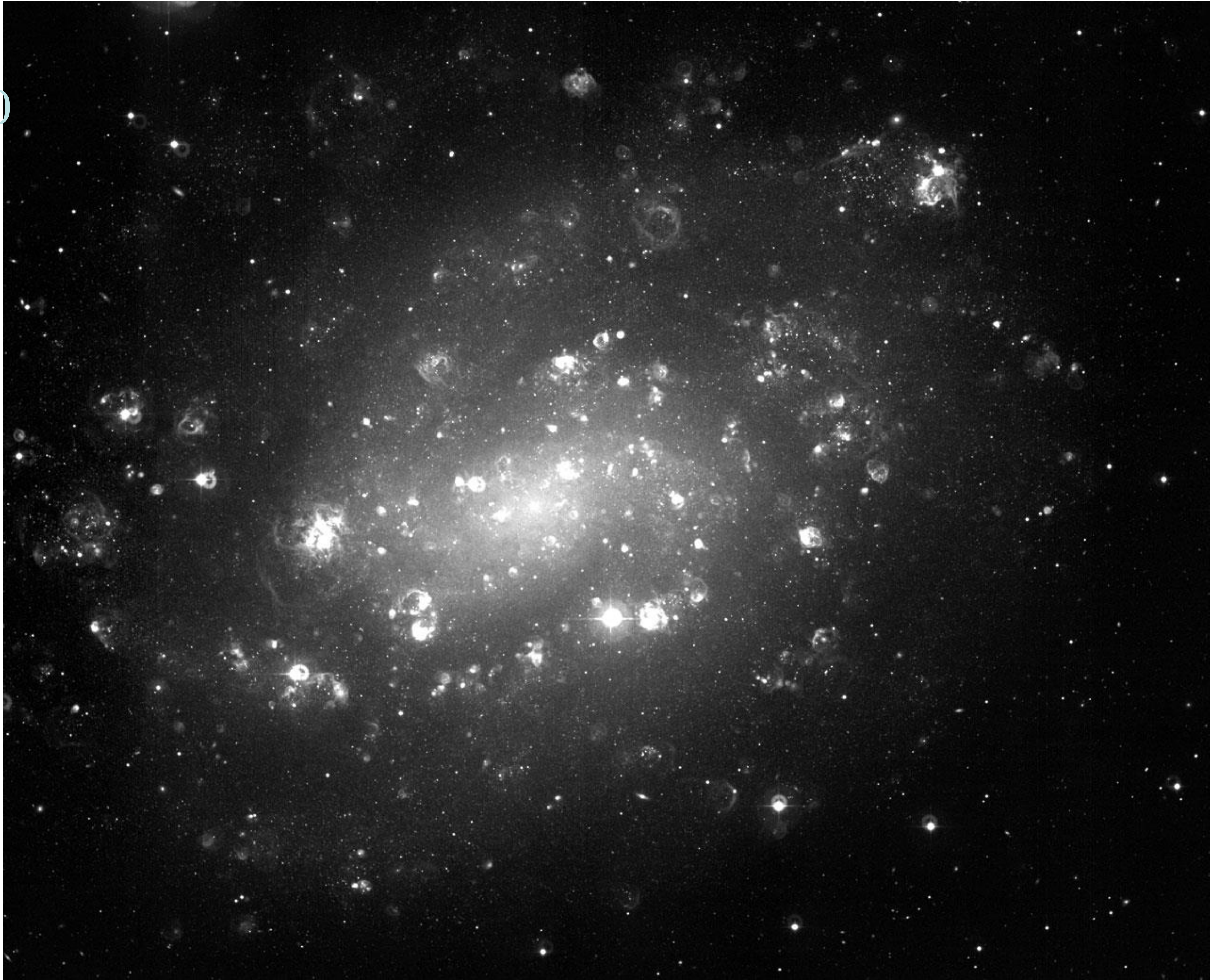

M51 (HST)

Strings of red H II "knots" delineate the arms of the Whirlpool Galaxy: sites of recent star formation

Strömgren Sphere

The region within which every H atom is photoionized by a UV-rich object (e.g., an OB star, a WD),

$[number\ of\ ionizing\ photons\ per\ s]$ by the star

$= [Total\ number\ of\ recombinations\ per\ s]$ of the nebula

$$R_s = \left(\frac{3L_{912}^*}{4\pi\alpha^{(2)}n_H^2}\right)^{1/3}$$

the Strömgren radius

He and C, too

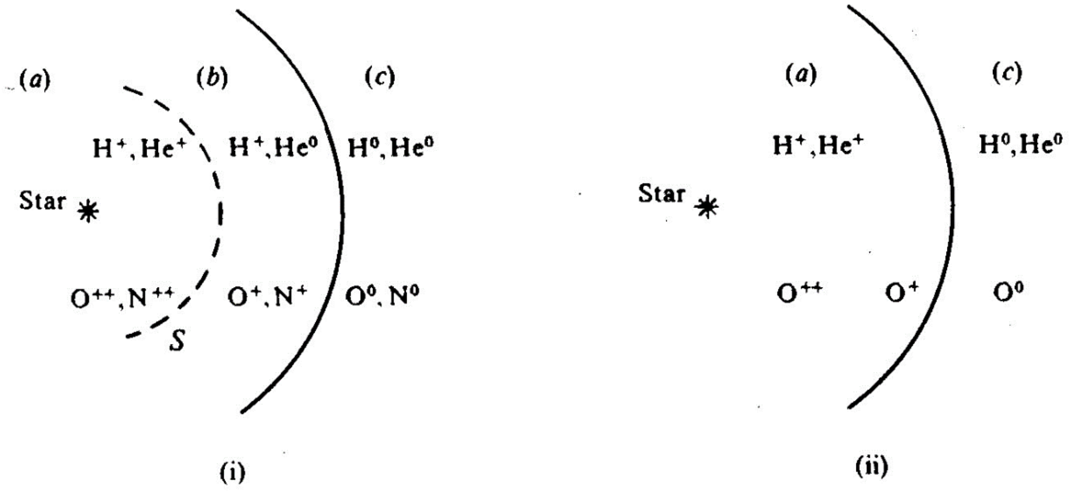

Figure 5.3. Ionization stratification in a nebula. (i) Low stellar temperature ($T_* \leq 40\,000$ K); (ii) High stellar temperature ($T_* \geq 40\,000$ K).

Dyson & Williams

Table 2.3

Calculated Strömgren radii as function of spectral types spheres

Spectral type	T_* (K)	M_V	log $Q(H^0)$ (photons/s)	log $n_e n_p r_1^3$ n in cm^{-3}; r_1 in pc	log $n_e n_p r_1^3$ n in cm^{-3}; r_1 in pc	r_1 (pc) $n_e = n_p$ = 1 cm^{-3}
O3 V	51,200	−5.78	49.87	49.18	6.26	122
O4 V	48,700	−5.55	49.70	48.99	6.09	107
O4.5 V	47,400	−5.44	49.61	48.90	6.00	100
O5 V	46,100	−5.33	49.53	48.81	5.92	94
O5.5 V	44,800	−5.22	49.43	48.72	5.82	87
O6 V	43,600	−5.11	49.34	48.61	5.73	81
O6.5 V	42,300	−4.99	49.23	48.49	5.62	75
O7 V	41,000	−4.88	49.12	48.34	5.51	69
O7.5 V	39,700	−4.77	49.00	48.16	5.39	63
O8 V	38,400	−4.66	48.87	47.92	5.26	57
O8.5 V	37,200	−4.55	48.72	47.63	5.11	51
O9 V	35,900	−4.43	48.56	47.25	4.95	45
O9.5 V	34,600	−4.32	48.38	46.77	4.77	39
B0 V	33,300	−4.21	48.16	46.23	4.55	33
B0.5 V	32,000	−4.10	47.90	45.69	4.29	27
O3 III	50,960	−6.09	49.99	49.30	6.38	134
B0.5 III	30,200	−5.31	48.27	45.86	4.66	36
O3 Ia	50,700	−6.4	50.11	49.41	6.50	147
O9.5 Ia	31,200	−6.5	49.17	47.17	5.56	71

Note: $T = 7{,}500$ K assumed for calculating α_B.

Osterbrock

Evolution of an H II region

- Original H I, $T \sim 100$ K; now H II, $T \nearrow\nearrow$ ($\sim 10^4$ K), ionization produces free electrons, so $n \nearrow$, hence pressure ($P \propto nT$) $\nearrow\nearrow$ → H II region expands, $v \sim$ sound speed of the hot gas ~ 10 km/s
- Sound speed in H I ~ 1 km/s → H II expansion highly supersonic → a shock (ionization) front
- H II continues to expand ($n \searrow$) until in pressure equilibrium with the H I region. This takes 10^7 to 10^8 years. But an early O star has a main-sequence lifetime of 10^6 years.

  ➔ H II regions are expanding!

- A **compact** H II region = young; newly formed H II regions = **ultra-compact** H II (UCHII) regions ($D < 0.3$ pc); **hyper-compact** H II regions ➔ massive star formation

Thermal (Bremsstrahlung; free-free) Emission

Hot, low-density plasma (e.g., HII regions, PNe, SNRs)
→ thermal radio emission

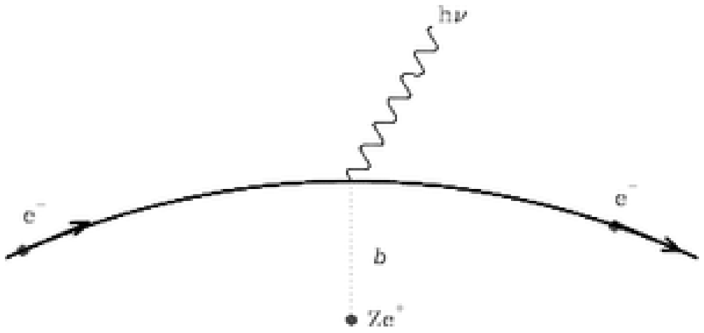

http://www.astro.utu.fi/~cflynn/

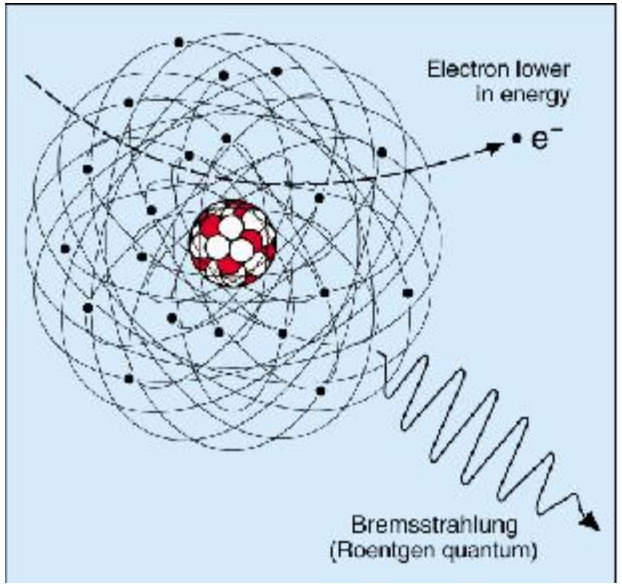

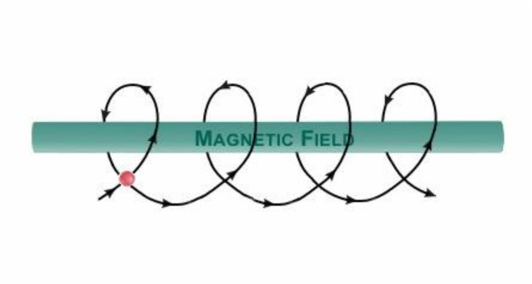

c.f. Synchrotron Radiation

Emission line observations suggest nebula $T_e \approx 10^4$ K, so in radio wavelengths, $h\nu \ll kT$, $e^{-h\nu/kT} \to 1$ (flat), and $B_\nu \approx 2kT\nu^2/c^2$

For free-free emission or bremsstrahlung (breaking radiation)

$$j_\nu \approx \frac{n_e n_i}{T_e^{1/2}} \implies \boxed{\kappa_\nu = \frac{j_\nu}{B_\nu} \approx \frac{n_e n_i}{T_e^{3/2}\,\nu^2}}$$

More rigorously, the optical depth

$$\tau = \int \kappa_\nu\, ds = \frac{8.235 \times 10^{-2}}{T_e^{1.35}\,\nu_{\mathrm{GHz}}^{2.1}}\ \mathrm{EM},$$

Bright HII regions
$n_e \approx n_p \approx 10^3\ \mathrm{cm}^{-3}$
over $\Delta s \approx 1$ pc
$\longrightarrow$ EM $\approx 10^6\ \mathrm{cm}^{-6}$ pc

where $\mathrm{EM} = \int n_e n_i\, ds$ [cm^{-6} pc] is the **emission measure**.

$\tau \searrow$ at higher ν (or long λ)

➔ **Plasma is more transparent at higher frequencies.**

Recall $\tau = \int \kappa_\nu \, ds \propto \frac{\text{EM}}{T_e^{1.5}\nu^2}$

✓ At high frequencies, $\tau \ll 1$,

$$I_\nu = B_\nu \tau \propto \frac{2kT\nu^2}{c^2}\frac{EM}{T^{3/2}\nu^2} \propto \frac{EM}{T^{1/2}} \quad \not\leftrightarrow \quad \nu$$

✓ At low frequencies, $\tau \gg 1$,

$$I_\nu = B_\nu = \frac{2kT\nu^2}{c^2}$$ Blackbody $\not\leftrightarrow$ n_e

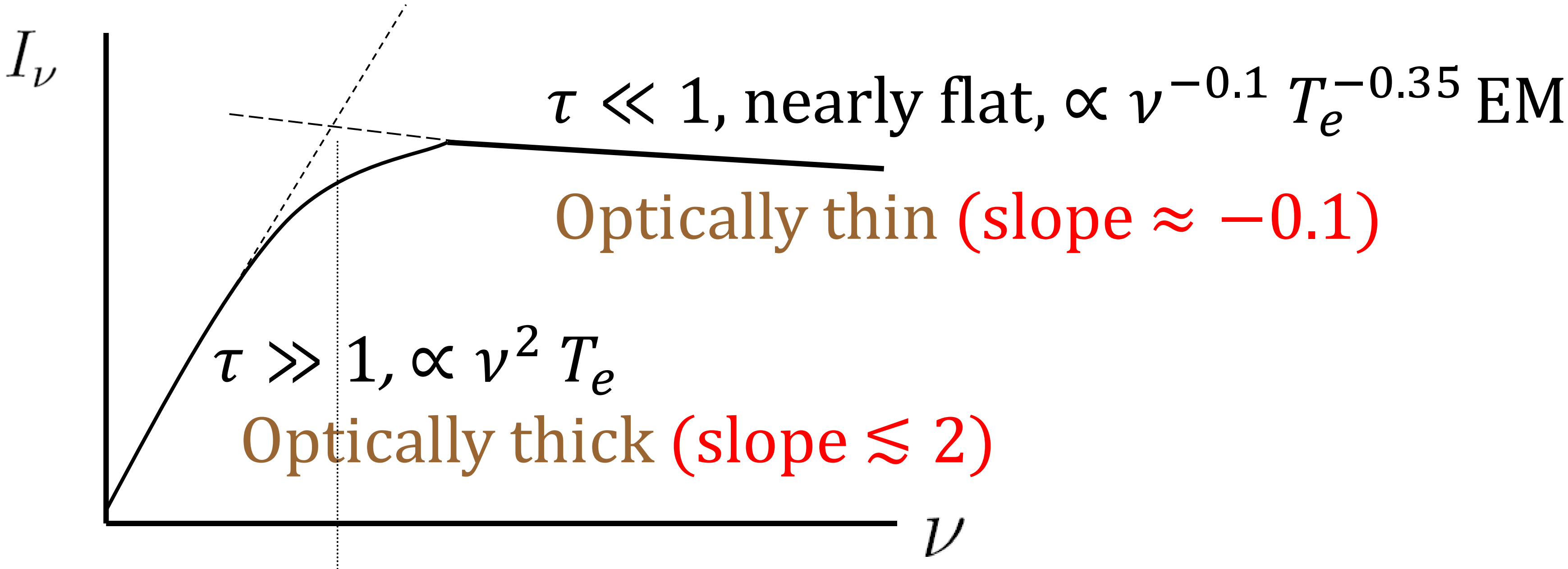

$$\tau = 1, \text{at } \nu_{\text{critical}} = 0.3\left(\frac{n_e^2 L}{T^{1.35}}\right) \text{ GHz}$$

Observations at $\tau \gg 1$, get T
Observations at $\tau \ll 1$, get n_e

Advantages of radio observations: less extinction; measures T directly at low freq.

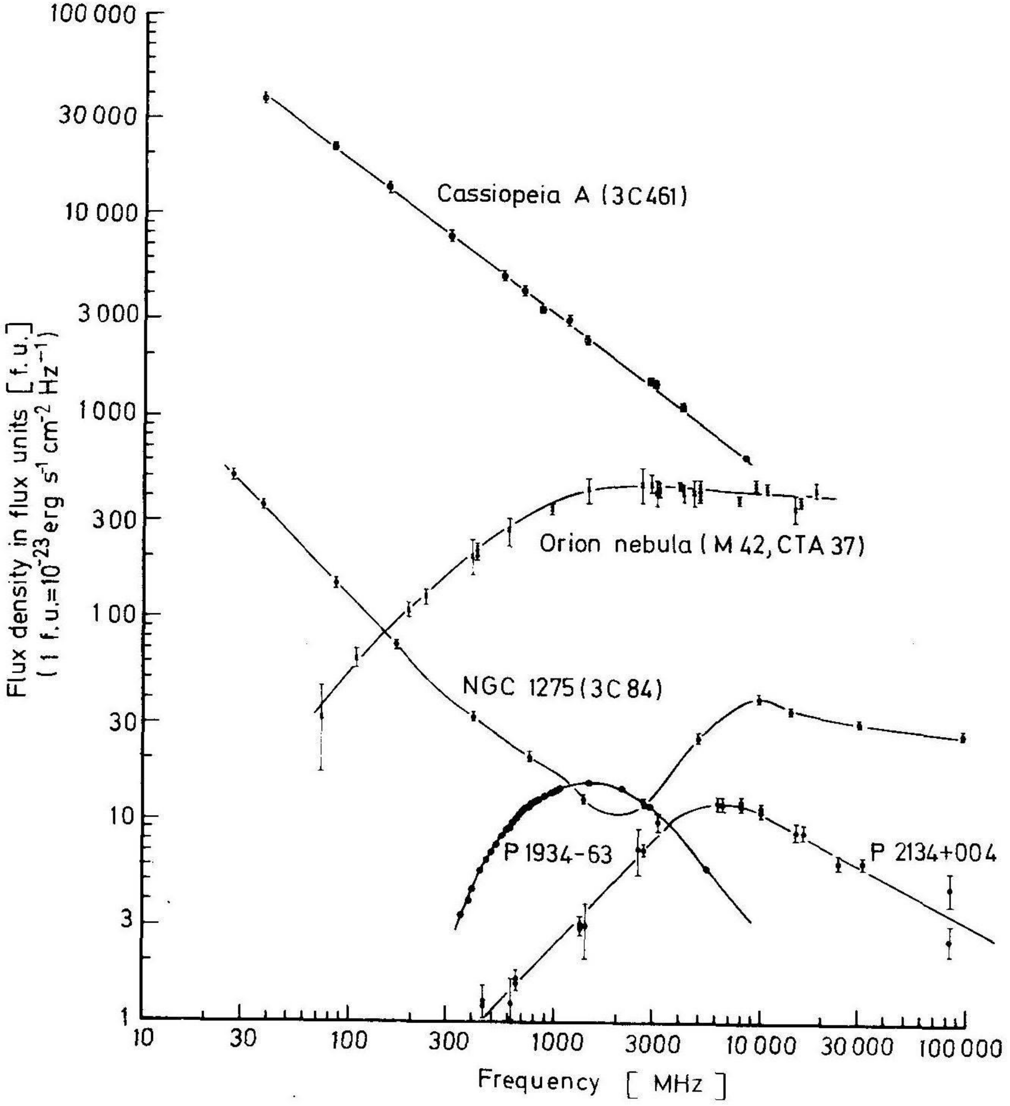

Fig. 4. Radiofrequency spectra of sources exhibiting the power law spectrum of synchrotron radiation (Casseopeia A), the flat spectrum of thermal bremsstrahlung radiation with low frequency self absorption (Orion Nebula), unusual high frequency radiation (NGC 1275), and low frequency absorption processes (P 1934 − 63 and P 2134 + 004). The data for P 2134 + 004 are from E. K. CONKLIN, and the other data are from KELLERMANN (1966), HJELLMING, and CHURCHWELL (1969), TERZIAN and PARRISH (1970), KELLERMANN, PAULINY-TOTH, and WILLIAMS (1969), and KELLERMANN *et al.* (1971)

Lang

W3= IC 1795

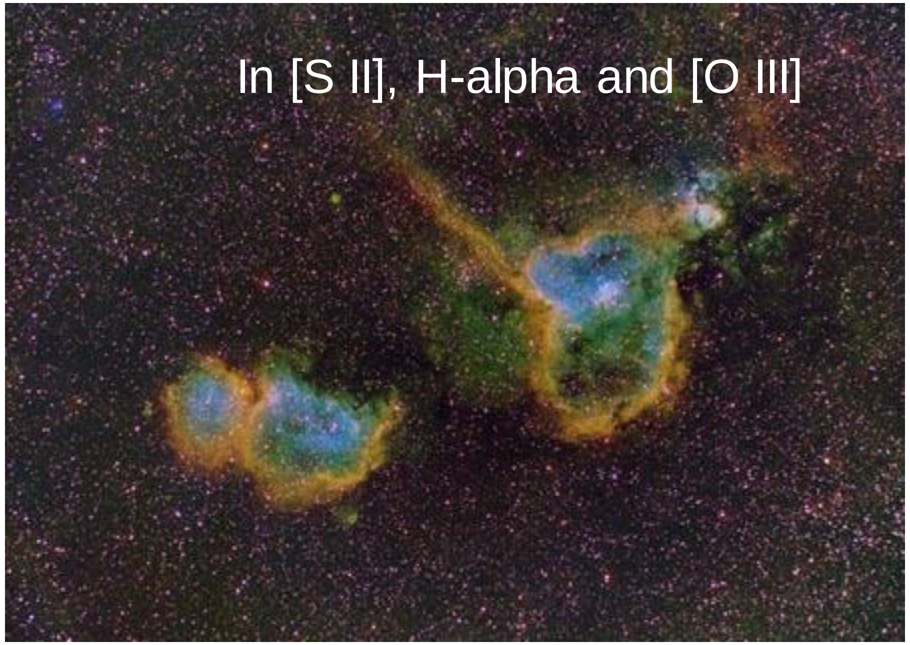

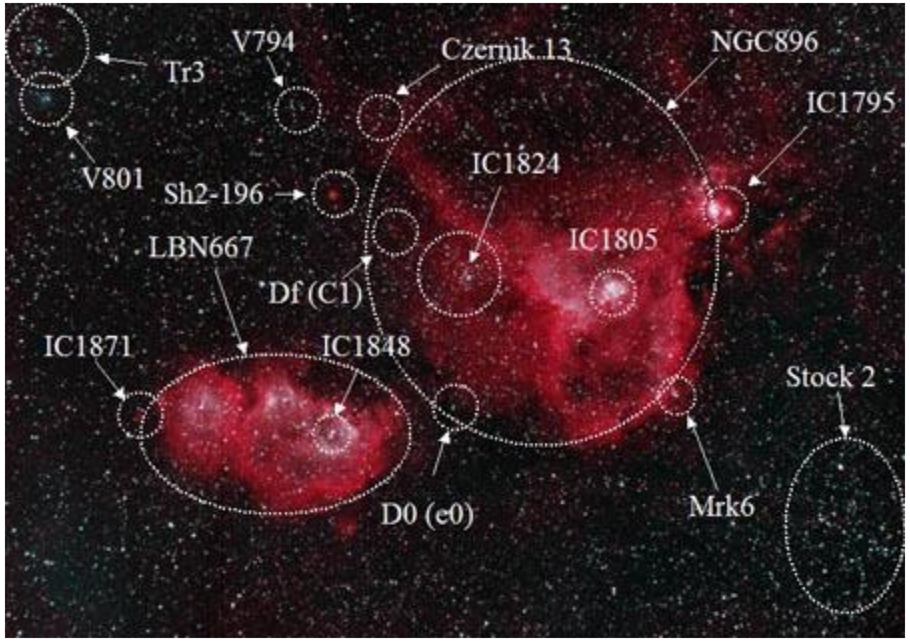

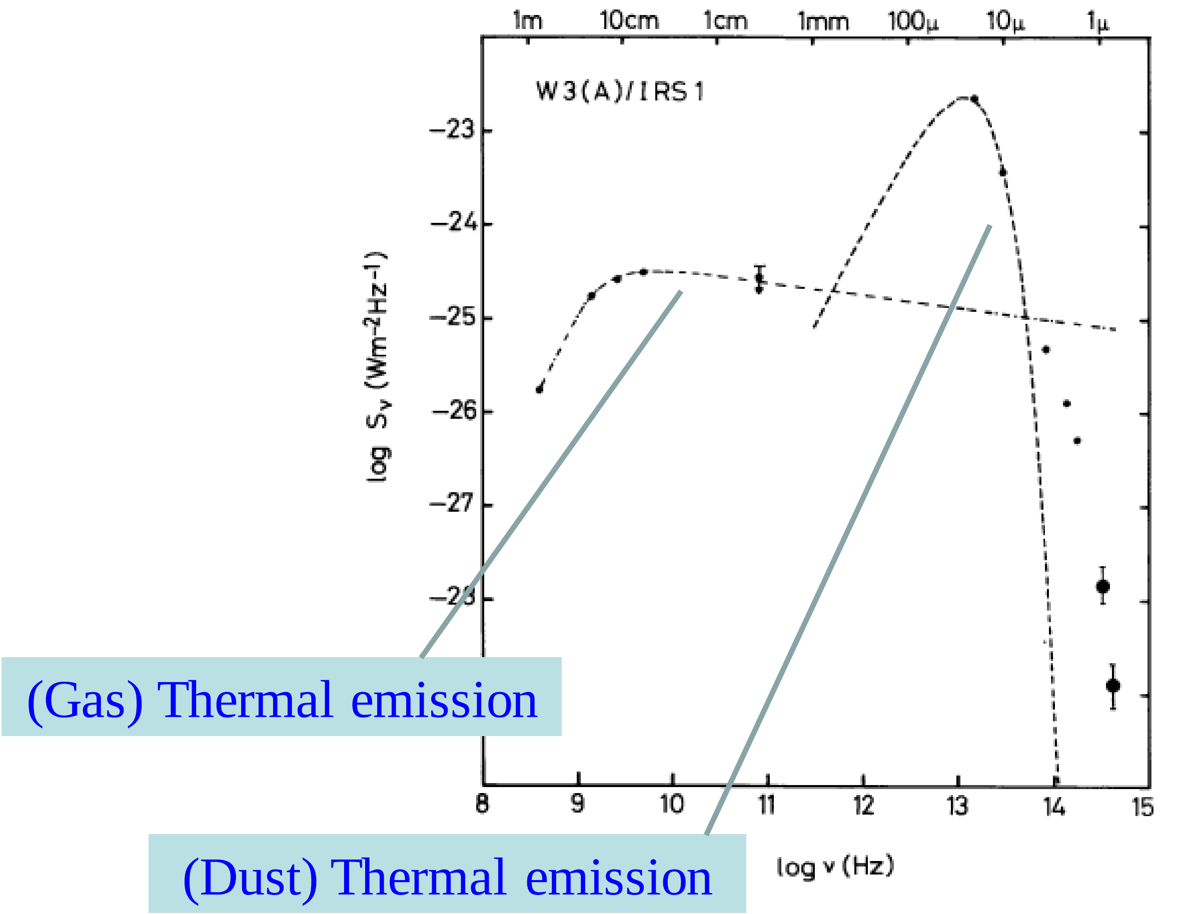

Fig. 2. Energy distribution of IRS 1 according to Wynn-Williams *et al.* (•) together with flux densities in *I* and *R* (●). Dashed lines: Predicted free-free emission from ionized hydrogen and thermal infrared radiation of dust, represented by Planck-curve with temperature $T = 200$ K

Beetz et al. (1974) A&A, 34, 335

ISM Solid State (dust grains)

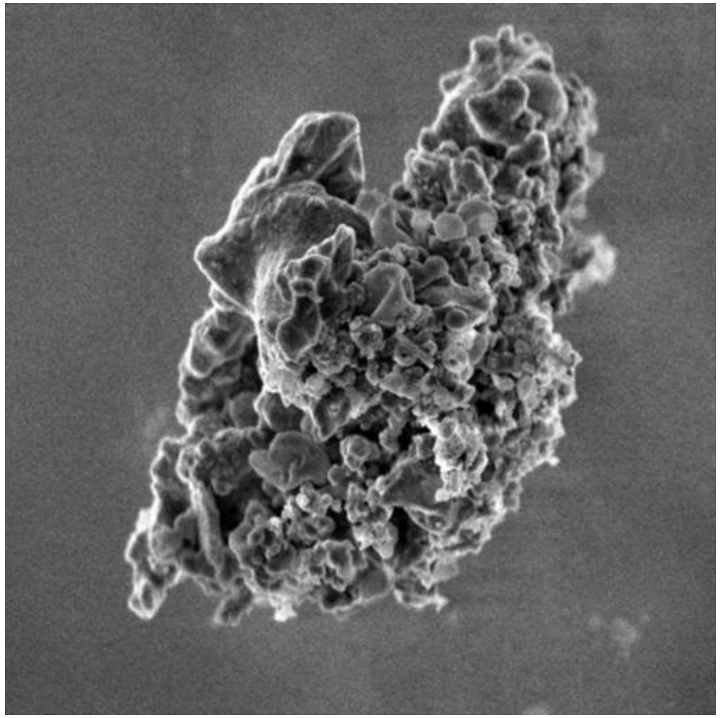

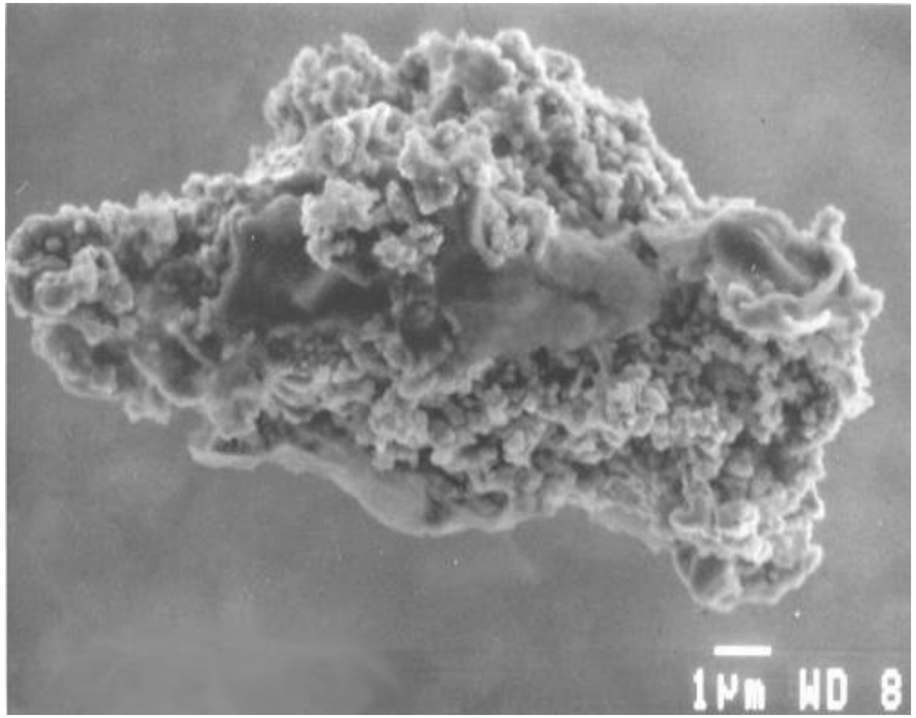

Grains appear to be loose (porous) conglomerations of smaller specks of material; stick together to grow in size.

Interstellar Extinction

<Extinction> = <Absorption> + <Scattering>

Cloud we are not aware of

Stars

Starlight dimmer and redder

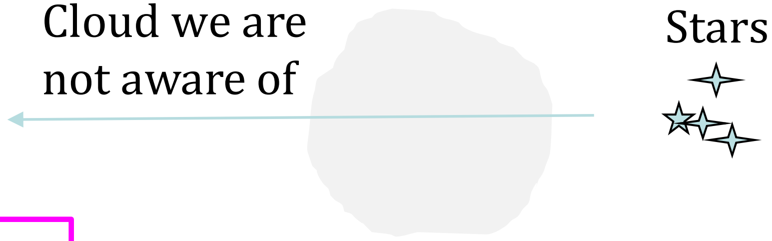

$$m_\lambda - M_\lambda = 5 \log r_{pc} - 5 + A_\lambda$$

Extinction severe in UV; much less in IR and X-rays

In UV/OIR, $A_\lambda \nearrow$ as $\lambda \searrow$

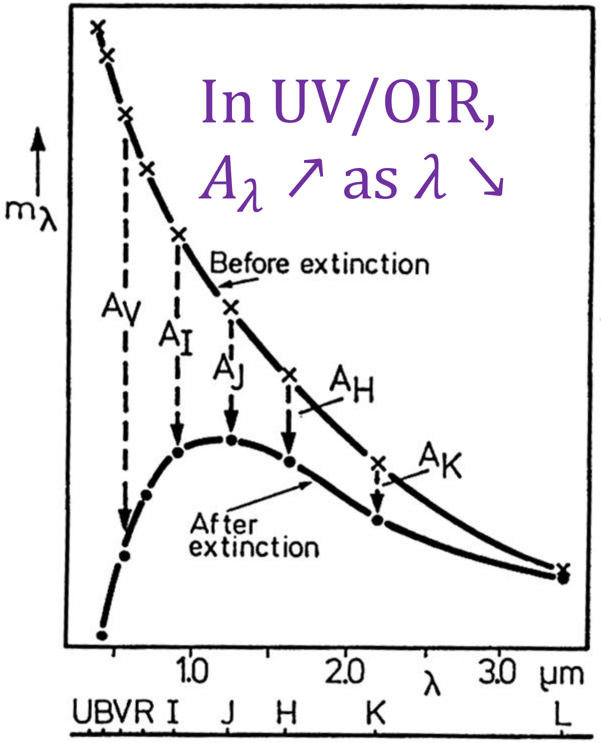

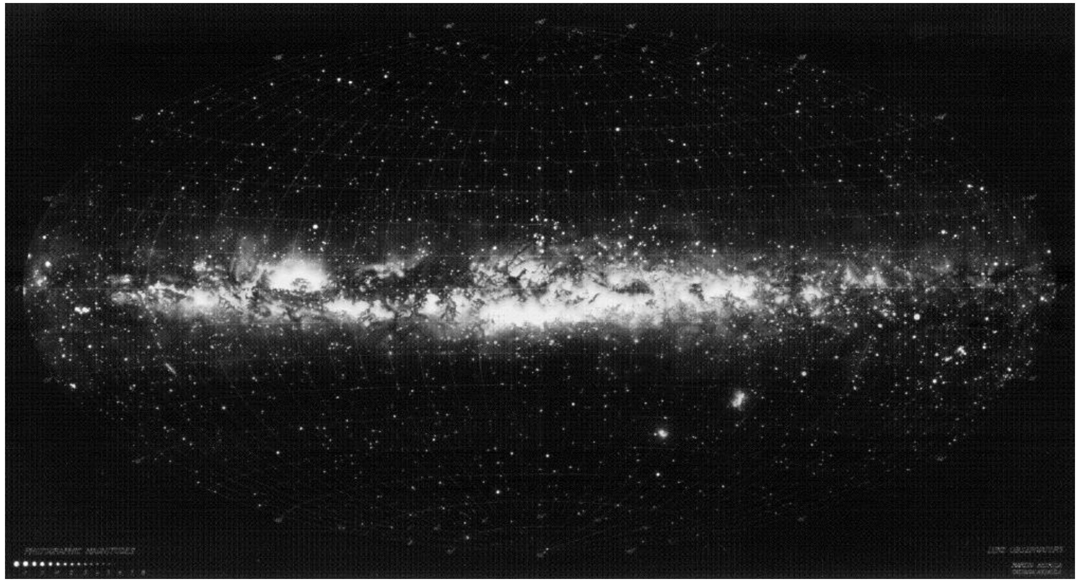

Background IR light shines through …

Pre-Collapse Black Cloud B68 (visual view)
(VLT ANTU + FORS 1)

ESO PR Photo 02a/01 (10 January 2001)

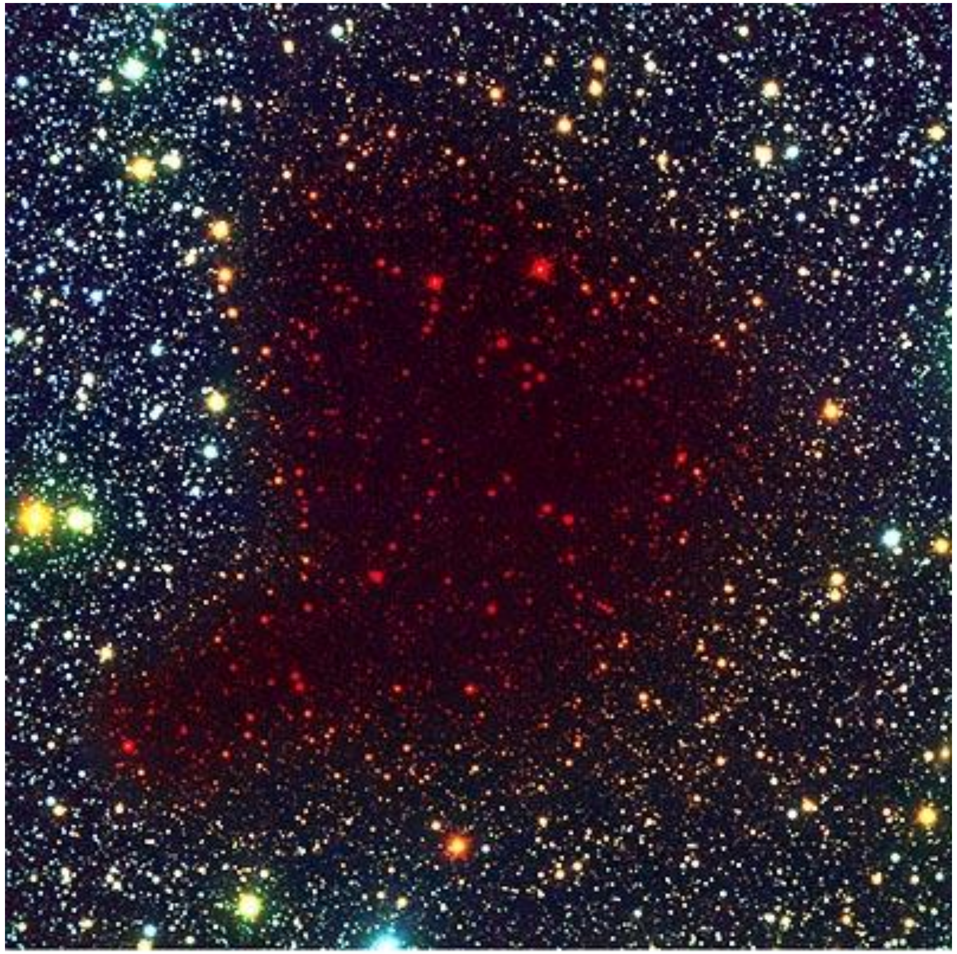

Seeing Through the Pre-Collapse Black Cloud B68
(VLT ANTU + FORS 1 - NTT + SOFI)

ESO PR Photo 02b/01 (10 January 2001)

- Dust affects our view therefore our study of celestial objects.
- Dust serves as the seed of grain growth toward planet formation.
- It is vital in cosmic energy budget (emissions from thermalized dust at long wavelengths easily escape).
- It exists in ISM (particular in cold clouds), and in cool (stellar, substellar, and planetary) atmospheres.

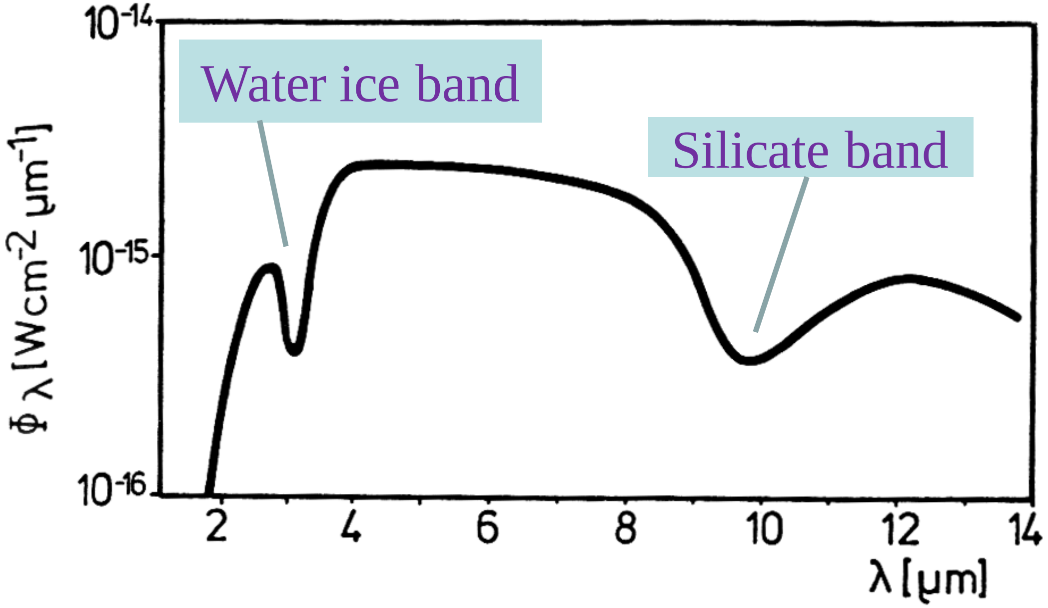

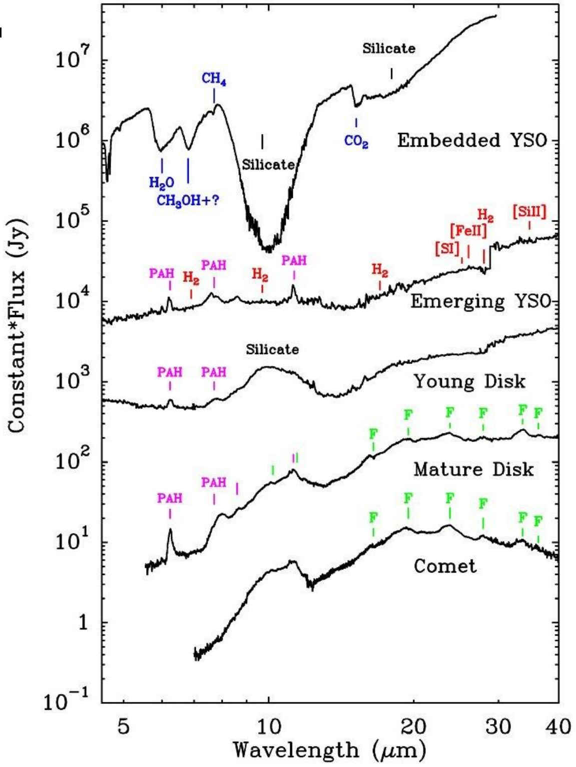

Scattering

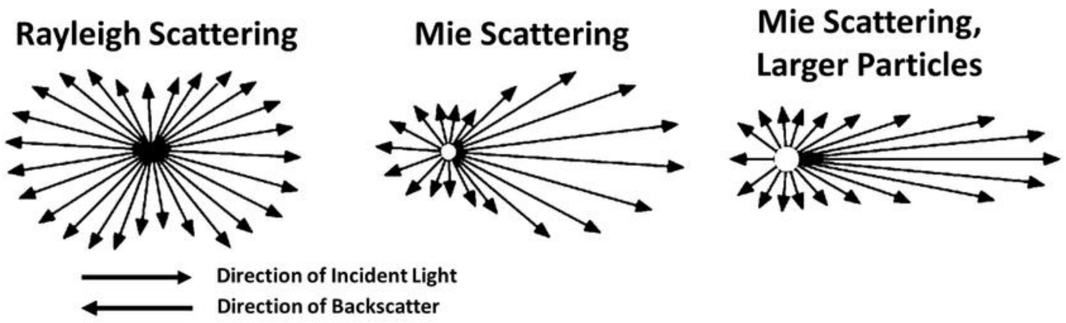

Size of particles a

- $2\pi a \ll \lambda \implies$ scattering $\leftrightarrow \lambda$

  $I_{\text{scattering}} \propto \lambda^{-4}$ (**Rayleigh scattering**)

  This is why a clear sky is blue.

- $2\pi a \gg \lambda \implies$ scattering $\not\leftrightarrow \lambda$ (cross section ~ geometric)

  $I_{\text{scattering}} \propto \lambda^{0}$

  This is why a cloudy sky is gray.

- $2\pi a \approx \lambda$ (dust $\bar{a} = 0.3\ \mu$m; λ in UV/visible)

  $I_{\text{scattering}} \propto \lambda^{-1}$

  This is interstellar reddening --- why distant/embedded stars are reddened (**interstellar reddening**).

Usually a size distribution, e.g., a power law, $n(a) \propto a^{-\beta}$

Gas and dust

In HI regions, $N(x)/N(H)$ depleted relative to atmospheres of Pop I stars $T_c \uparrow \rightarrow$ *condensed first* $\rightarrow$ *depletion* $\uparrow$

At $T \nearrow\nearrow$, grains evaporated.

... by atomic number ... by condensation temperature

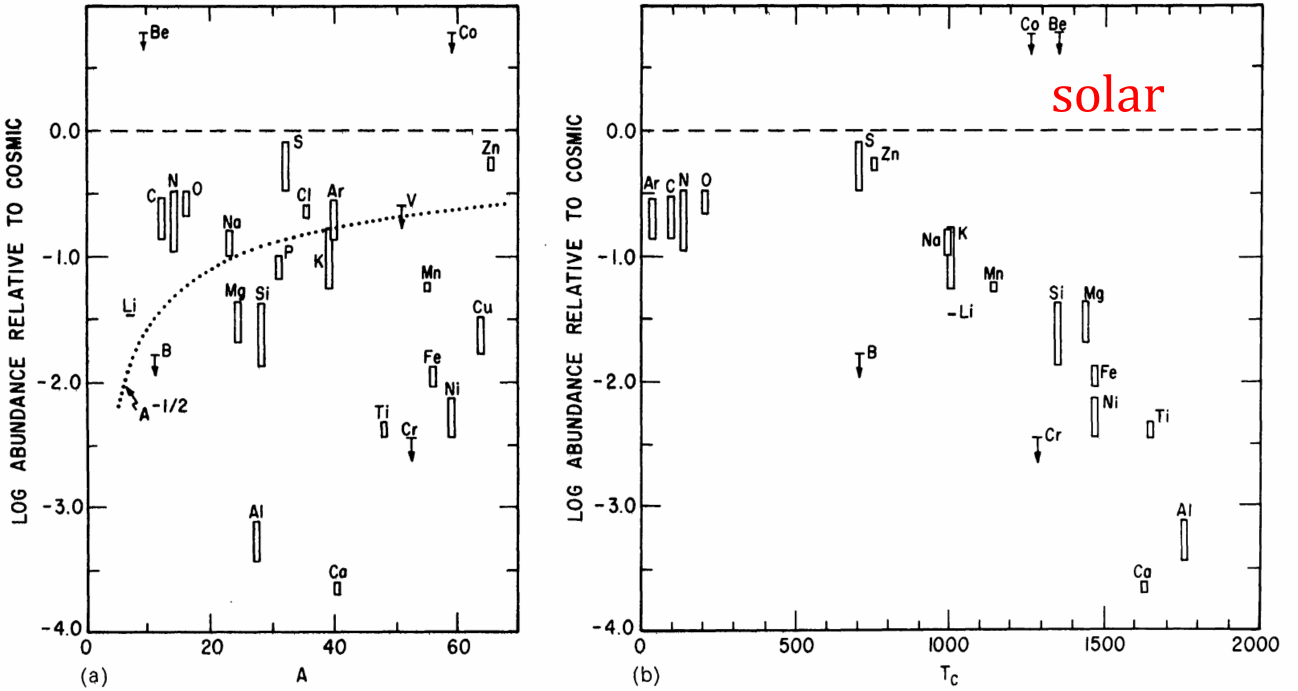

Figure 5 Depletion below solar abundances for elements in their atomic form in the H I gas toward ζ Oph, plotted against atomic mass *A* in (*a*) and condensation temperature T_c in (*b*). The vertical width of each bar represents the experimental error arising from uncertainties in the respective element's curve of growth. For grains and atoms of a given charge, the nonequilibrium accretion rate in cool interstellar clouds should be proportional to $A^{-1/2}$, illustrated by the dotted line in (*a*). All elements shown here except N, O, and Ar should be predominantly ionized in H I regions.

Field76

Polarized Starlight

Magnetic field in the ISM first discerned by linearly polarized starlight (~1%) (Hiltner 1949 and Hall 1949)

It is thought that the partial polarization of starlight is produced by <u>elongated dust grains aligned by magnetic fields</u> in the ISM

Unpolarized starlight

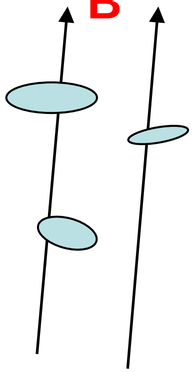

Grains preferentially spin with the minor axes $\parallel \vec{B}$

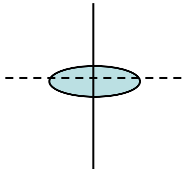

Polarized starlight observed

$$\vec{P} \parallel \vec{B}$$

A thermalized ISM elongated grain tends to spin along its minor axis: $\vec{\omega} \longrightarrow \vec{B}$

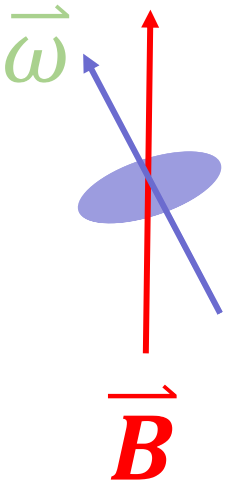

[Davis-Greenstein](http://bgandersson.net/grain-alignment) alignment mechanism --- paramagnetic dissipation

http://bgandersson.net/grain-alignment

Observations in OIR

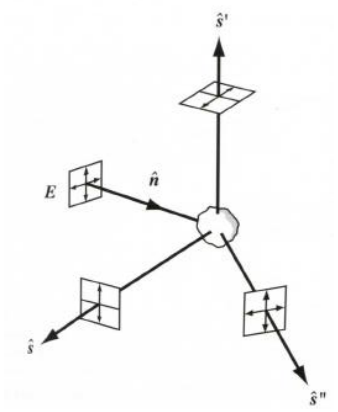

Stahler & Pallo 2004

Scattering by dust

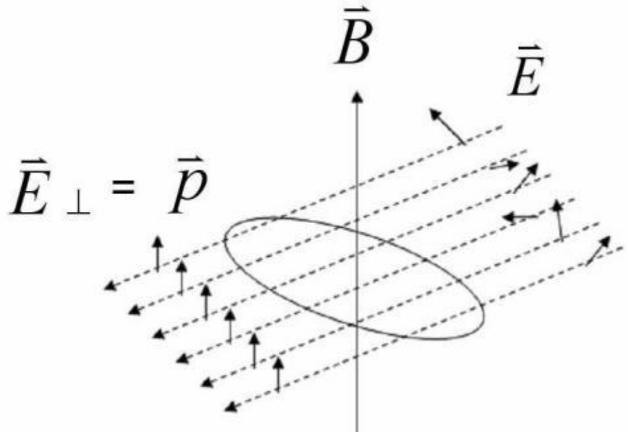

Dichroic extinction by aligned dust

Observations in FIR to mm

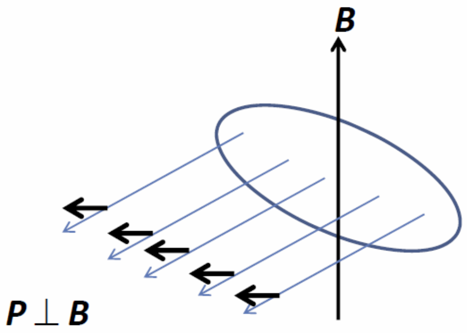

Polarized thermal emission by dust aligned by ***B***

Courtesy: Tamura

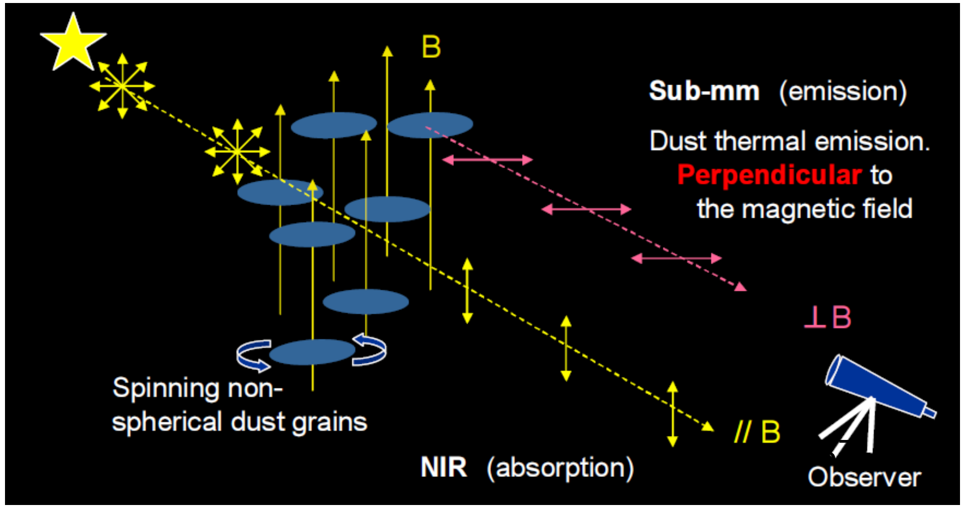

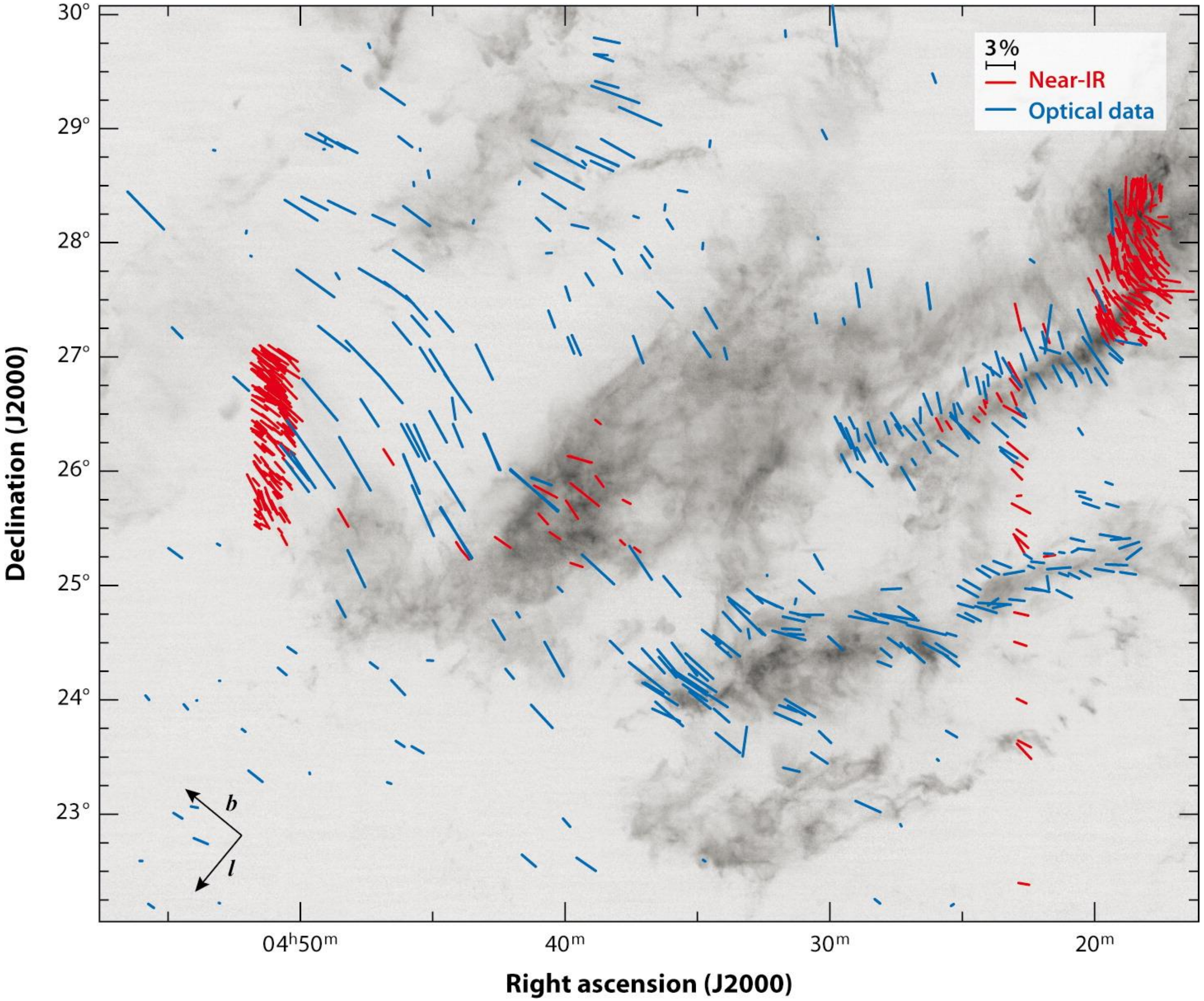

Crutcher RM. 2012.
Annu. Rev. Astron. Astrophys. 50:29–63

<u>Organized</u> magnetic field morphology in the Taurus dark-cloud complex superposed on a ^{13}CO map (Chapman et al. 2011). Blue lines show polarization measured at <u>optical</u> wavelengths and red lines show <u>near-IR</u> (*H*-band and *I*-band) polarization.

Dichroic extinction by dust (optical and near-IR) $\vec{P} \parallel \vec{B}$

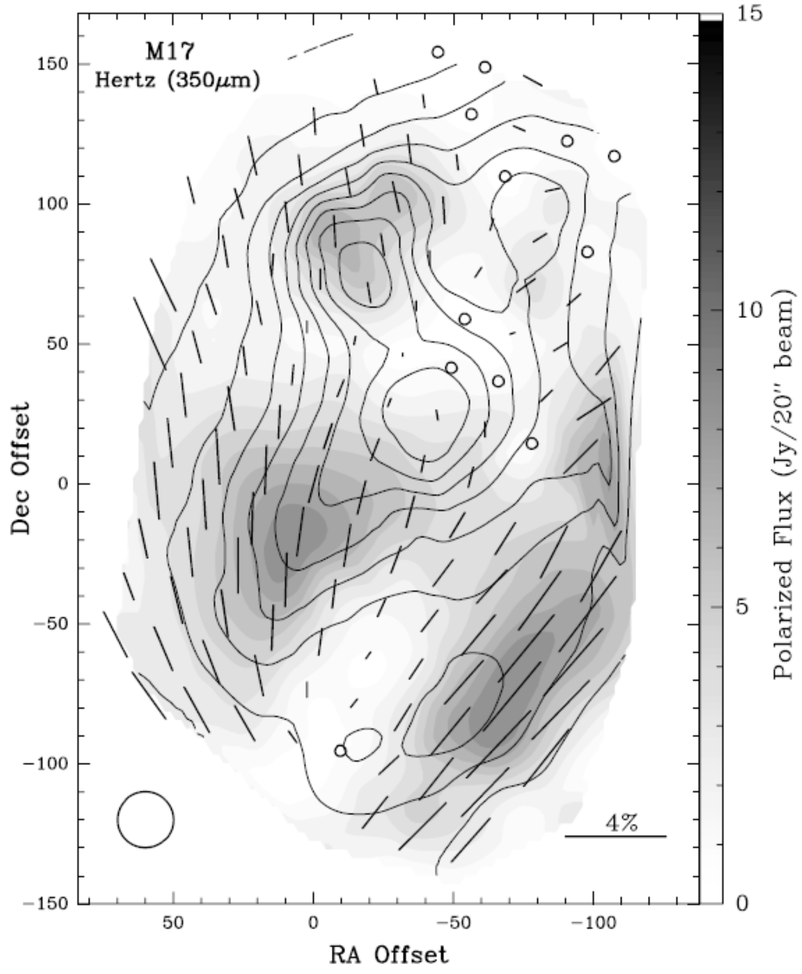

FIG. 6.—HERTZ polarization map of M17 at 350 μm. All of the polarization vectors shown have a polarization level and error such that $P > 3\sigma_P$. Circles indicate cases where $P + 2\sigma_P < 1\%$. The contours delineate the total continuum flux (from 10% to 90% with a maximum flux of ≈700 Jy), whereas the underlying gray scale gives the polarized flux according to the scale on the right. The beam width (≃20″) is shown in the lower left corner and the origin of the map is at R.A. = $18^h17^m31^s.4$, decl. = −16°14′25″.0 (B1950.0).

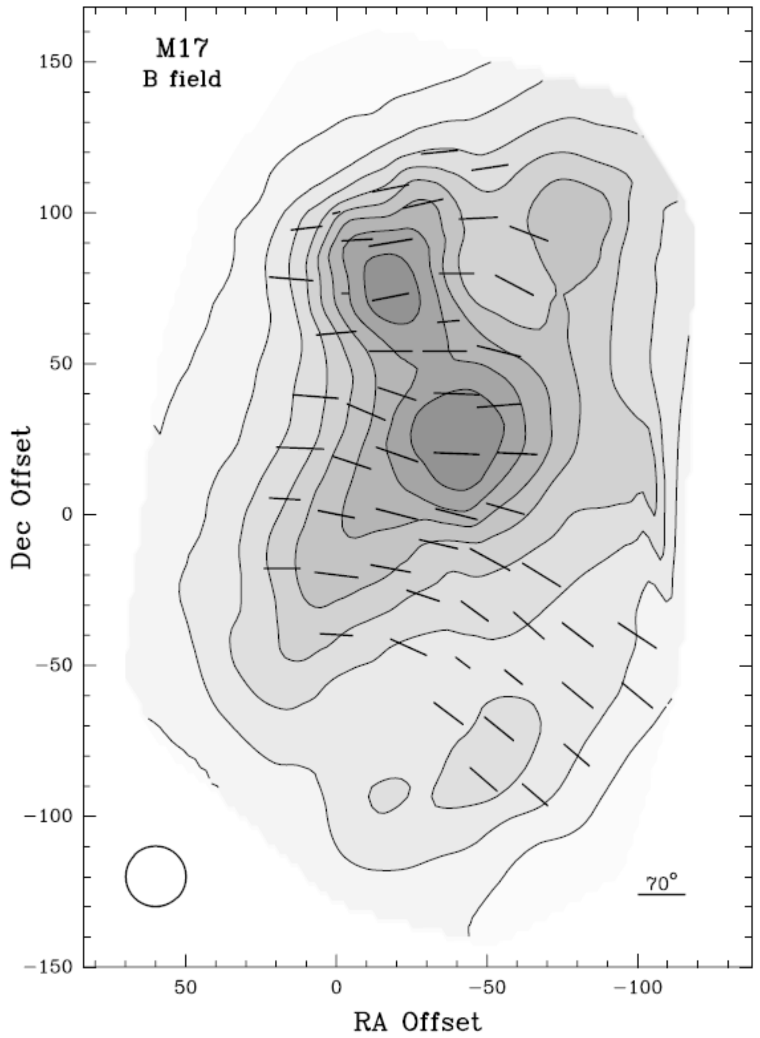

FIG. 11.—Orientation of the magnetic field in M17. The orientation of the projection of the magnetic field in the plane of the sky is shown by the vectors and the viewing angle is given by the length of the vectors (using the scale shown in the bottom right corner). The contours and the gray scale delineate the total continuum flux. The beam width (≃20″) is shown in the lower left corner, and the origin of the map is at R.A. = $18^h17^m31^s.4$, decl. = −16°14′25″.0 (B1950.0).

Thermal emission directly by dust (far-IR, and smm)

$\vec{P} \perp \vec{B}$

Houde et al. (2002)

Polarization

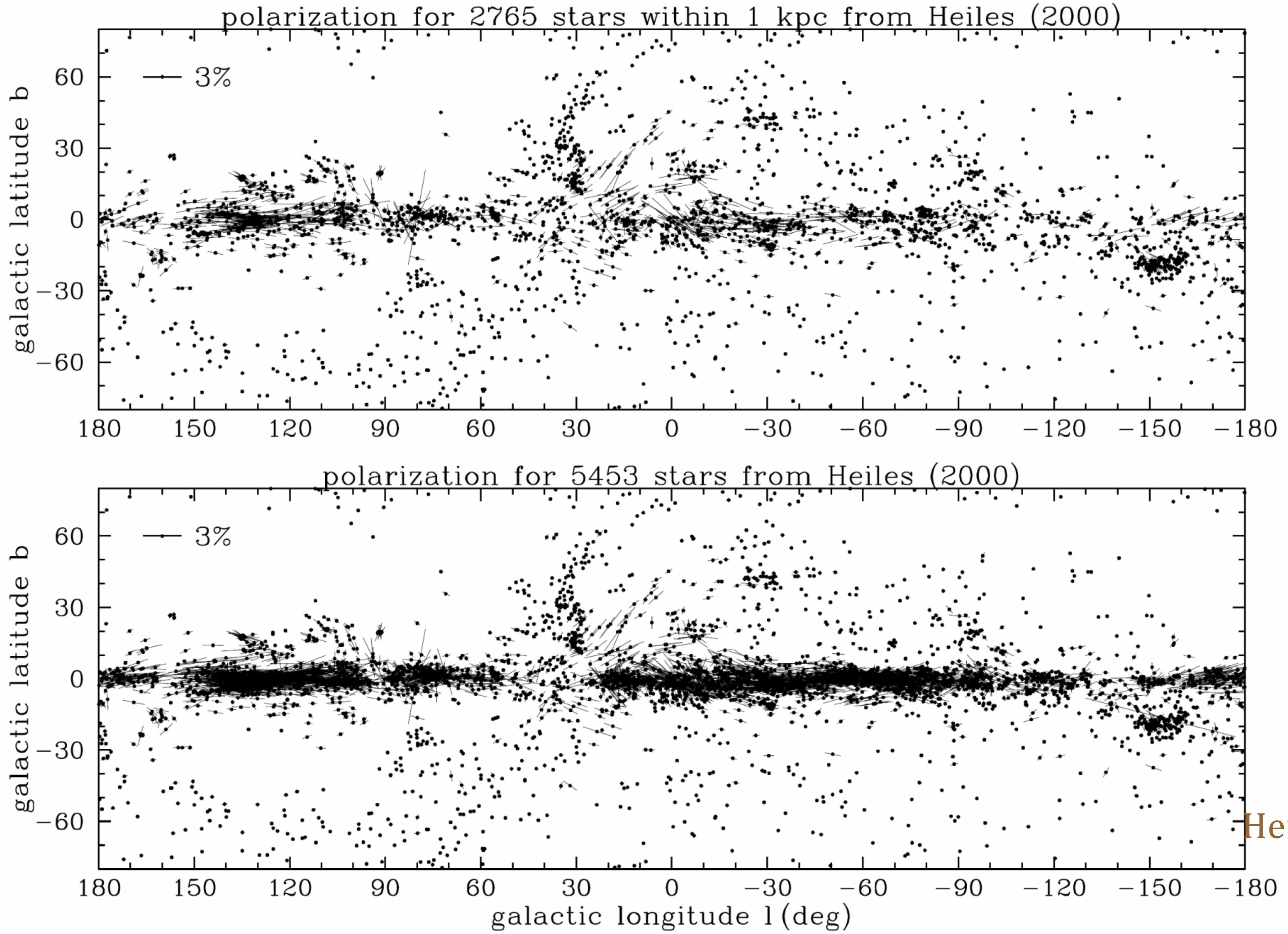

Heiles (2000)

Star Formation

- Stars are formed in dense molecular cloud cores, whereas planets are formed, contemporaneously, in young circumstellar disks.

Compression of gas from a cloud size $\sim 10^{18}$ cm (parsec) down to a stellar size $\sim 10^{11}$ cm, i.e., density increase by a factor of $\sim 10^{21}$.

$\rightarrow$ Large dynamical range in size, density, and time

Filamentary Molecular Clouds

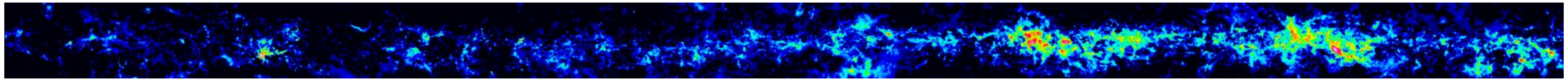

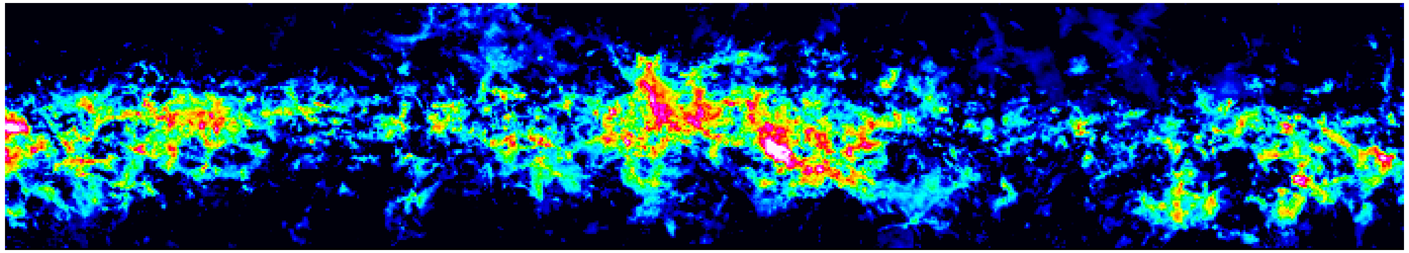

Fractal structure

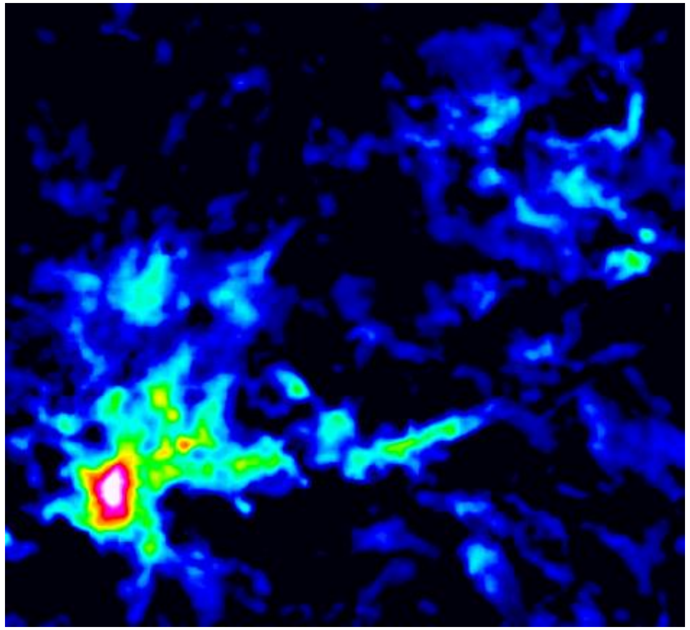

Giant Molecular Clouds

- $D = 20 - 100$ pc
- $\mathcal{M} = 10^5 - 10^6\ \mathcal{M}_\odot$
- $n \approx 10 - 300\ \mathrm{cm}^{-3}$
- $T \approx 10 - 30$ K
- $\Delta v \approx 5 - 15\ \mathrm{km}^{-1}$

Molecular clumps/ clouds/condensations

- $n \sim 10^3\ \mathrm{cm}^{-3}$, $D \sim 5$ pc, $M \sim 10^3\ \mathcal{M}_\odot$

Dense molecular cores

- $n \geq 10^4\ \mathrm{cm}^{-3}$, $D \sim 0.1$ pc, $M \sim 1 - 2\ \mathcal{M}_\odot$

http://www.bu.edu/galacticring/outgoing/PressRelease/

H_2 (dihydrogen, molecular hydrogen)

- It is the main constituent of cold clouds; not important in stars, except in the coolest substellar objects (brown dwarfs or planetary-mass objects)
- Lacking a **permanent electric dipole moment**, cold H_2 is very difficult to detect. A rotationally excited molecule would radiate through a relatively slow electric quadrupole transition.
- Only in a heated medium (e.g., a photodissociation PDR region between HII and a molecular cloud) where stellar radiation or stellar wind excites vibrational and electronic states which then decay relatively quickly.

$\mathcal{E}_{\text{dissociation}} = 4.48 \text{ eV; H} - \text{H bond}$

https://en.wikipedia.org/wiki/Bond-dissociation_energy

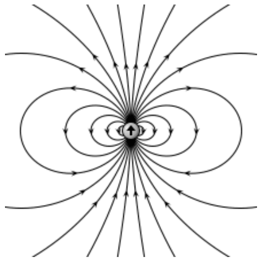

Zero electric dipole moment

CO molecules

- Simple and most abundant next to H_2
- Strong $\mathcal{E}_{\text{dissociation}}$ =11.16 eV; $\mathrm{C} \equiv \mathrm{O}$, strongest bond among neutral molecules, self-shielding against stellar UV field
- with a permanent electric dipole moment; radiating strongly at radio frequencies.
- $^{12}C^{16}O$ easiest to detect; isotopes $^{13}C^{16}O$, $^{12}C^{18}O$, $^{12}C^{17}O$, $^{13}C^{18}O$ useful as diagnosing tools
- Low critical density for excitation → CO used to study large-scale distribution of clouds, as a tracer of H_2, $n(\mathrm{CO}) \approx 10^{-4} n(\mathrm{H_2})$

$$n^*_{NH_3} \approx 10^3\ \mathrm{cm^{-3}} \qquad n^*_{HCN} \approx 10^5\ \mathrm{cm^{-3}}\ (\text{for } J = 1 \rightarrow 0)$$

- $^{12}C^{16}O$ almost always **optically thick**.
  so brightness temperature ≈ molecular gas kinetic temperature, i.e., little dependence on column density

- Lines from rarer isotopes usually **optically thin**
  → estimate of column density (total mass) of molecular gas
  $N_H = 10^6\, N_{^{13}CO}$

  Intensity ratios of optically thin lines from different J levels → excitation temperature

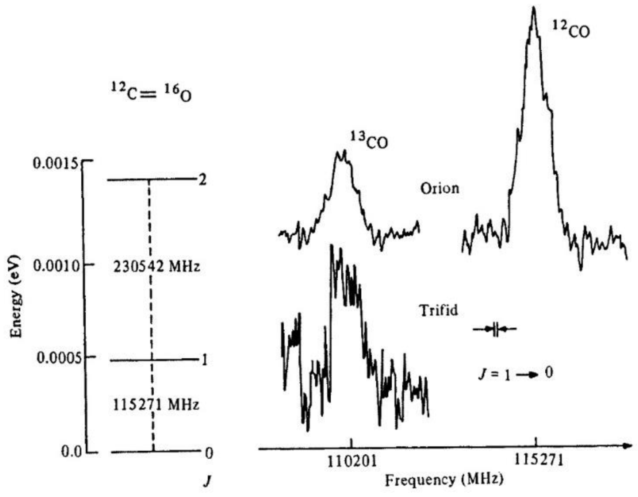

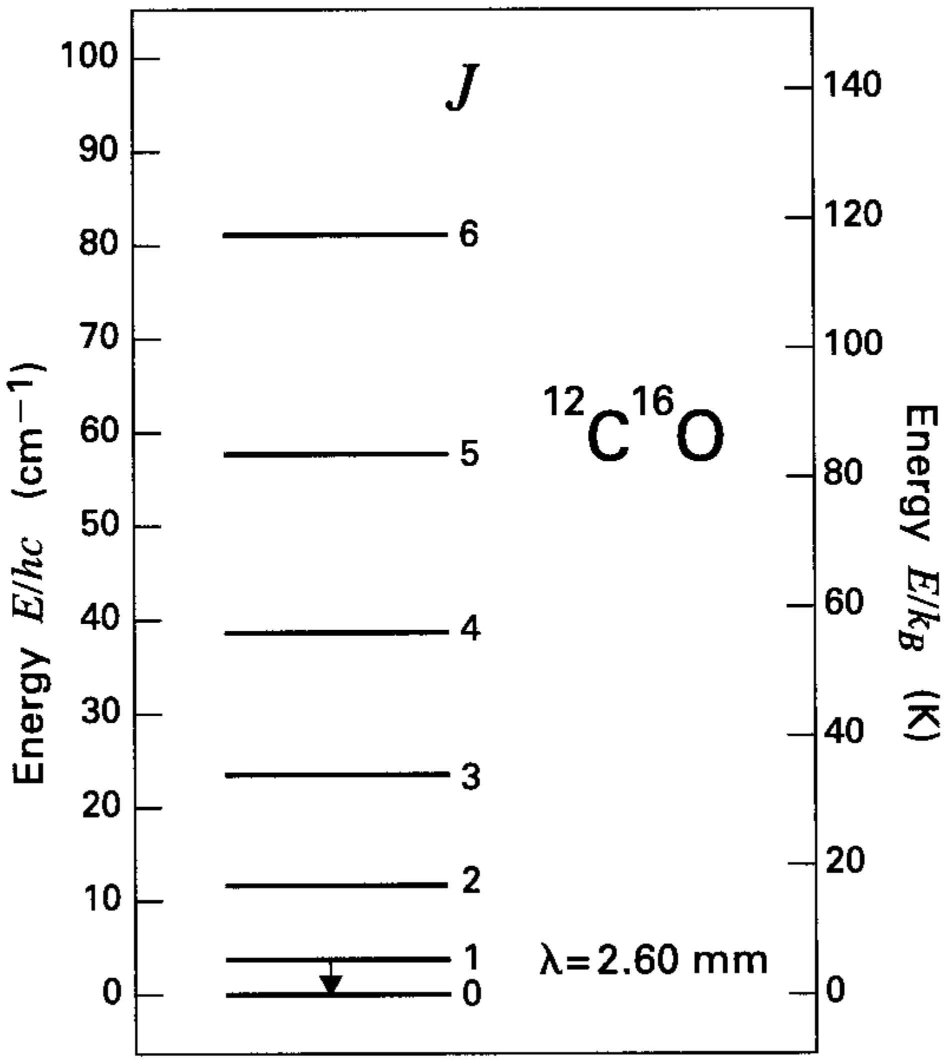

Figure 5.6 Rotational levels of $^{12}C^{16}O$ within the ground ($v = 0$) vibrational state. The astrophysically important $J = 1 \rightarrow 0$ transition at 2.60 mm is shown.

$J = 1 - 0$, 2.60 mm = 115 GHz

Only 5 K above the ground level … can be excited by collisions with ambient molecules or CMB photons

$J = 2 - 1$, 1.30 mm
$J = 3 - 2$, 0.87 mm

$J = 1 - 0$, 2.67 mm for $^{12}C^{17}O$
2.72 mm for $^{13}C^{16}O$

Stahler & Palla

Stars form in groups → seen as a star cluster if the group survives disintegration and remains gravitationally bound. Groups of young stellar objects are found in the dense regions of the molecular clouds (*dense molecular clouds*).

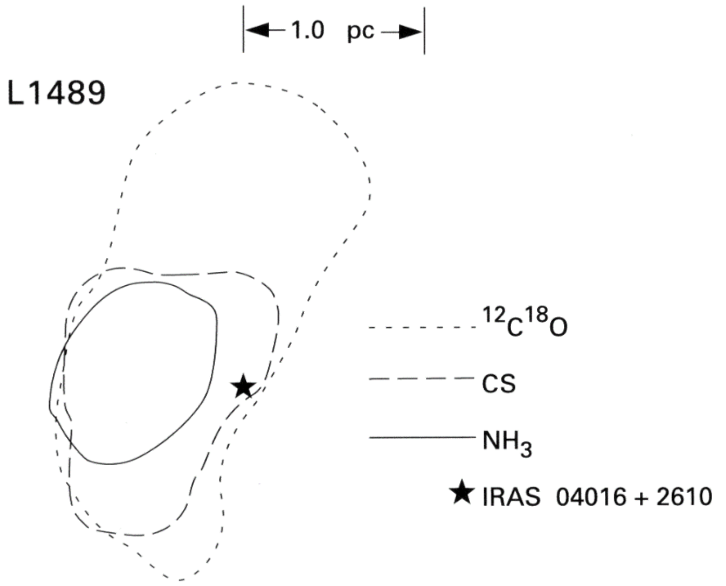

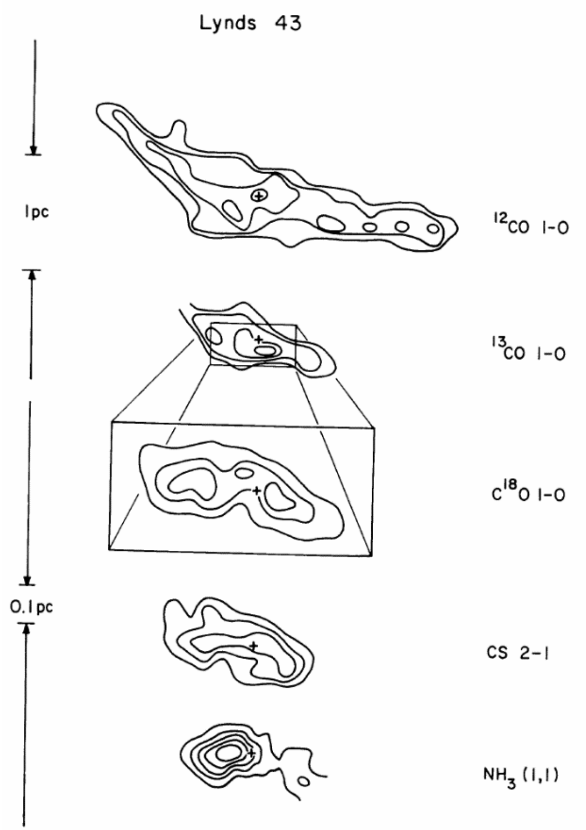

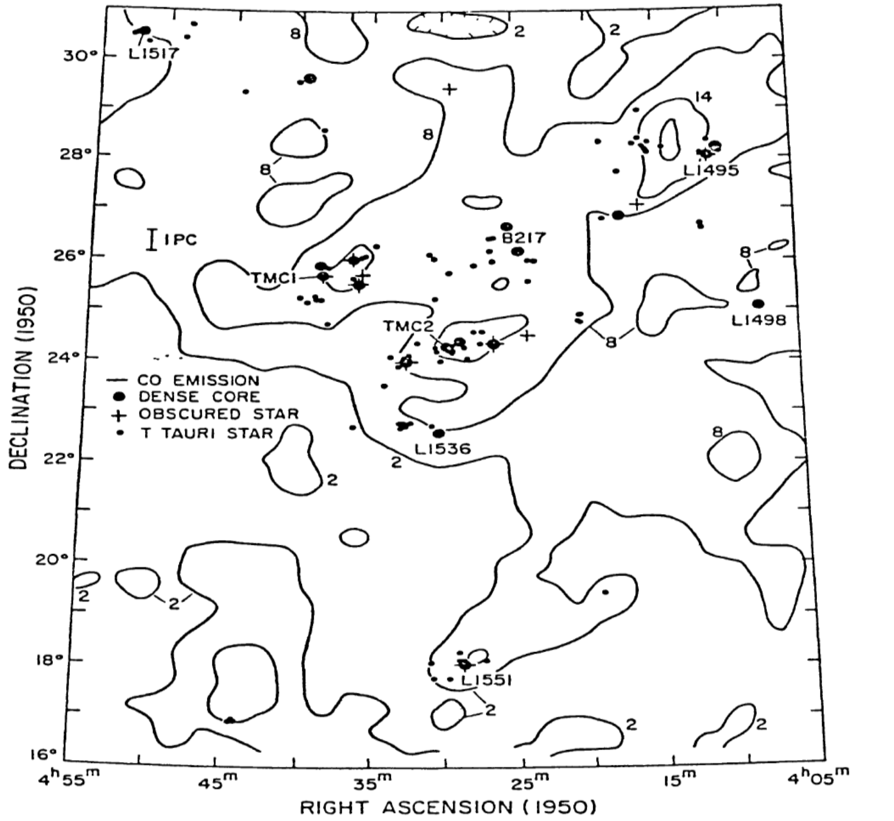

Figure 2 CO contour map of the Taurus molecular cloud with positions of dense NH_3 cores, embedded infrared sources, and visible T Tauri stars (from Myers 1986).

Molecular clouds observed by different tracers …

Taurus molecular cloud

Nearby Examples

Massive Star-Forming Regions

- *Per OB2* (350 pc)
- *Orion OB Association* (350--400 pc) … rich

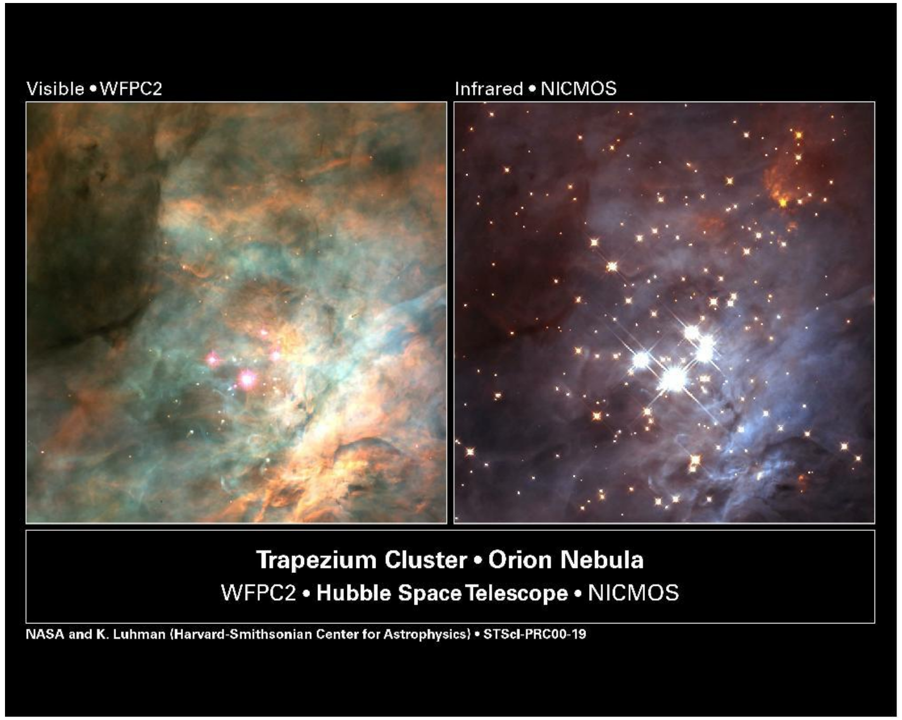

Low-Mass Star-Forming Regions

- *Taurus Molecular Cloud (TMC-1)* (140 pc)
- *Rho Ophiuchi cloud* (130 pc)
- *Lupus* (140 pc)
- *Chamaeleon* (160 pc)
- *Corona Australis* (130 pc)

} 4/5 in the southern sky … why?

Stability: The Virial Theorem

In a spherically symmetric cloud of temperature T, for each particle, the equation of motion is $\boldsymbol{F}_i = m_i \ddot{\boldsymbol{r}}_i = \dot{\boldsymbol{p}}_i$, the momentum change with time.

Sum up all particles and take time derivative

$$\frac{d}{dt}\sum_i \boldsymbol{p}_i \cdot \boldsymbol{r}_i = \sum_i \dot{\boldsymbol{p}}_i \cdot \boldsymbol{r}_i + \sum_i \boldsymbol{p}_i \cdot \dot{\boldsymbol{r}}_\mathrm{i}$$

$$= \sum_i \boldsymbol{F}_i \cdot \boldsymbol{r}_i + \sum_i m_i \dot{\boldsymbol{r}}_i \cdot \dot{\boldsymbol{r}}_\mathrm{i}$$

$$= E_p + 2E_k$$

$$\frac{d}{dt}\sum_i m_i \dot{r}_i \cdot r_i$$

$\sum_\mathrm{i} \boldsymbol{F}_i \cdot \boldsymbol{r}_i$ = virial of Clausius

For moment of inertia, $I = \sum_i m_i \, r_i^2$,

$$\frac{d^2 I}{dt^2} = \frac{d}{dt}\left[\sum_i m_i 2\, r_i\, \dot{r}_i\right]$$

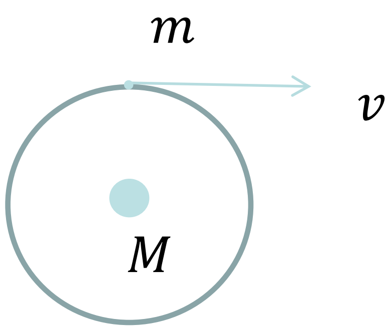

Hence

$$\frac{1}{2}\frac{d^2 I}{dt^2} = 2E_k + E_p$$

$$\frac{GmM}{r^2} = m\frac{v^2}{r}$$

To be stable, LHS = 0

$$2E_k + E_p = 0$$

$$2\left({}^{1}/_{2}\right) mv^2 = GmM/r$$

$\mathrm{LHS} = 0$ → stable

$\mathrm{LHS} < 0$ → collapsing

$\mathrm{LHS} > 0$ → expanding

$\boldsymbol{E_K}$ **a variety of <u>kinetic</u> energies**

- ✓ Kinetic energy of molecules
- ✓ Bulk motion of clouds
- ✓ Rotation
- ✓ …

$\boldsymbol{E_P}$ **a variety of <u>potential</u> energies**

- ✓ Gravitation
- ✓ Magnetic field
- ✓ Electrical field
- ✓ …

<u>Note</u>:

Virial theorem governs the motion status,
whereas the total energy

$$\boldsymbol{E_{\text{total}} = E_K + E_P}$$
$$\boldsymbol{= E_K + \Omega \;(\text{mostly})}$$

governs whether the system is dynamically bound.

A tossed coin (less than the escape velocity) is bound either upward or downward.

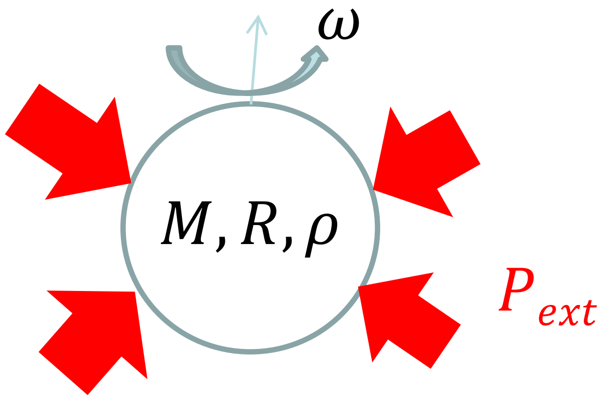

Cloud of mass M, radius R, rotating at ω

$$E_{rot} = \frac{1}{2} I \omega^2 \qquad I = \frac{2}{5} M R^2 \qquad \Omega = -\frac{3}{5}\frac{GM^2}{R}$$

Generalized virial theorem

$$\frac{1}{2}\frac{d^2 I}{dt^2} = 2 < E_K > + \int \vec{r}\cdot\vec{F} dm + 3\int P dV - \oint P\vec{r}\cdot d\vec{s}$$

If $\omega = 0$, and $P_{ext} = 0$ $\qquad 2\cdot\frac{3}{2}\frac{M}{\mu m_H} kT - \frac{3}{5}\frac{GM^2}{R} = 0$

$$R_J = \frac{1}{5}\frac{GM\mu m_H}{kT}$$

This is the **Jeans length**.

$\mu \approx 2.37$ for solar abundance with H_2

Jeans length = critical spatial wavelength (length scale)

If the perturbation length scale is longer

→ Medium is decoupled from self-gravity ➔ stable

$$M_J = \frac{4}{3}\pi R_J^3\,\rho \qquad R_J = \left(\frac{15}{4\pi}\frac{kT}{\mu m_H G\rho}\right)^{1/2} \sim \sqrt{\frac{T}{\rho}}$$

$$M_J = \left(\frac{\pi kT}{4\mu m_H G}\right)^{3/2}\sqrt{\frac{1}{\rho}} \sim \frac{T^{3/2}}{\rho^{1/2}}$$

This is the **Jeans mass** …
the **critical** mass for onset of gravitational collapse

If cloud mass $M > M_{\text{Jeans}}$ ➔ cloud collapse

Note the above does not consider external pressure, or other internal supporting mechanisms.

A non-magnetic, isothermal cloud in equilibrium with external pressure → a **Bonnor-Ebert sphere** (Bonnor 1956, Ebert 1955)

$$2E_K + E_P - 3P_{\text{ext}}V = 0$$

The potential term may include, other than the gravity, also rotation, magnetic field, etc.

At first, the cloud is optically **thin**.

Contraction → density ↑ → collisions more frequent
→ molecules excited and radiating → photons escaped
→ cooling → less resistance to the contraction
➔ cloud collapse (free fall)

$R_J \approx c_s \, \tau_{\text{ff}}$ = [isothermal sound speed] * [free fall time]

To maintain $2E_K + E_P = 0$, <u>the total energy</u> $E_t = E_K + E_P$ <u>must change</u>. The gravitational energy

$$\Omega \sim -\frac{GM^2}{r} \longrightarrow d\Omega \sim \frac{dr}{r^2}$$

For contraction, $dr < 0$, so $d\Omega < 0$, then

$$dE_t = dE_k + d\Omega = {}^1/_2 \, d\Omega = Ldt$$

This means to maintain quasi-static contraction, **half** of the gravitation energy from the contraction is radiated away.

Eventually the cloud becomes dense enough (i.e., optically **thick**) and contraction leads to temperature increase.

The cloud's temperature increases while energy is taken away
→ negative heat capacity

Numerically,

$$M_J = 1.0 \left(\frac{T}{10\ \mathrm{K}}\right)^{3/2} \left(\frac{n_{\mathrm{H}_2}}{10^4\ \mathrm{cm}^{-3}}\right)^{-1/2} \quad [\mathcal{M}_\odot]$$

- <u>H I clouds</u>

  $T \approx 100$ K, $n_H \approx 100$, $R_J \approx 25$ pc; $M_J \approx 300\ \mathcal{M}_\odot > M_{\mathrm{obs}}$

  So H I clouds are <u>not</u> collapsing.

- <u>Dark molecular clouds</u>

  $T \approx 15$ K, $n_H \approx 10^5$, $M_J \approx 20\ \mathcal{M}_\odot < M_{\mathrm{obs}} \approx 100{-}1000\ \mathcal{M}_\odot$

  So H_2 clouds (dense cores and Bok globules) should be on the verge of collapsing. But observations show that most are not. → Additional support, e.g., thermal pressure, e.g., rotation, magnetic field, turbulence, etc.

Recall $M_J \approx 1.2 \times 10^5 \left(\frac{T}{100\ K}\right)^{3/2} \left(\frac{\rho_0}{10^{-24}\ \mathrm{g\ cm^{-3}}}\right)^{-1/2} \frac{1}{\mu^{3/2}}\ [M_\odot]$

$$\propto T^{3/2}/\rho^{1/2}$$

A small/decreasing M_J favors cloud collapse.

During collapse, ρ always ↑, so the behavior of M_J depends on T.

Optically thin → gravitational energy radiated away, **isothermal** collapse, T = const, so $M_J \propto \rho^{-1/2}$ ➔ collapse continues, local M_J ↓ → subregions become unstable and continue to collapse to ever smaller M_J (**fragmentation**)

Until optically thick, **adiabatic** contraction →T ↗↗ → stars

Formation of a cluster of stars ~~

Equation of motion for a spherical surface at r is

$$\frac{d^2r}{dt^2} = -\frac{GM}{r^2}$$

Dimensional analysis yields

$$\frac{R}{t^2} \sim \frac{GM}{R^2} \Longrightarrow t_{ff} \sim \frac{1}{\sqrt{G\rho}}$$

More accurately, $\boxed{t_{\rm ff} = \left(\frac{3\pi}{32\, G\rho_0}\right)^{\frac{1}{2}}} = \frac{3.4 \times 10^7}{\sqrt{n_0}}$ [yr] $=$ $35/\sqrt{\rho}_{\rm cgs}$ [min]

It takes the Sun ~30 minutes to collapse (the **free-fall time scale**).

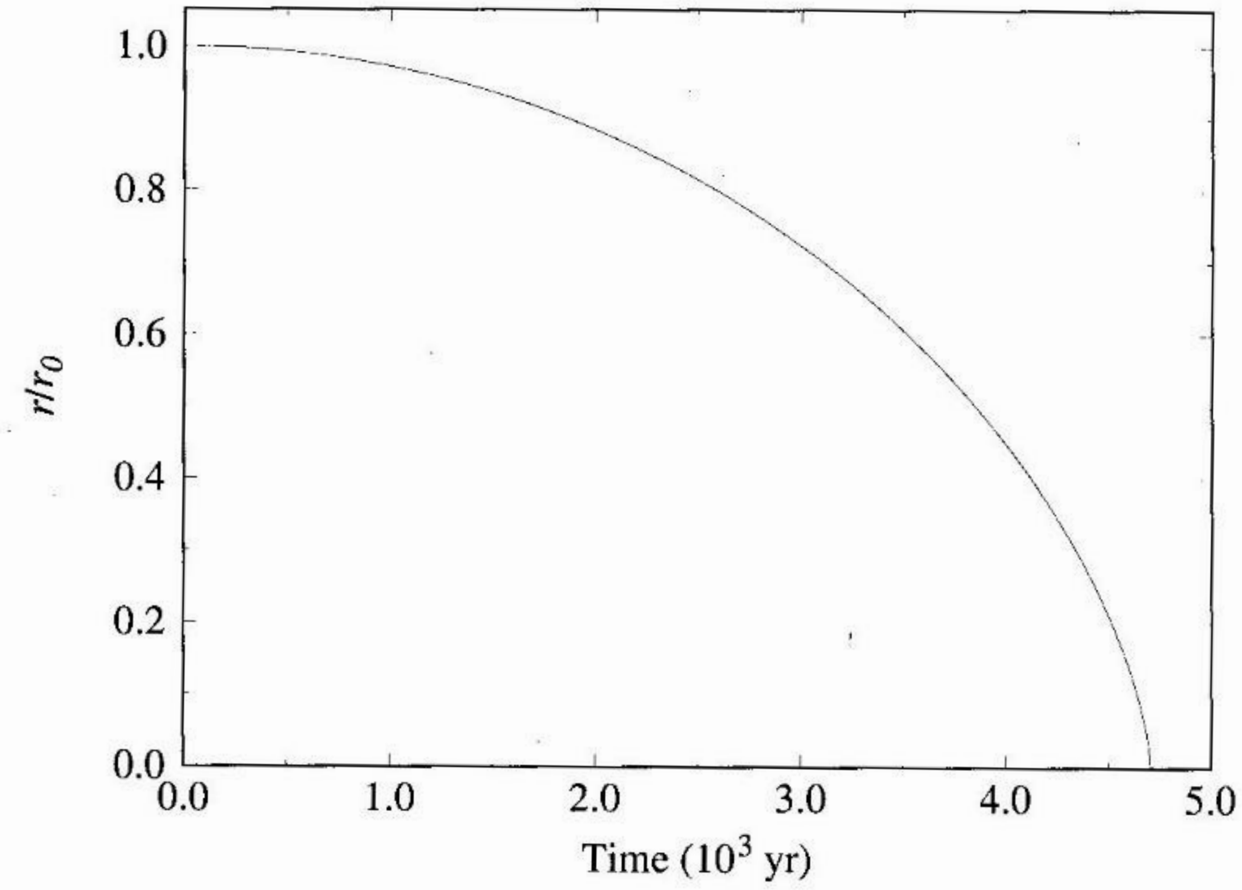

Figure 12.5 The ratio of the radius relative to its initial value as a function of time for the homologous collapse of a molecular cloud. The collapse is assumed to be isothermal, beginning with a density of $\rho_0 = 2\times10^{-16}$ g cm^{-3}.

Carroll & Ostlie

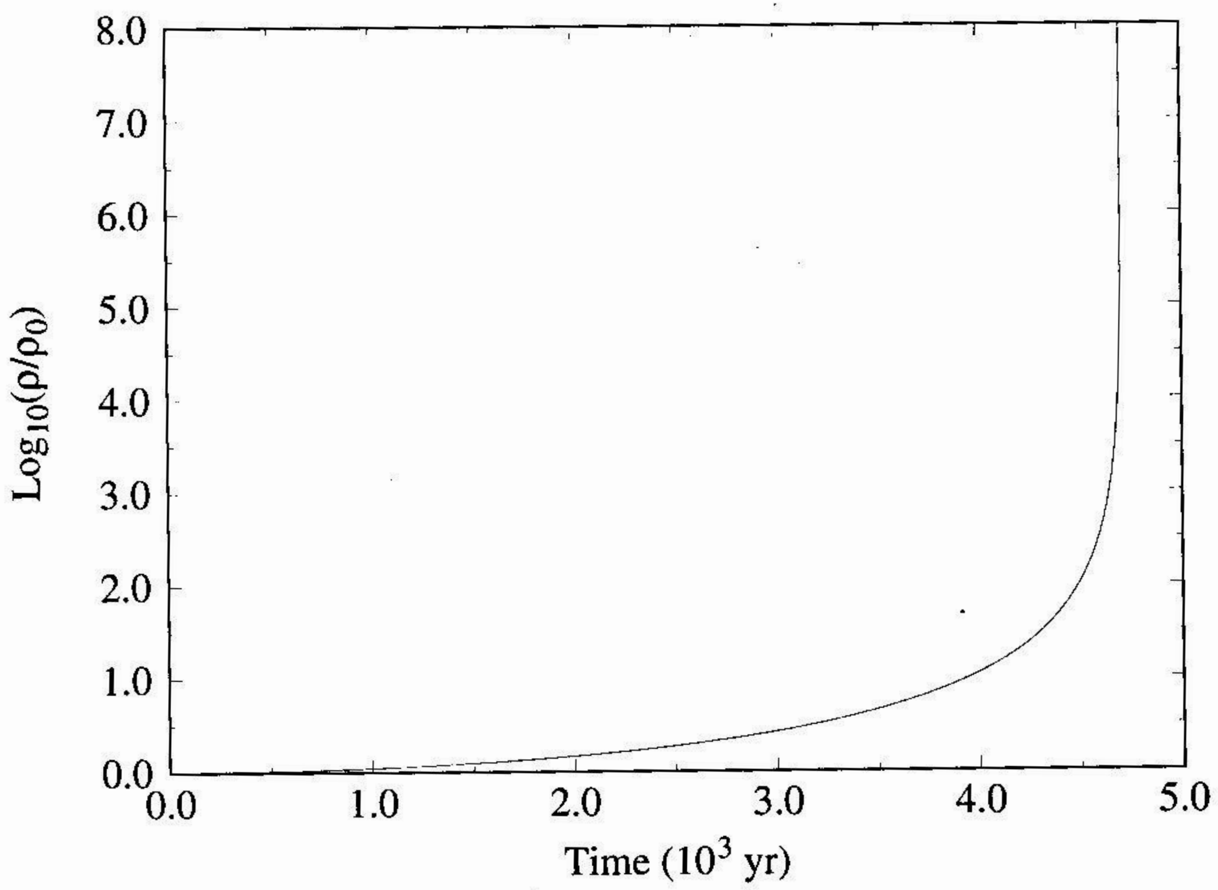

Figure 12.6 The ratio of the cloud's density relative to its initial value as a function of time for the isothermal, homologous collapse of a molecular cloud with an initial density of $\rho_0 = 2 \times 10^{-16}$ g cm^{-3}.

Carroll & Ostlie

Note that $t_{\rm ff} \propto \frac{1}{\sqrt{G\rho_0}}$ has no dependence on r_0.

If ρ_0 is uniform, all m collapse to the center at the same time

→ **homologous collapse**

In reality, ρ_0 is somewhat centrally condensed, as observed,
e.g., $\rho_0 \propto r^{-1}$ to r^{-2}, inner region (small r), $t_{\rm ff}\downarrow\downarrow$

→ **inside-out collapse**

A protostellar core is formed, followed by material "raining down" from the envelop → **accretion**

Gravitational energy → kinetic energy → heat

$L_{\rm acc} \sim GM_* \dot{M}/R_*$

Ann. Rev. Astron. Astrophys. 1987. 25: 23–81

STAR FORMATION IN MOLECULAR CLOUDS: OBSERVATION AND THEORY

Frank H. Shu, Fred C. Adams, and Susana Lizano

Astronomy Department, University of California, Berkeley, California 94720

Dense cores form within molecular clouds → Seeds of individual stars

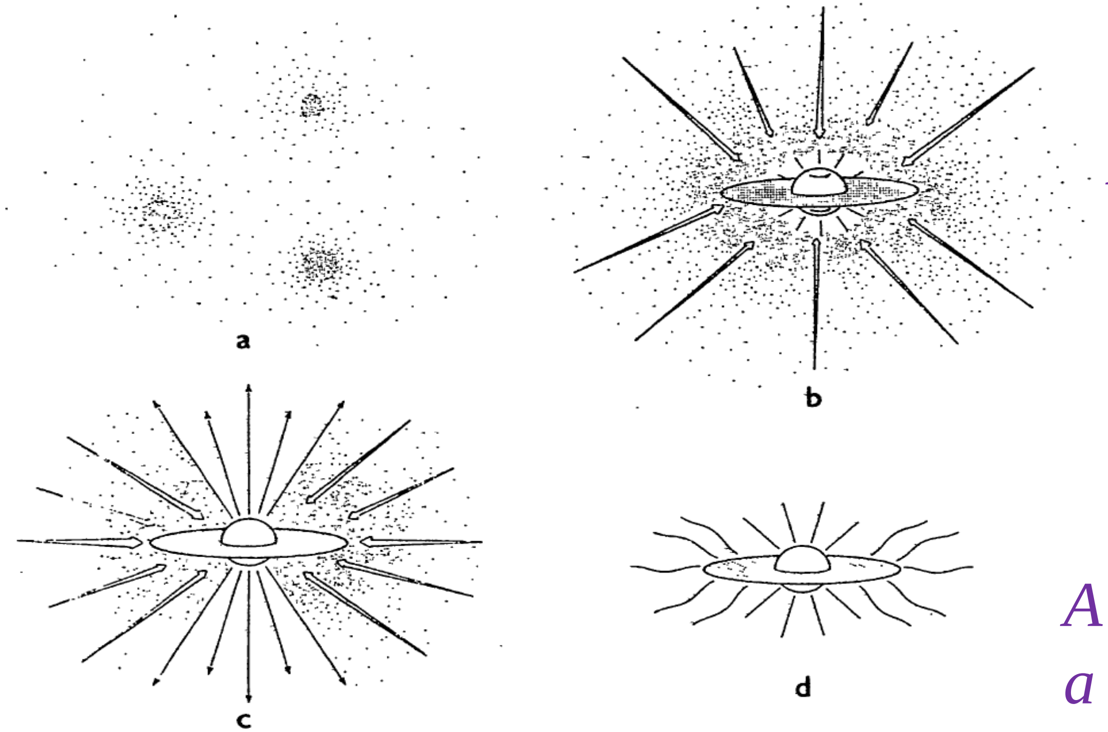

A core collapse inside-out and form a protostar with a toroid.

A stellar wind with a bipolar flow forms.

A star is formed with a circumstellar disk.

Figure 7 The four stages of star formation. (*a*) Cores form within molecular clouds as magnetic and turbulent support is lost through ambipolar diffusion. (*b*) A protostar with a surrounding nebular disk forms at the center of a cloud core collapsing from inside-out. (*c*) A stellar wind breaks out along the rotational axis of the system, creating a bipolar flow. (*d*) The infall terminates, revealing a newly formed star with a circumstellar disk.

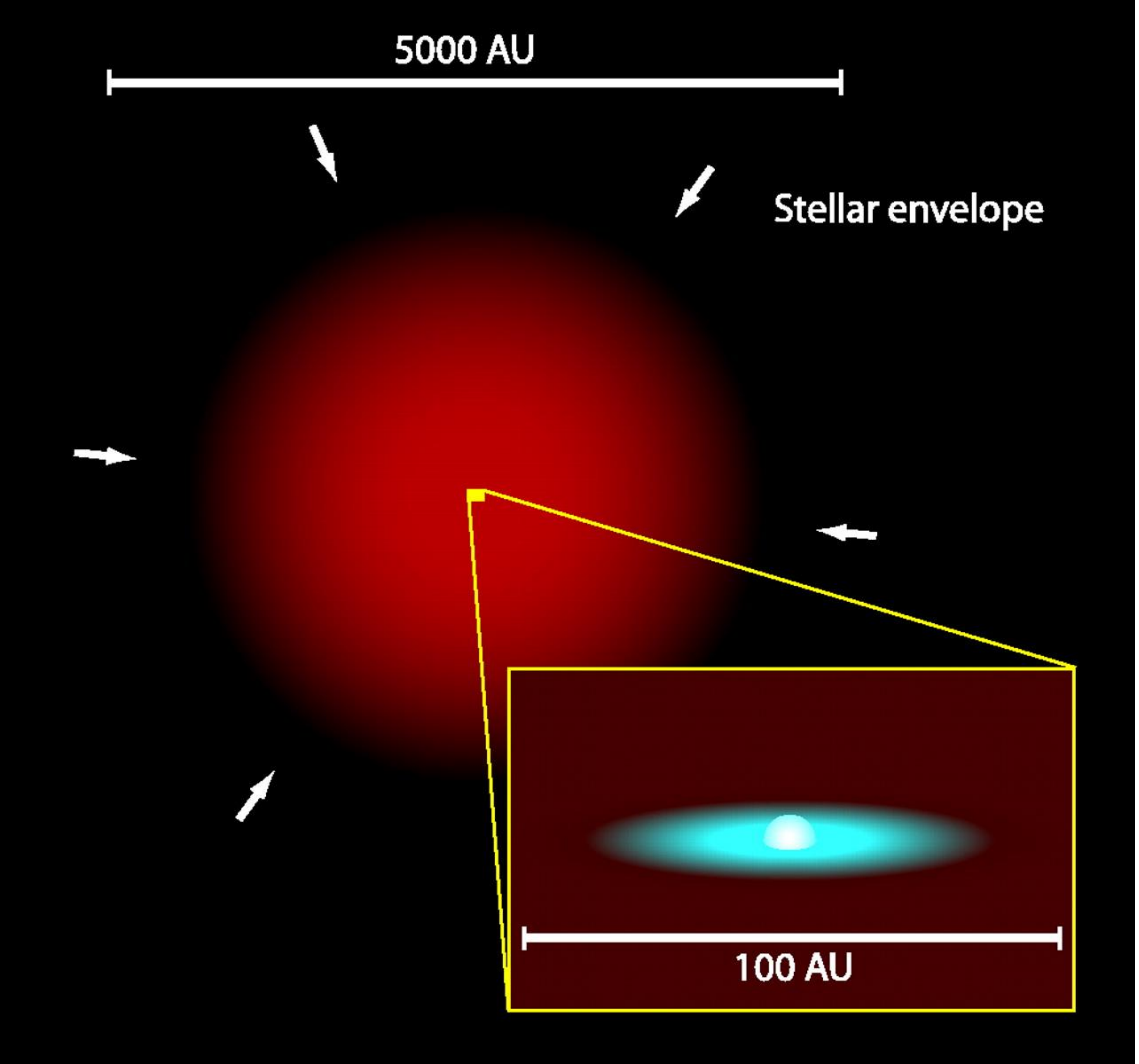

Central condensed protostar,
$r \sim$ a few $R_\odot$

Circumstellar disk,
$r \sim 100$ au

Surrounding envelope,
$r \sim 5000$ au

Matter accretes from the envelope via the disk onto the protostar

Ward-Thomson (2002)

Spectral energy distribution

F_λ vs λ
or $\log \lambda F_\lambda$ vs $\log \lambda$

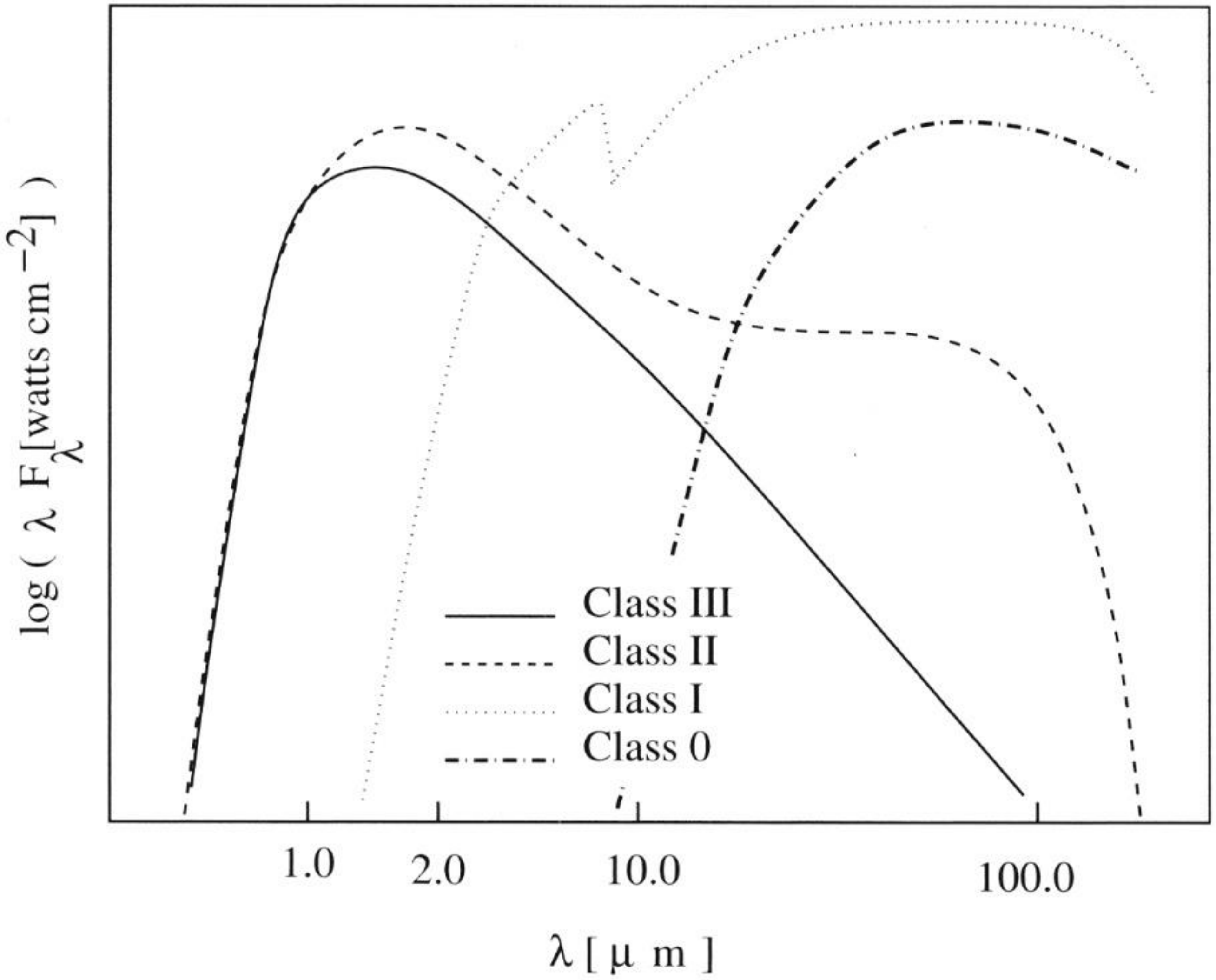

Spectral index useful to classify a young stellar object (YSO)

$$\alpha = \frac{d\log(\lambda F_\lambda)}{d\log(\lambda)}$$

where λ wavelength, between 2.2 and 20 μm; F_λ=flux density

Class 0 sources --- undetectable at $\lambda < 20$ μm
Class I sources --- $\alpha > 0.3$
Flat spectrum sources --- $0.3 > \alpha > -0.3$
Class II sources --- $0.3 > \alpha > -1.6$
Class III sources --- $\alpha < -1.6$

➔ Evolutionary sequence in decreasing amounts of circumstellar material (disk clearing)

Annu. Rev. Astron. Astrophys. 1996. 34:111–54

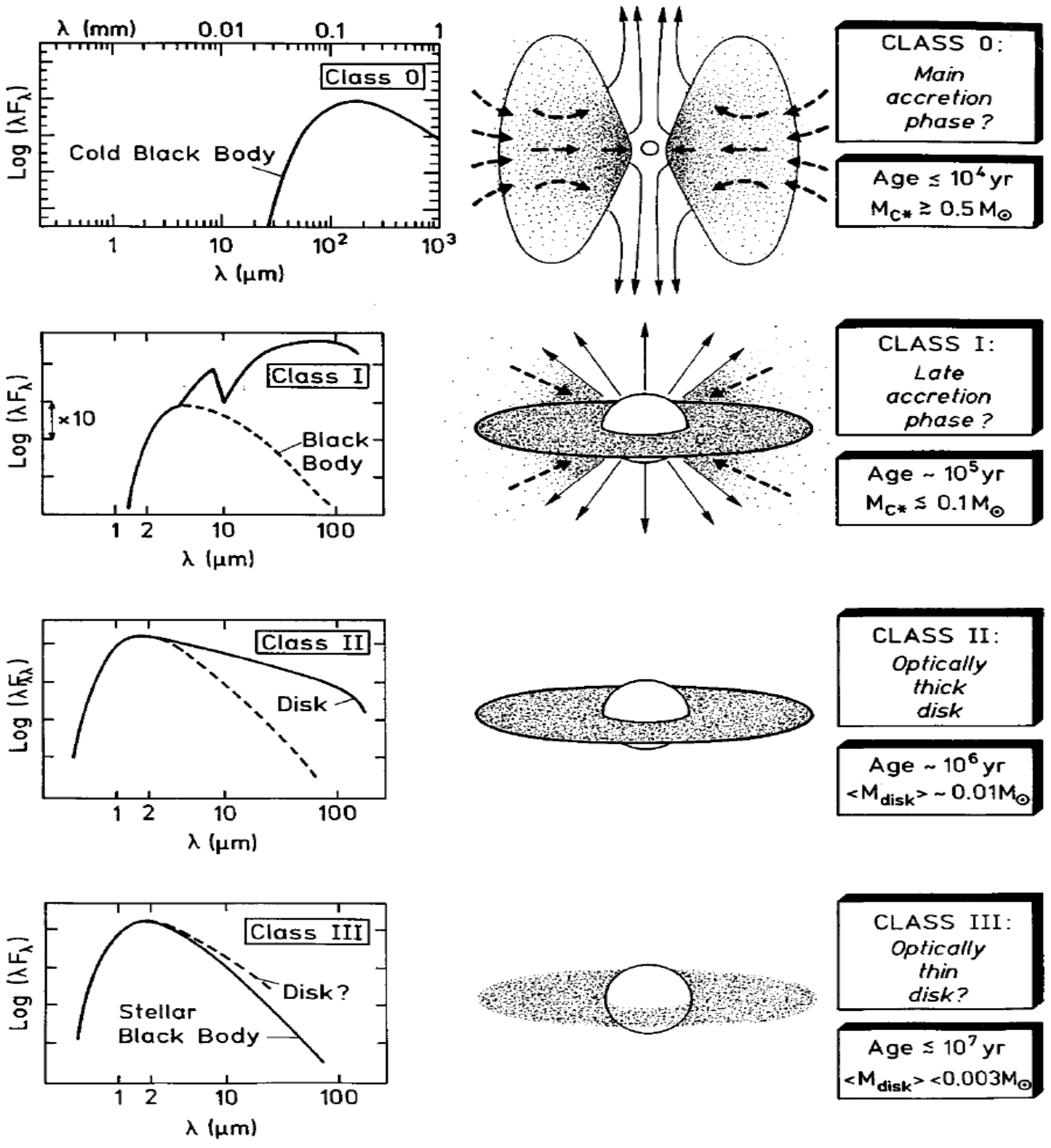

Figure 11 Evolutionary sequence of the spectral energy distributions for low-mass YSOs as proposed by André (1994). The four classes 0, I, II, and III correspond to successive stages of evolution.

Class 0
Submilimeter cores

Class I
Protostars

Class II
Classical T Tauri stars

Class III
Weak-lined T Tauri stars

Rafael Bachiller

Star Formation Rate (SFR): The rate at which gas and dust forms stars.
[Solar masses]/[Year] [unit area in disk]

Milky Way galaxy: 1~3 $M_\odot\ yr^{-1}$ (a few new-born stars per year)
M31: 0.4 $M_\odot\ yr^{-1}$

SFR $\Leftrightarrow$ LFIR, L(H_α, UV) …
Kennicutt-Schmidt empirical "law": $\Sigma_{SFR} \propto (\Sigma_{gas})^n, n \approx 1.4$ (surface?)

Star Formation Efficiency (SFE): Within a region, the ratio of
[Mass of stars formed]/[Total mass of the gas and dust available],
usually a few percent; e.g., nearby
star clusters 10% to 30% (Lada & Lada 03)

or SFR per unit of gas,
e.g., SFE(H_2) (Leroy+08)

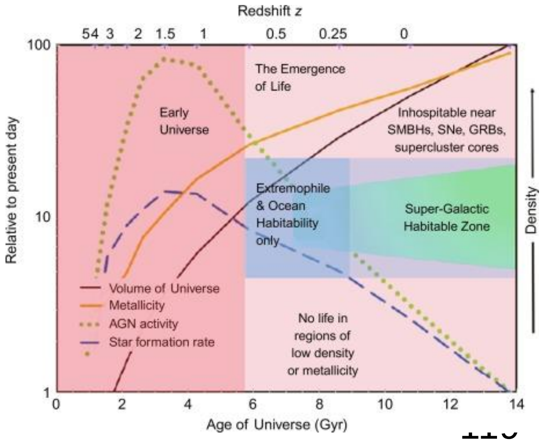

https://www.sciencedirect.com/topics/earth-and-planetary-sciences/star-formation-rate

Massive Star Formation and Feedback

Triggered/sequential/induced SF

Stellar winds + radiation

Radiation-Driven Implosion

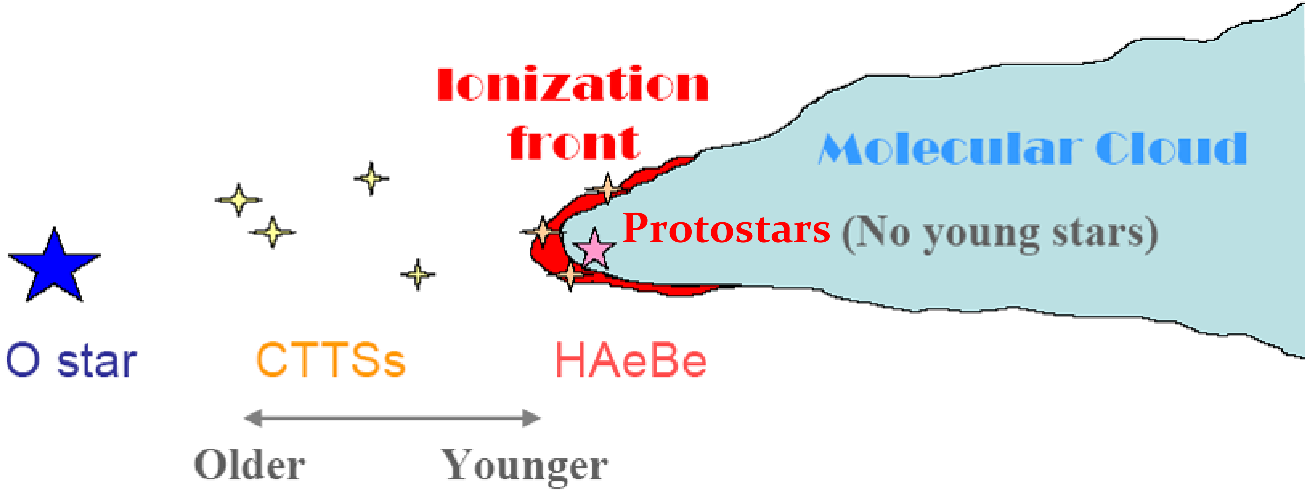

Other possible triggerers:

SNe, cloud-cloud collisions, density waves (spiral-arm), merging galaxies, etc.

Collect-and-Collapse

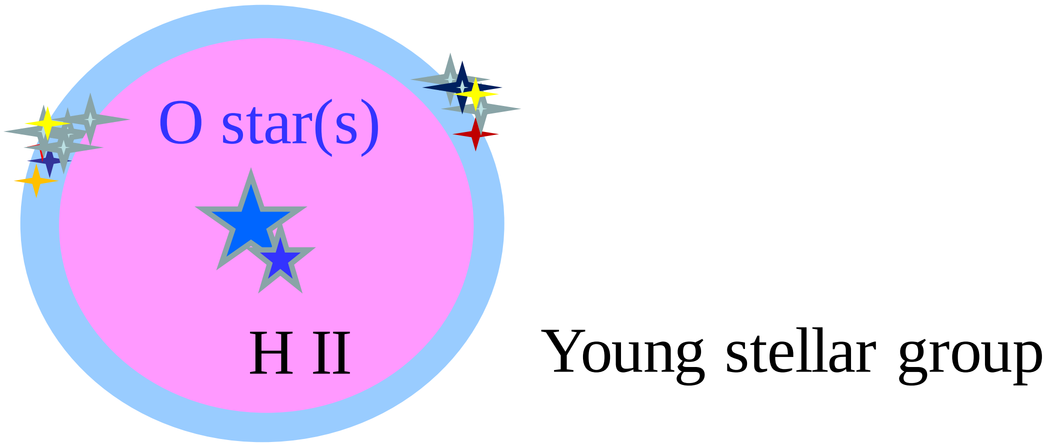

Antennae Galaxies

HST image of NGC 4038 (top) and NGC 4039 (bottom)

HST (blue, young stars) and ALMA (red, pink, and yellow; cold gas)

Conclusions

- ISM has a variety of forms (atomic, ionic, molecular) in solid or gaseous state, under differing conditions (temperature, density, composition …)
- Stars form out of cold, dense ISM cloud cores. Rotation, magnetic field, turbulence, etc. play crucial roles. Planets/life … → A universal initial stellar mass function … more lower-mass stars
- Stars continue to interact with ISM. Evolved stars condense dust in their atmospheres. Dying stars enrich the ISM with complex elements ("metals") from which new stars form.
- Some galaxies are rich in such gas and dust, some not. Our Milky Way galaxy is producing stars. Cosmic SF history?